



IFPiLM

INSTYTUT FIZYKI PLAZMY I LASEROWEJ MIKROSYNTEZY
IM. SYLWESTRA KALISKIEGO



EUROfusion

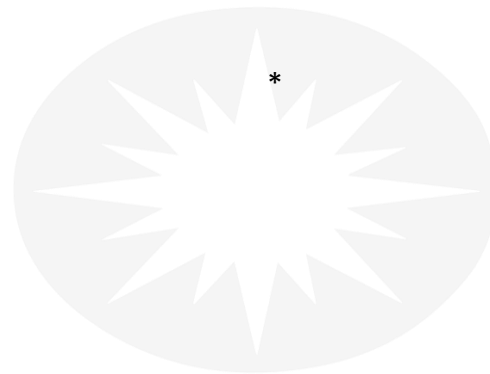


MAX-PLANCK-GESELLSCHAFT



Overview of the Wendelstein 7-X project – Polish contribution, recent results and plans

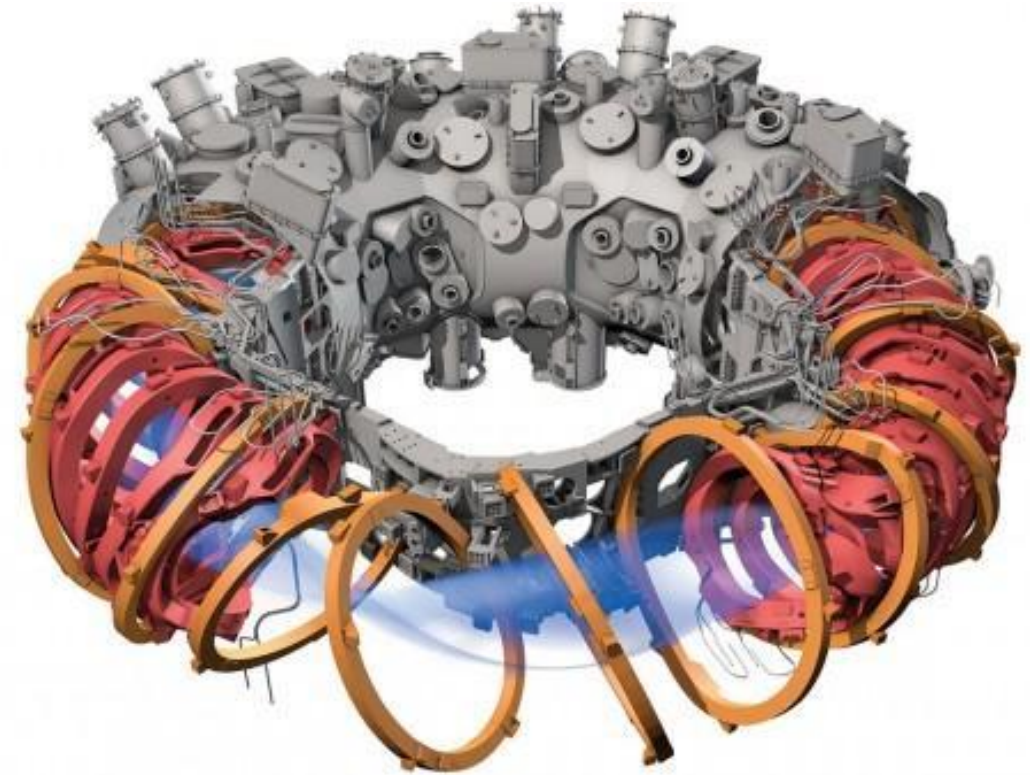
Monika Kubkowska for the W7-X team



9.03.2023, Seminarium IFJ PAN

Outline

1. Why Fusion?
2. Tokamak vs stellarators
3. Wendelstein 7-X project
4. Polish involvement in W7-X
5. Exemplary results
6. Plans



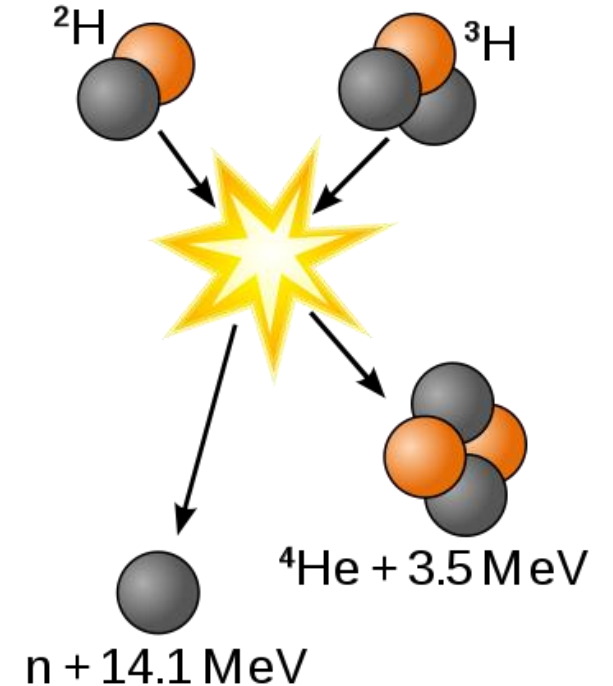
Why Fusion?

Fusion is the process that powers the stars.

Fusion science indicates that fusion energy will require small amounts of fuel, produce very little nuclear waste, and its reactions can be shut down swiftly.

The urgency of the climate crisis highlights the need to accelerate and intensify experiments to create new forms of energy, including the design and development of fusion devices.

Experiments are needed for proof of concepts, to test alternative choices, and to hone technical performance.



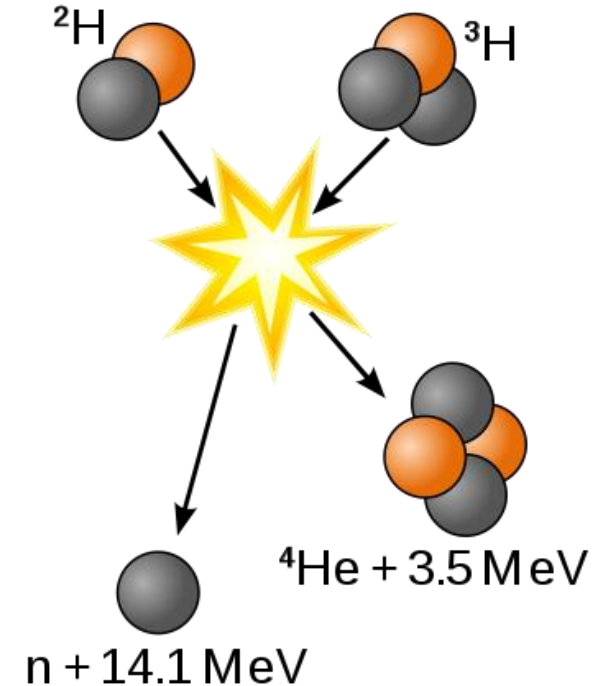
Why Fusion?

Fusion is the process that powers the stars.

Fusion science indicates that fusion energy will require small amounts of fuel, produce very little nuclear waste, and its reactions can be shut down swiftly.

The urgency of the climate crisis highlights the need to accelerate and intensify experiments to create new forms of energy, including the design and development of fusion devices.

Experiments are needed for proof of concepts, to test alternative choices, and to hone technical performance.

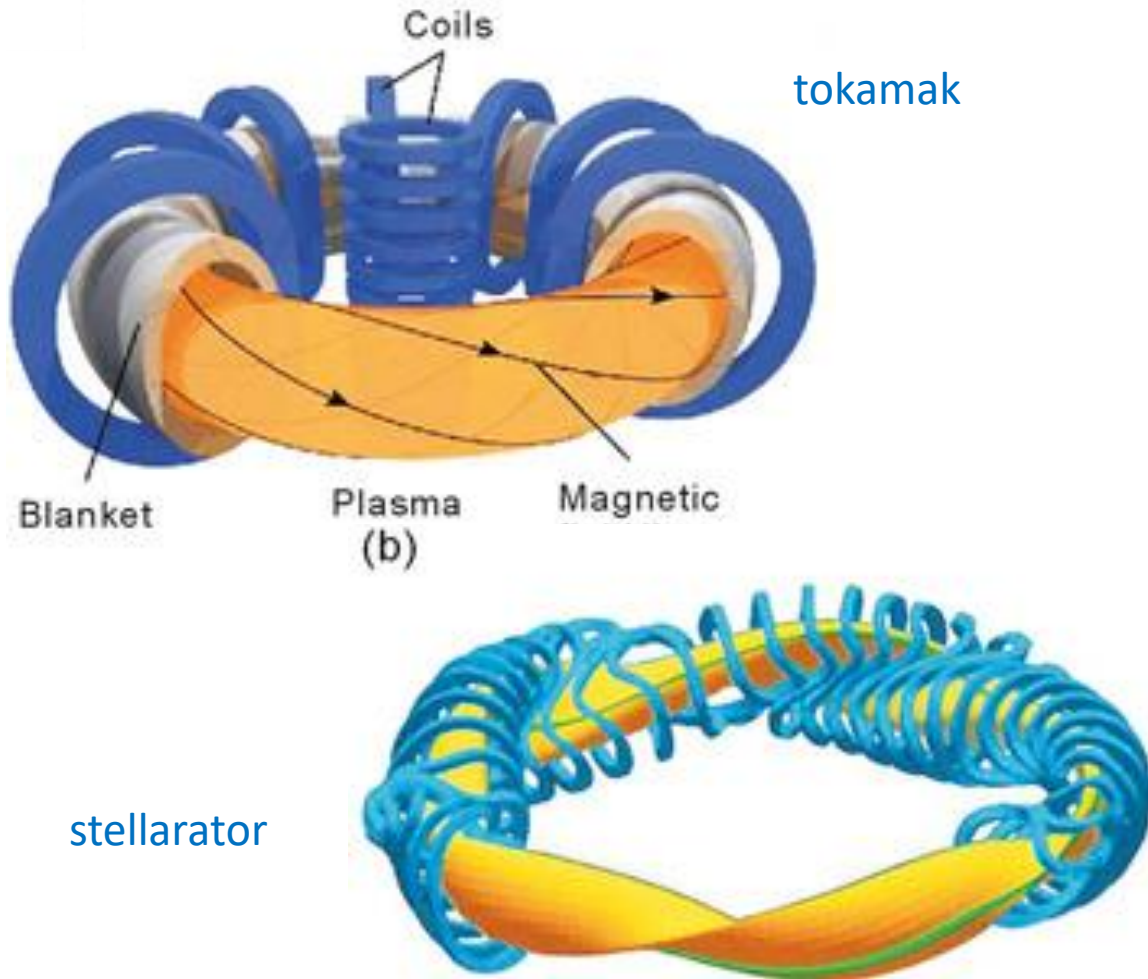


Statements from World Economic Forum 2020

<https://www.weforum.org/agenda/2020/12/fusion-experiments/>

Confinement

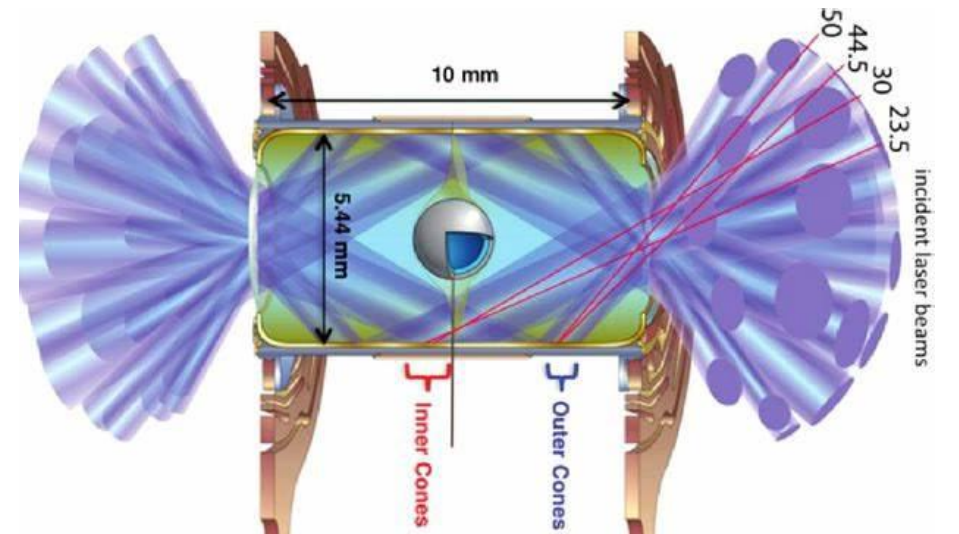
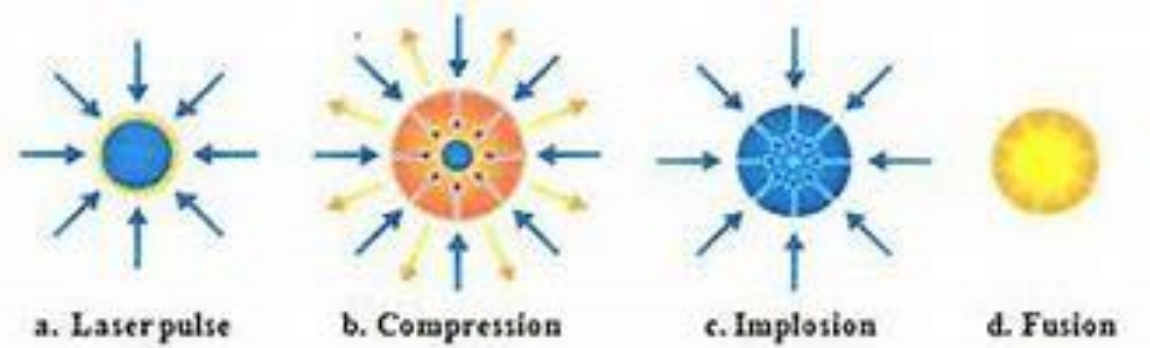
Magnetic confinement



tokamak

stellarator

Inertial confinement

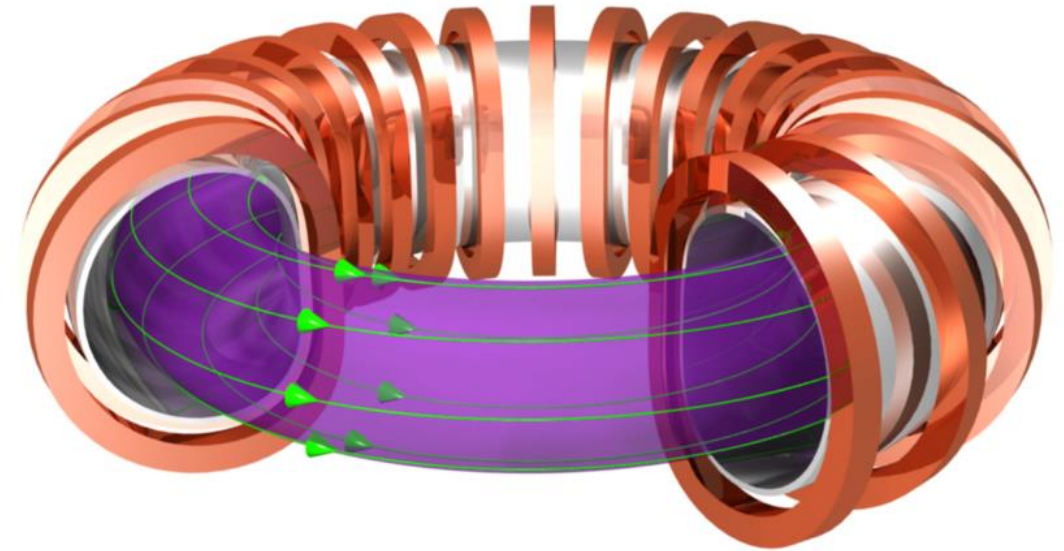


Magnetic confinement

For a toroidal plasma confinement system, the plasmas are confined by a magnetic field. In order to have an equilibrium between the plasma pressure and the magnetic forces it is necessary to have a rotational transform of the toroidal magnetic field. Such a rotational transform may prevent the drift shape of the guiding center of plasma particles towards the wall.

There are three different ways to twist the magnetic field:

- creating a poloidal field by a toroidal electric current;
- rotating the poloidal cross-section of stretched flux surfaces around the torus;
- making the magnetic axis non-planar.



Y. Xu / Matter and Radiation at Extremes 1 (2016) 192e200

Magnetic confinement

For a toroidal plasma confinement system, the plasmas are confined by a magnetic field. In order to have an equilibrium between the plasma pressure and the magnetic forces it is necessary to have a rotational transform of the toroidal magnetic field. Such a rotational transform may prevent the drift shape of the guiding center of plasma particles towards the wall.

There are three different ways to twist the magnetic field:

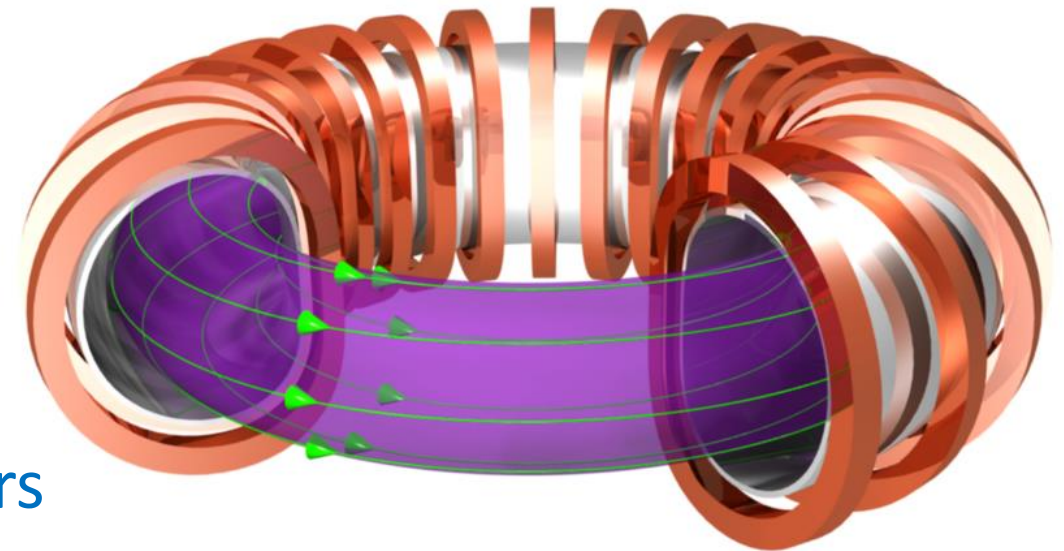
➤ creating a poloidal field by a toroidal electric current;

tokamaks

➤ rotating the poloidal cross-section of stretched flux surfaces around the torus;

➤ making the magnetic axis non-planar.

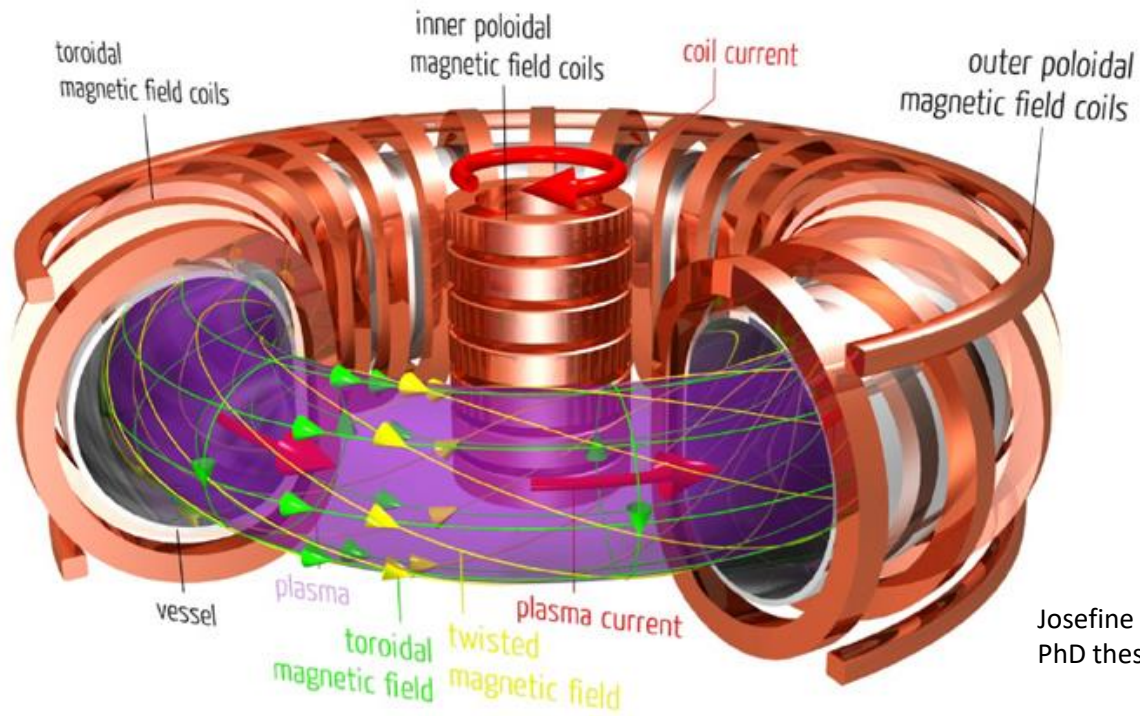
stellarators



Y. Xu / Matter and Radiation at Extremes 1 (2016) 192e200

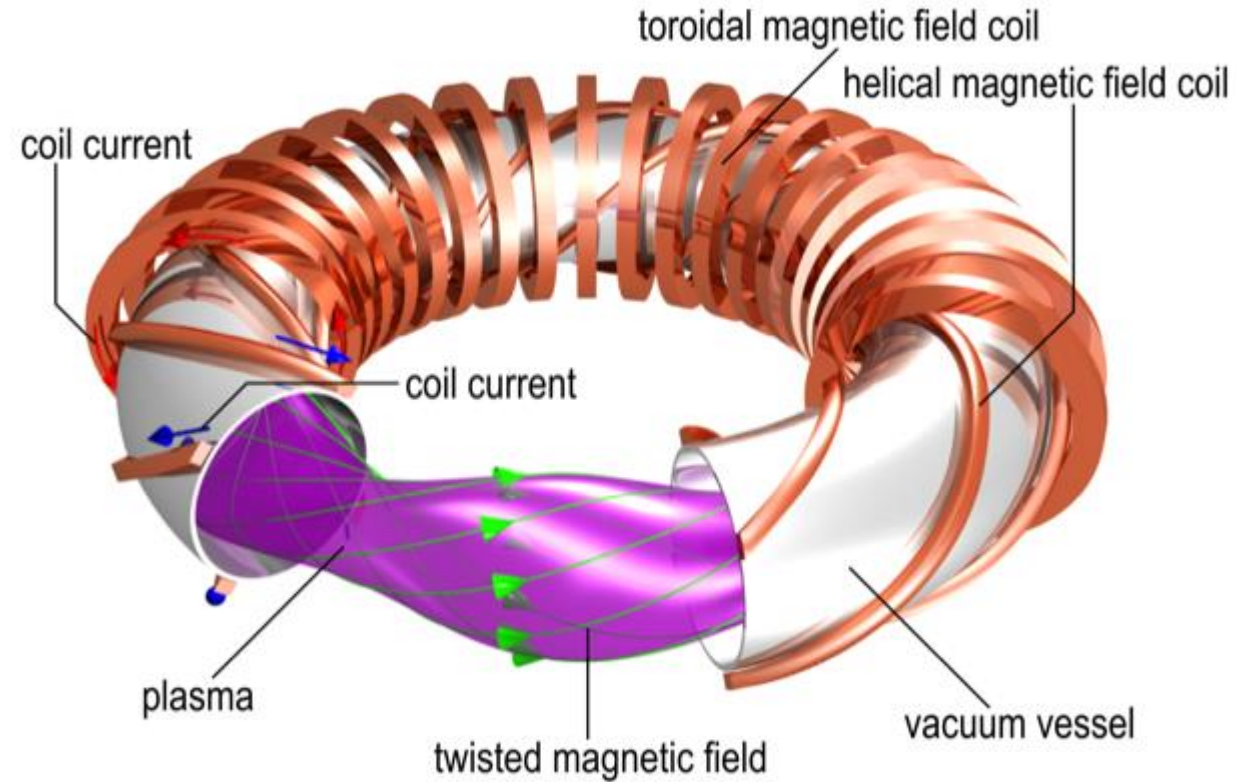
Tokamak vs stellarator

tokamak



Josefine Henriett
PhD thesis, 2013

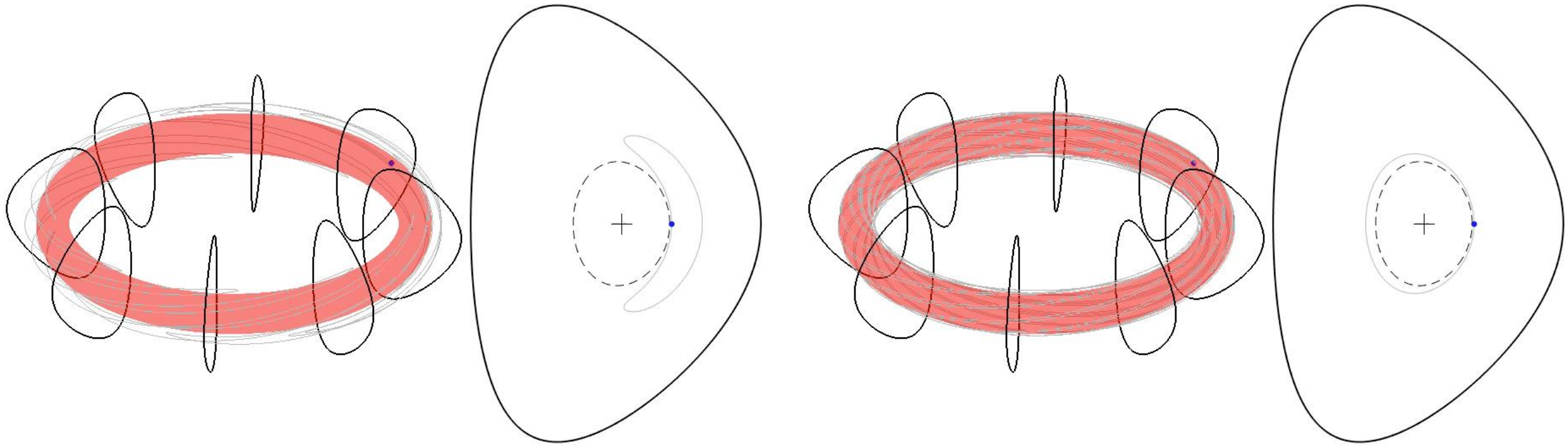
stellarator



In tokamak, one set of coils generate an intense toroidal field while a central solenoid (a magnet carrying electric current) creates a poloidal field, confining the plasma particles. A third set of magnetic coils creates an outer poloidal field to shape and position the plasma within the torus. The toroidal current is normally generated by a transformer, which makes the device vulnerable to current-driven instabilities and difficult to operate in a steady state. The stellarators, on the other hand, are inherently current free, and thus, able to operate the plasma in a steady state. But more unconfined particle orbits in stellarators can lead to high neoclassical transport of energetic and thermal particles.

Particles in tokamak

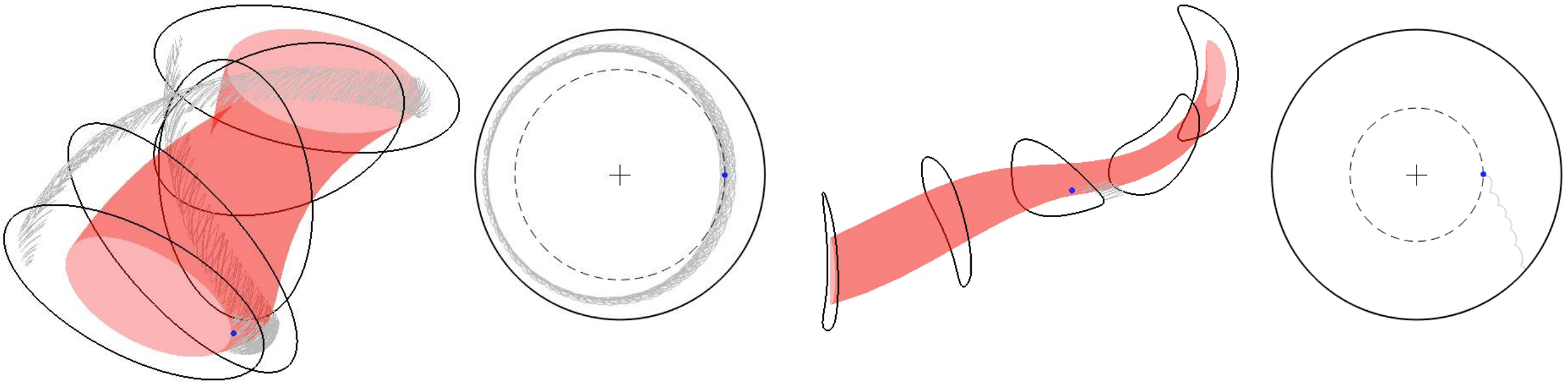
- Magnetic drifts and mirror behavior of particles cause particles to move across flux surfaces
- This results in so-called banana, potato, and stochastic orbits



Particle in stellarators

Stellarator tend to be more quiescent but generally have poor confinement

- The three-dimensional fields of stellarator suppresses many MHD activity present in tokamaks
- These fields open the possibility of helically trapped along with toroidally trapped particles.
- These magnetic fields can result in ripple trapping and loss of particles.



S. Lazerson, 23rd ISHW

Why stellarators?

Stellarators are the main alternative MCF concept to the tokamaks

External coils generate rotational transform: 3D confinement w/o plasma current

Pros & Cons

- + steady-state, intrinsically
- + no current disruptions
- + no current driven instabilities
- + no significant current drive
- + no runaway electrons
- + operation above Greenwald-limit* feasible
- + lower alpha-particle pressure (given P_{fusion})

- 3D engineering
- 3D core impurity transport
- 3D plasma/fast ion confinement
- high neoclassical losses**
- 3D MCF: one generation behind
- divertor concept to be verified
- operation scenarios to be developed

*an operational limit for the density in magnetic confinement devices $n_G = \frac{I_p}{\pi a^2}$

Stellarators in the EU fusion Roadmap

W7-X is a proof-of-concept experiment for a new class of MCF devices

It's sufficiently large/powerful to:

- Resolve 3D MCF show-stoppers and good performance (w.r.t. tokamak)
- Address drawbacks of tokamaks
- steady-state Fusion technology
- Study fundamentally new 3D plasma physics

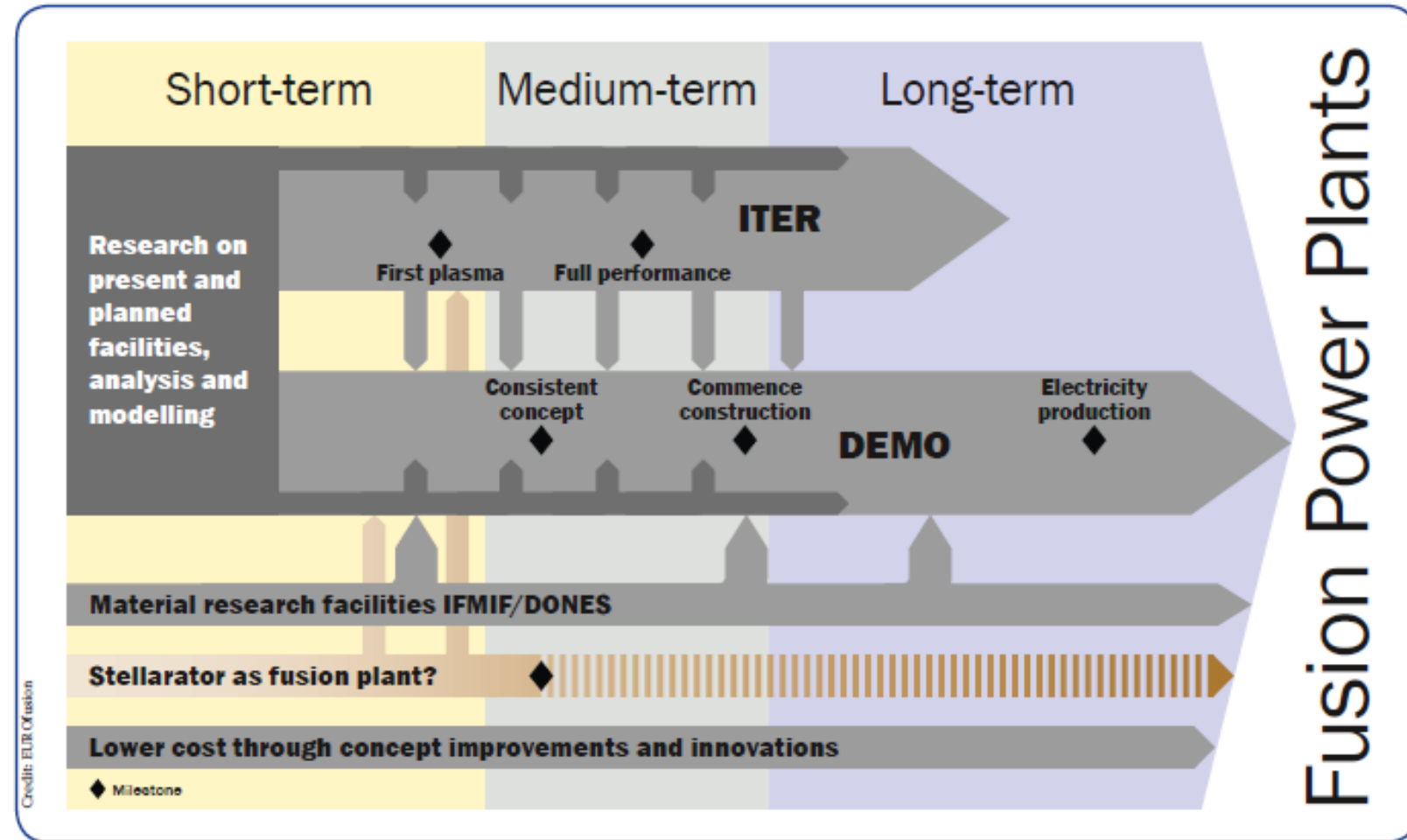


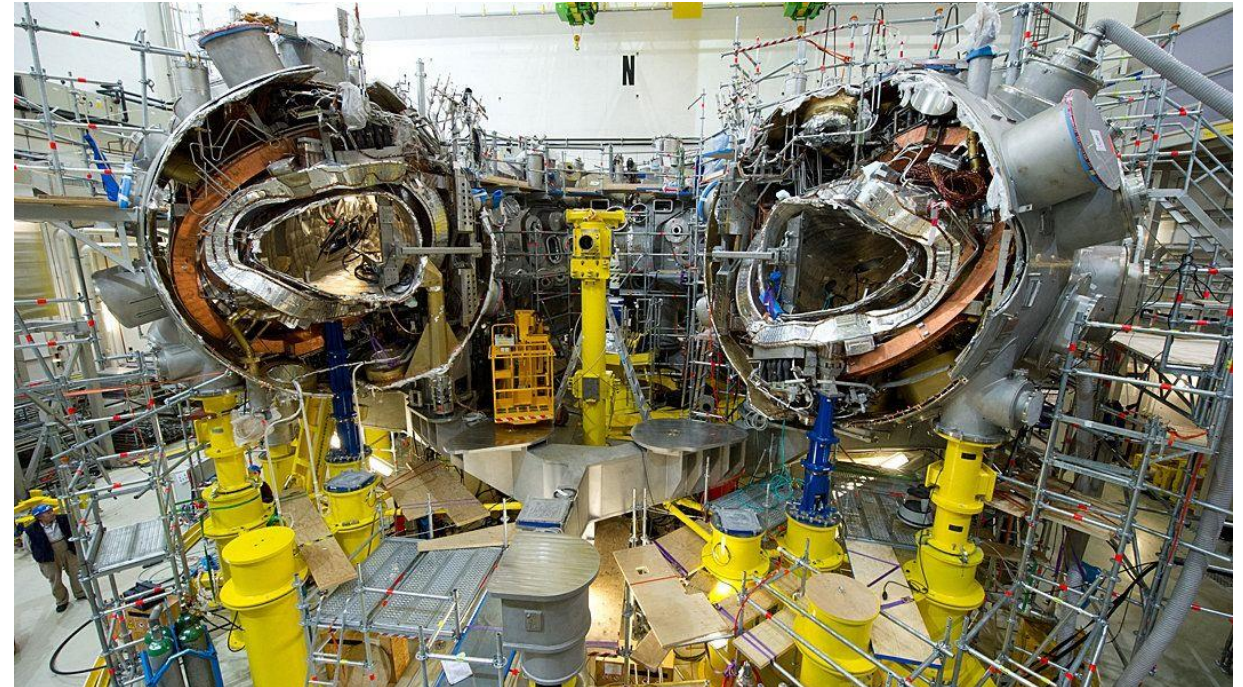
Figure 10: Mission 8 elements of the roadmap (coloured) involve exploitation of Wendelstein 7-X as well as pre-conceptual studies into a Helias-based fusion power plant.

Wendelstein 7-X project

It is a HELIAS type stellarator - HELical Axis Advanced Stellarator (Neoclassical Optimization)

The construction of Wendelstein 7-X has officially started in the year 1996 in Greifswald, Germany.

The first large components had arrived in 2004 on site and device assembly took about 10 years in total.



Participation of Polish institutions in the Wendelstein 7-X project



Institute of Plasma Physics and Laser Microfusion (IPPLM), Warsaw
Diagnostic systems - PHA, MFS; Plasma modelling



The Henryk Niewodniczański Institute of Nuclear Physics (IFJ PAN), Cracow
Cooperation on device assembly; Detection of the delayed neutrons



National Center for Nuclear Research (NCBJ), Otwock-Swierk
Neutral Beam Injection system for Wendelstein 7-X



Warsaw University of Technology (WUT)
Numerical analysis of the structural mechanical behaviour of magnet system of W7-X



Opole University, Opole
C/O monitor system for W7-X



KrioSystem, Wrocław
Manufacturing and delivery of cryogenic systems



Construction phase of W7-X

According to the agreement **IFJ PAN** was responsible for the assembly of the bus bar system powering 70 superconducting coils on five modules of the W7-X stellarator.



More than 50 engineers and technicians were involved and trained in the assembly process of the bus bars.

Construction phase of W7-X

NCBJ contributed to the construction of Neutral Beam Injector NBI system.

System consists of:

- Support structures for NBI boxes as well as hydraulic system for positioning and displacement of boxes,
- Two gates valves separating the NBI boxes from the stellarator torus,
- Cooling system ensuring the heat dissipation from ion sources, rf-generators and plasma grids
- Two reflection magnets.



Construction and operation phase of W7-X

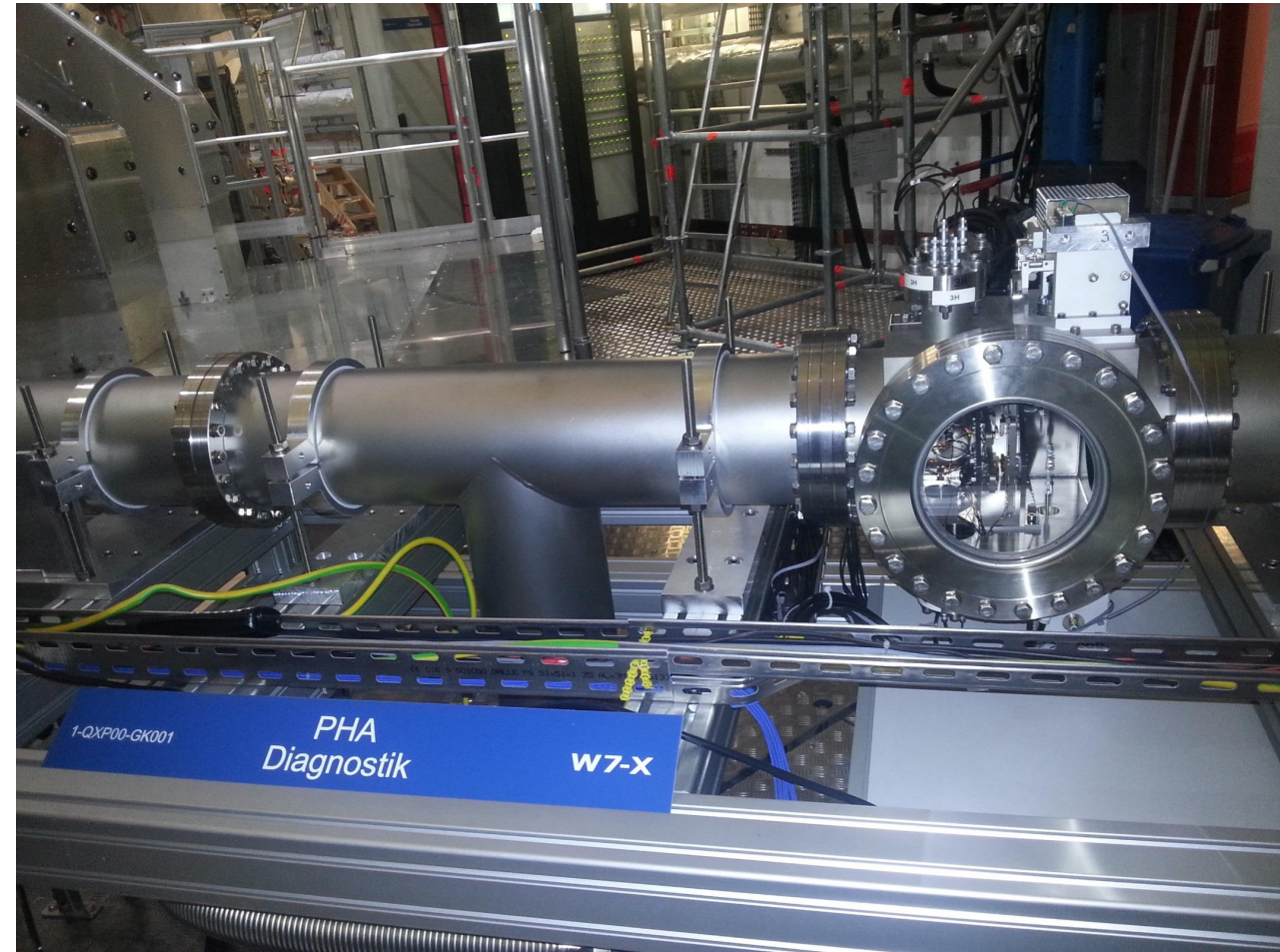
IPPLM was responsible for the development of soft X-ray spectrometry systems: **Pulse High Analysis (PHA)** and **Multi-Foil System (MFS)**

PHA system – is intended to provide the spectral energy distribution with an energy resolution of about 150-200 eV along a central line of sight

Measurements of the X-ray spectra will allow:

- to identify the impurity line radiation
- to determine impurity concentration
- to determine the electron temperature
- to determine Z_{eff} in the plasma.

MFS system is still under design.



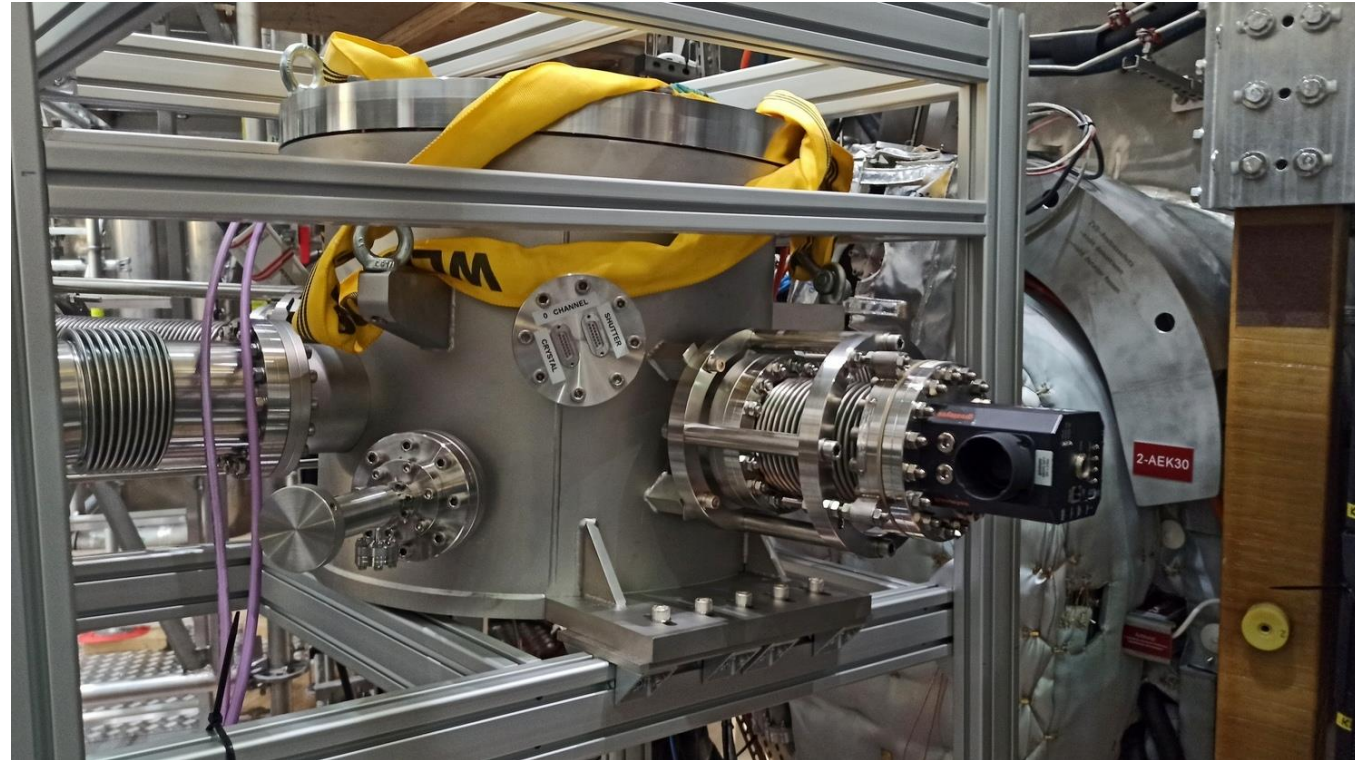
Construction and operation phase of W7-X

Opole University was involved in development of C-O- Monitor system (IFJ PAN supported OU in electronics for the detector – Multi Strip Gaseous Chamber)

- dedicated EUV/soft X-ray spectrometer
- no spatial resolution, central line-of-sight (fixed);
- 4 channels at fixed wavelengths of H-like impurity ions:

from 2014 in collaboration with IPPLM

- oxygen, 1.9 nm (general wall condition),
- carbon, 3.4 nm (plasma interaction with CFC/carbon wall) ,
- nitrogen, 2.5 nm (vacuum leakage),
- boron, 4.9 nm (quality of boron layer).



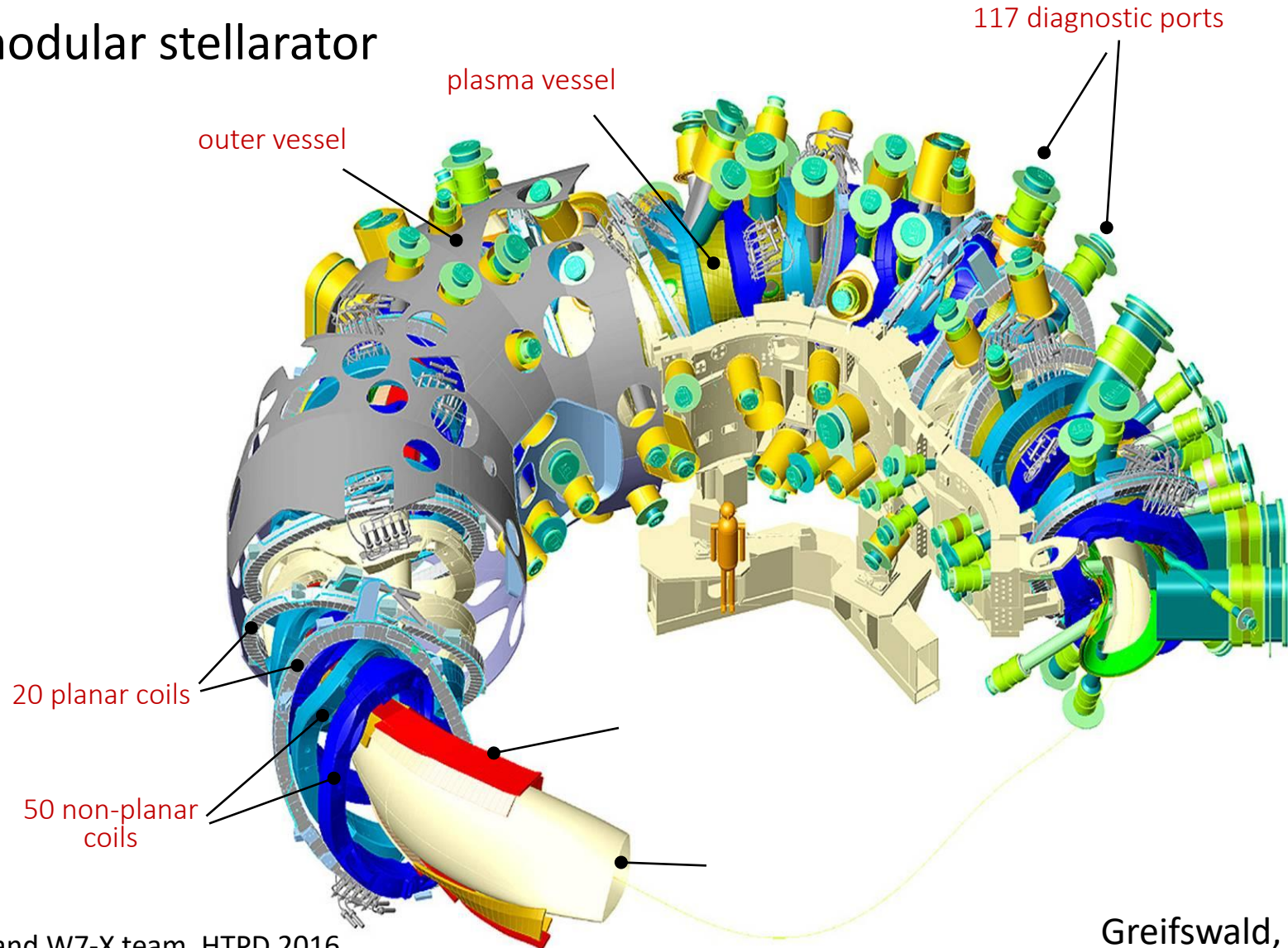
Wendelstein 7-X

➤ Superconducting modular stellarator

- $R = 5.6 \text{ m}$
- $a = 0.5 \text{ m}$
- Mass: 725 t
- $V_{\text{plasma}} = 30 \text{ m}^3$
- $\iota = 5/6 - 5/4$
- $B \leq 3 \text{ T}$

➤ Mission

- Steady state operation
 - Pulses up to 30 min.
- Several optimizations

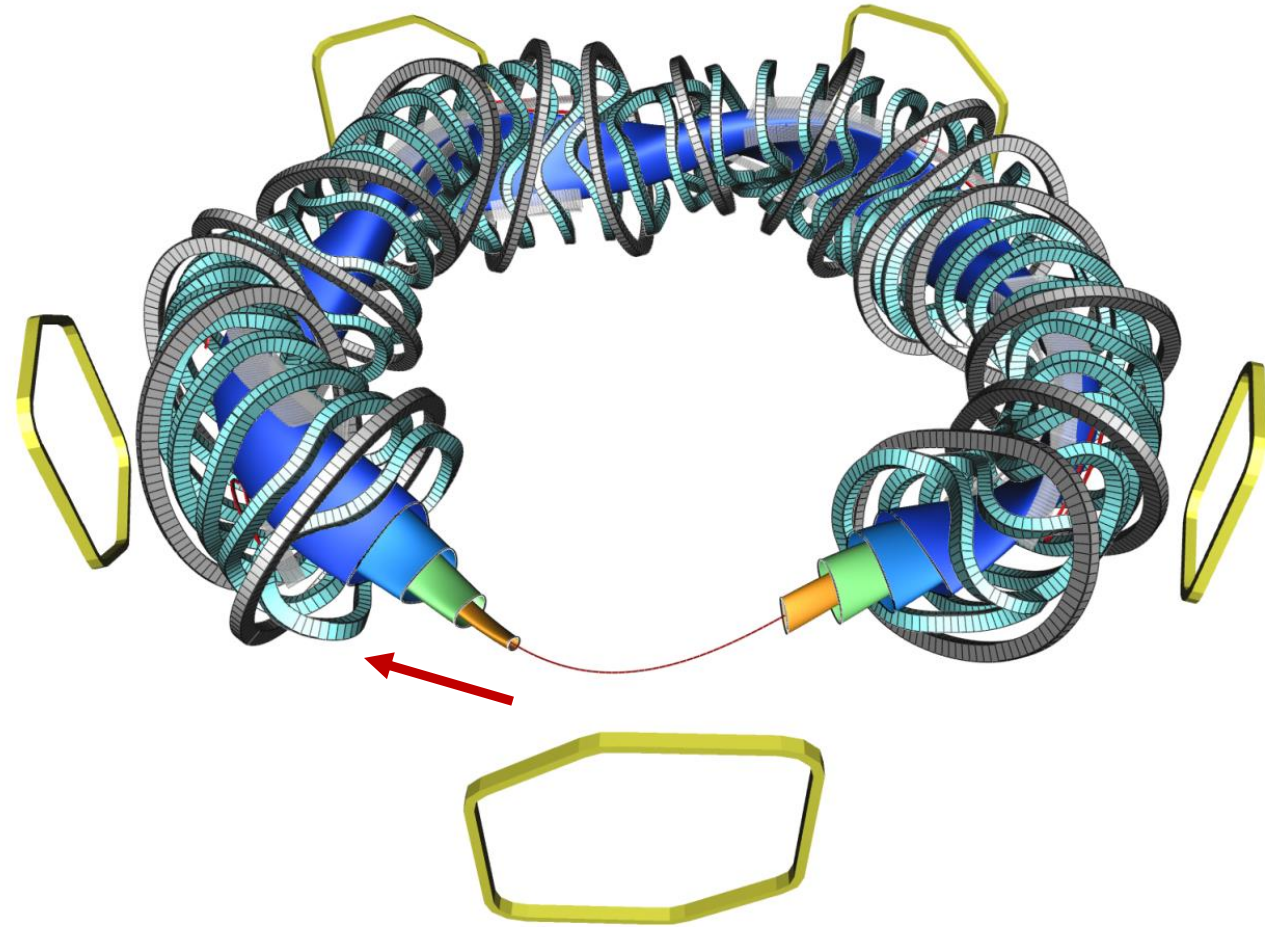
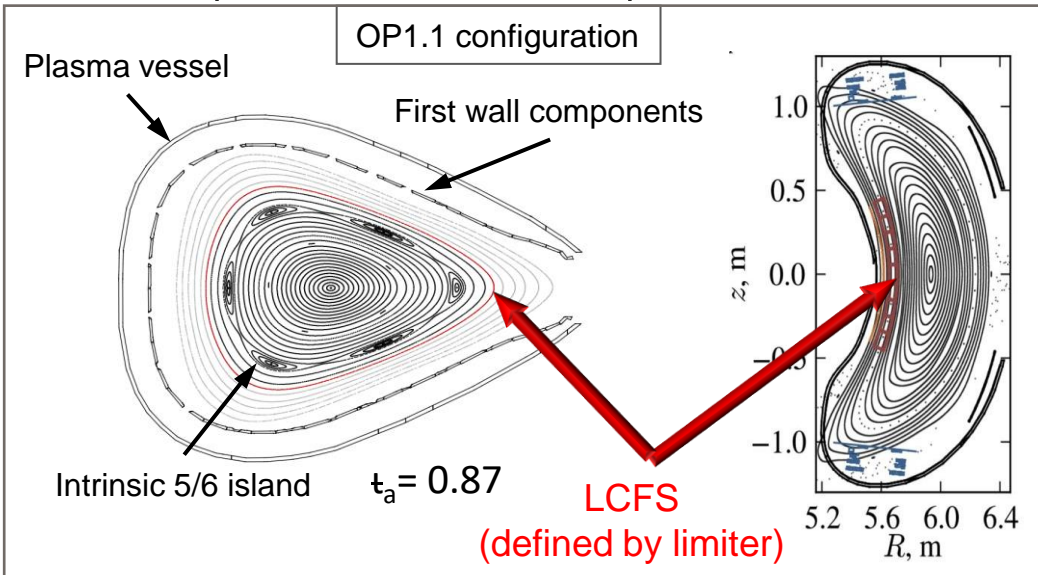


From M. Krychowiak and W7-X team, HTPD 2016

Greifswald, Niemcy

Wendelstein 7-X

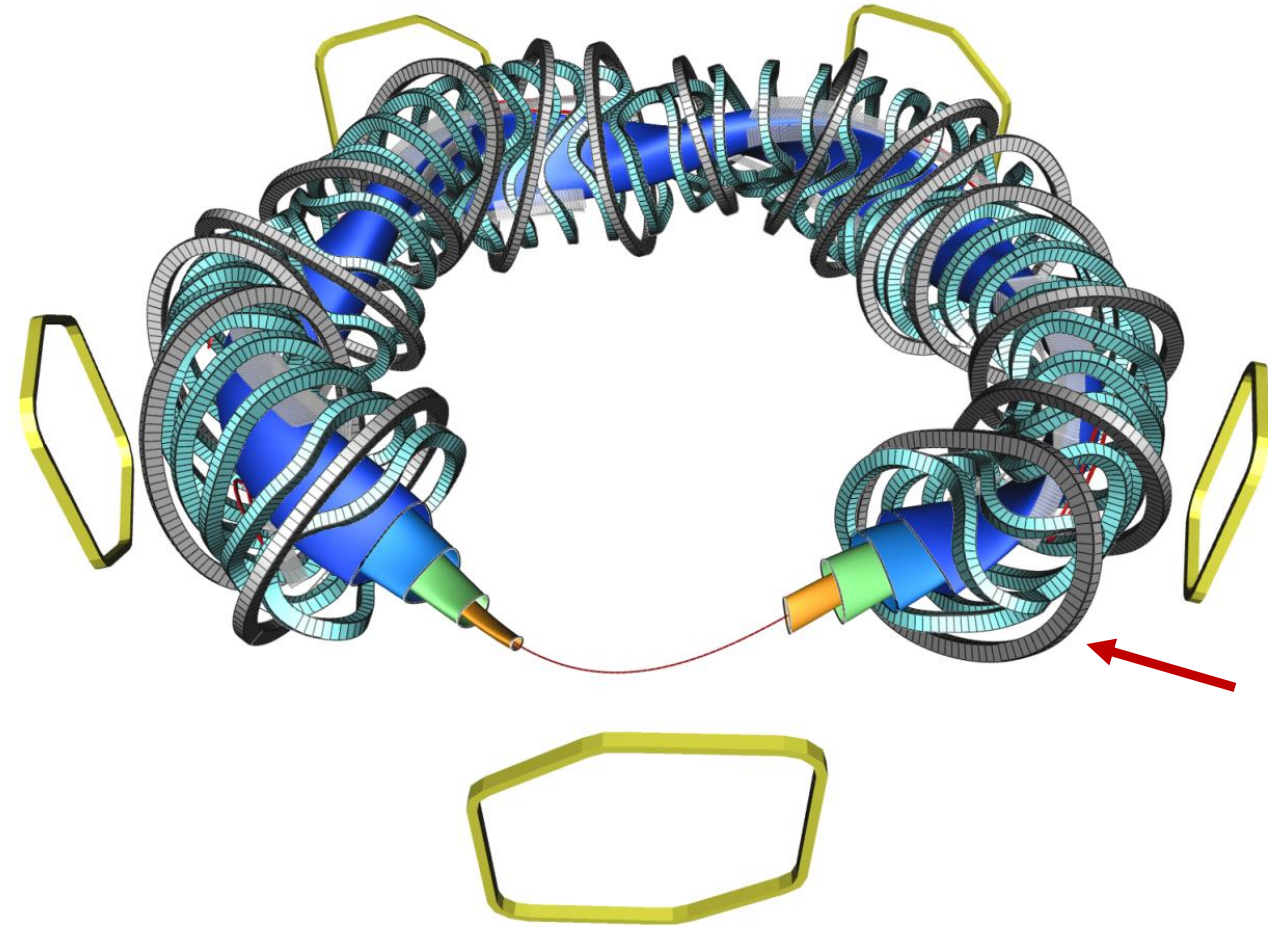
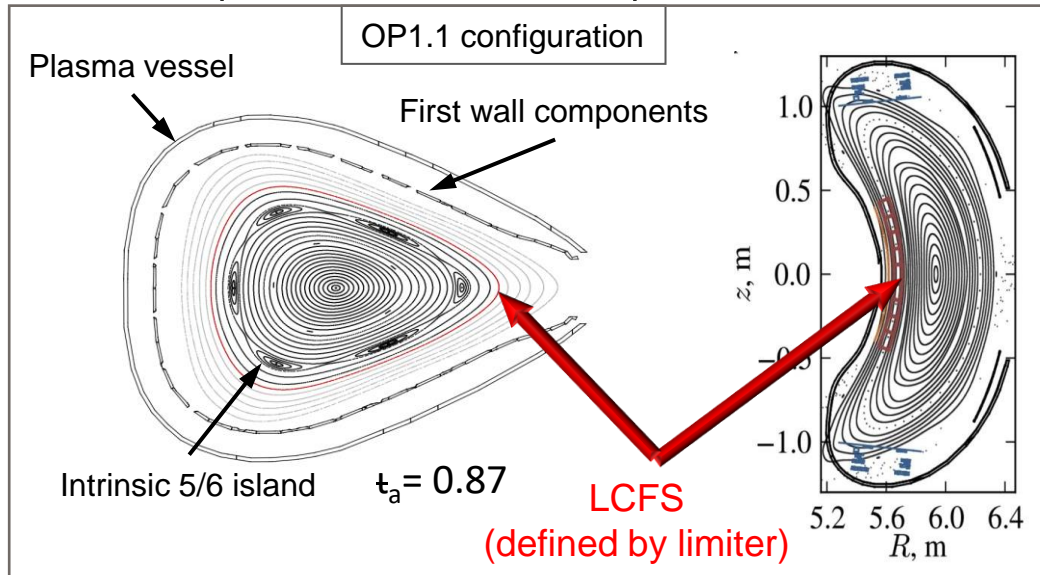
- Main helical field: 50 non-planar coils (18 kA, superconducting)
- Adjusting iota: 20 planar coils (12 kA, superconducting)
- Move island position at divertors: 10 control coils (water cooled)
- Correction of 1/1 field error: 5 trim coils (2 kA, water cooled)



From M. Krychowiak and W7-X team, HTPD 2016

Wendelstein 7-X

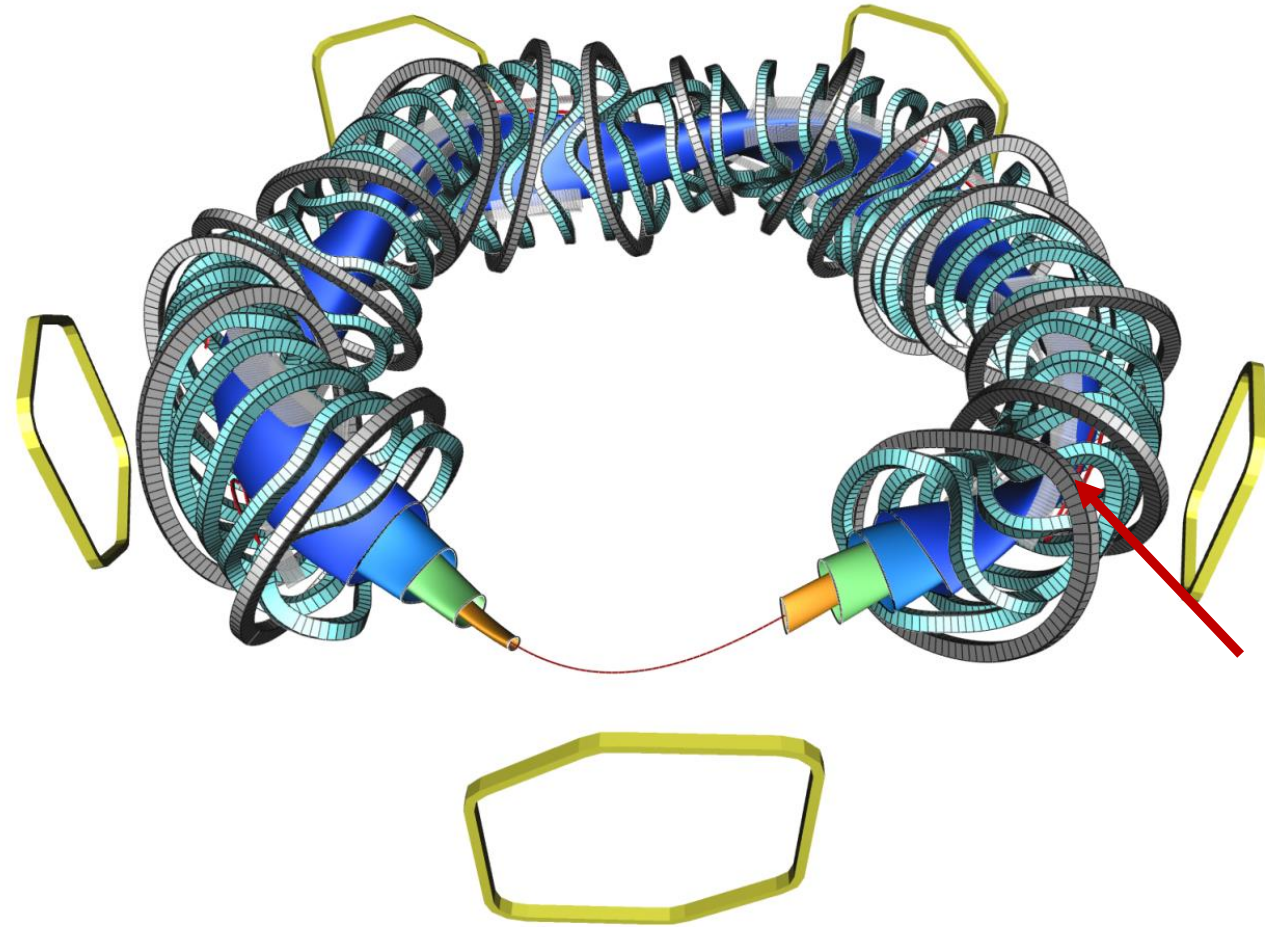
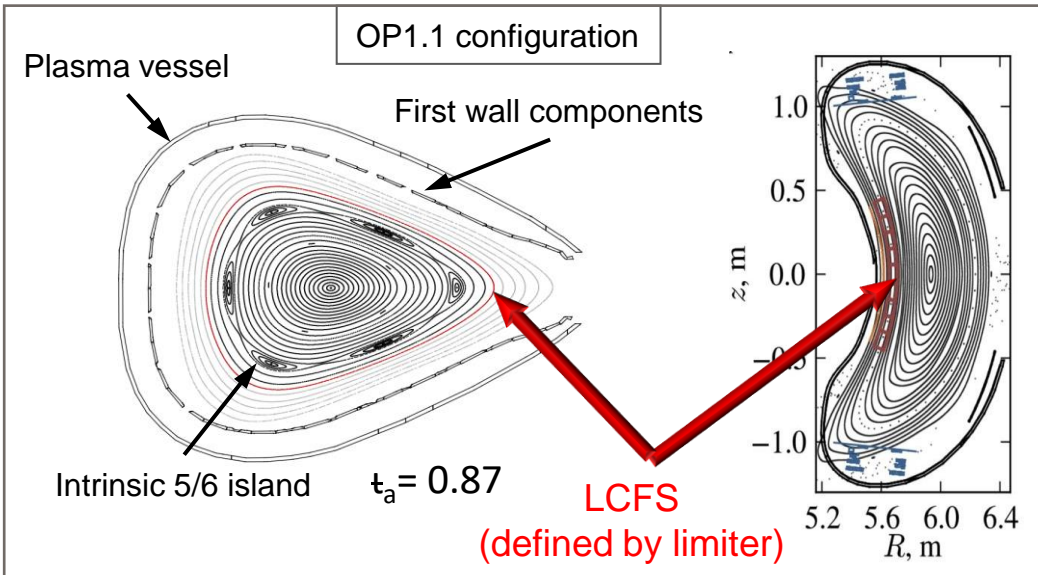
- Main helical field: 50 non-planar coils (18 kA, superconducting)
- Adjusting iota: 20 planar coils (12 kA, superconducting)
- Move island position at divertors: 10 control coils (water cooled)
- Correction of 1/1 field error: 5 trim coils (2 kA, water cooled)



From M. Krychowiak and W7-X team, HTPD 2016

Wendelstein 7-X

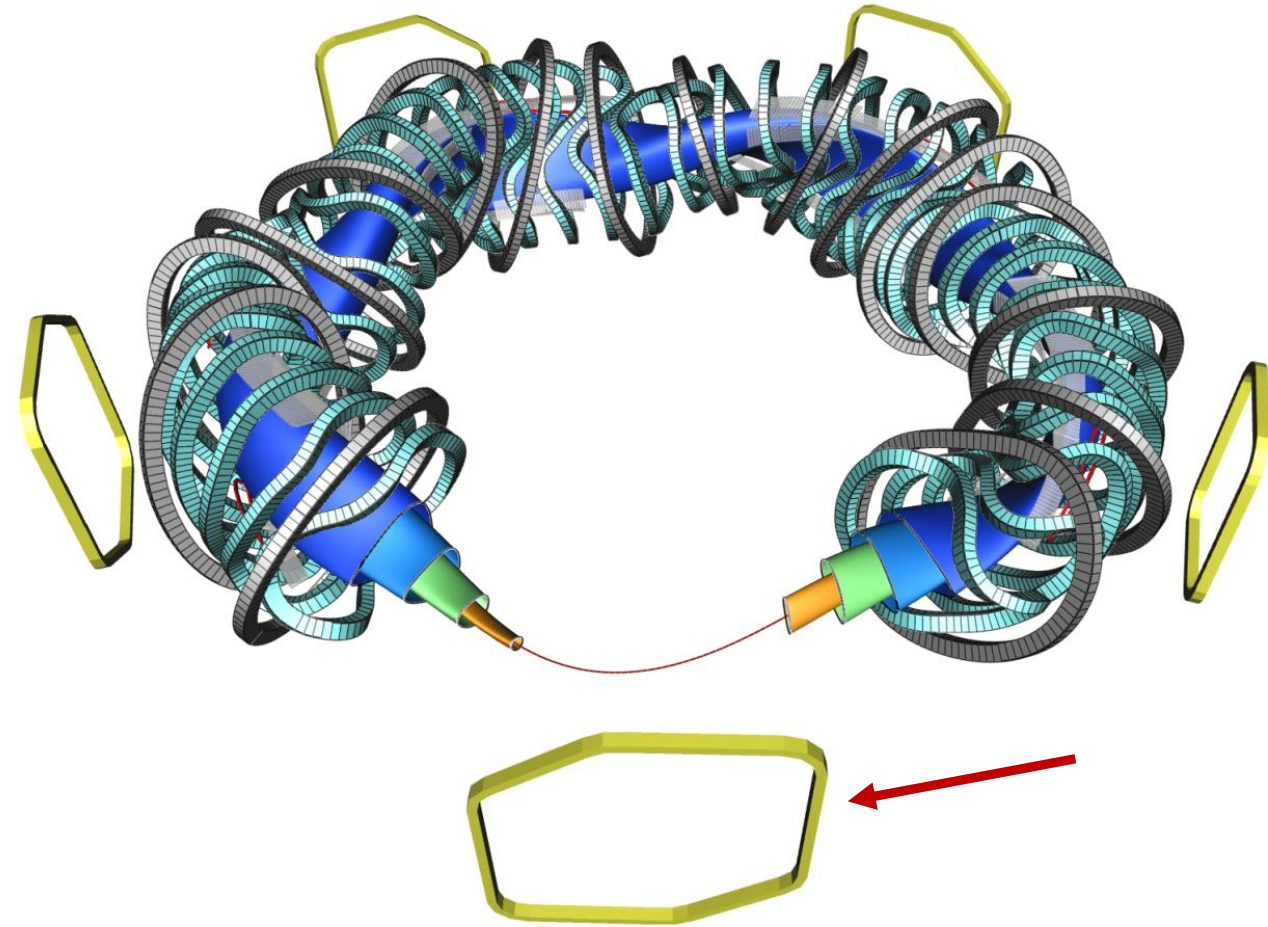
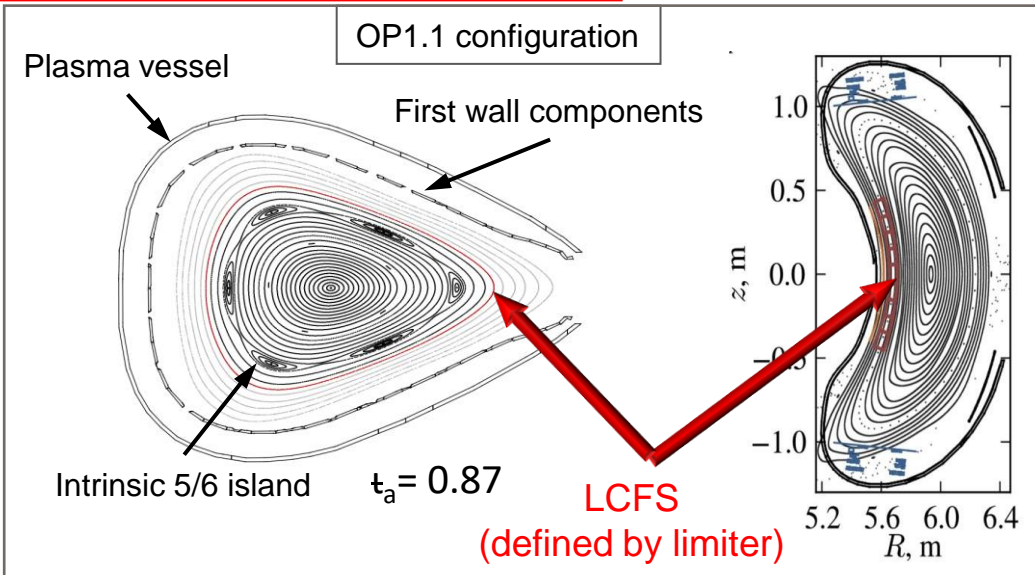
- Main helical field: 50 non-planar coils (18 kA, superconducting)
- Adjusting iota: 20 planar coils (12 kA, superconducting)
- Move island position at divertors: 10 control coils (water cooled)
- Correction of 1/1 field error: 5 trim coils (2 kA, water cooled)



From M. Krychowiak and W7-X team, HTPD 2016

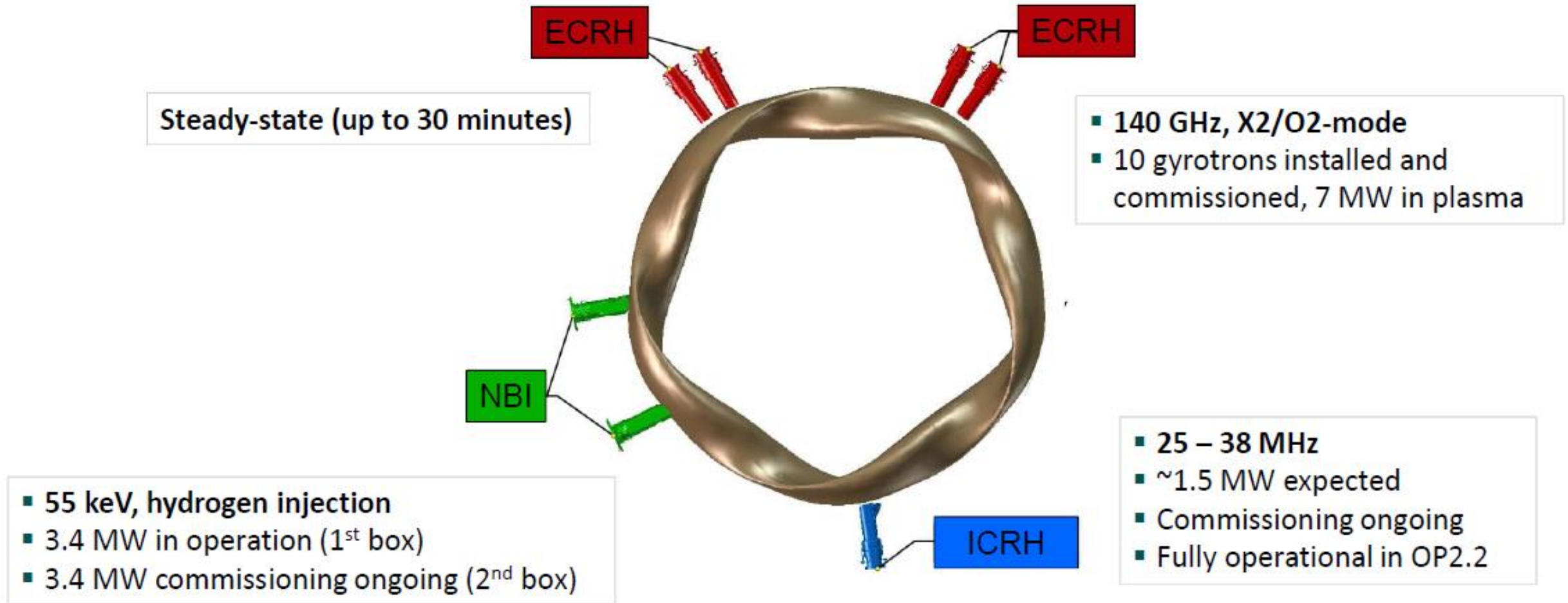
Wendelstein 7-X

- Main helical field: 50 non-planar coils (18 kA, superconducting)
- Adjusting iota: 20 planar coils (12 kA, superconducting)
- Move island position at divertors: 10 control coils (water cooled)
- Correction of 1/1 field error: 5 trim coils (2 kA, water cooled)






From M. Krychowiak and W7-X team, HTPD 2016

Wendelstein 7-X heating systems



Stellarator Wendelstein 7-X

		Energy limit	Heating	Plasma parameters
OP1.1 2015-2016	First W7-X operation, graphite limiter	$P < 4.3$ MW (e.g. 0.8 MW for 5 sec.)	ECRH 6 gyrotrons 5 MW	$t_{\text{pulse}} \sim 1$ s, $P=2.7$ MW $t_E \sim 0.1$ s, $T_e > 4$ keV, $T_i = 2.2$ keV $n_e = 3.5 \times 10^{19}$ m ⁻³ $n_i T_i t_E = 0.08 \times 10^{20}$ keV m ⁻³ s
				
OP1.2 2017-2018	Uncooled graphite divertor (TDU)	$P < 9$ MW ~ 80 MJ (on divertor) (e.g. 8 MW for 10 sec.)	$P_{\text{ECRH}} \sim 8.8$ MW (cw) $P_{\text{NBI}}^H \sim 7$ MW (10s)	$t_{\text{pulse}} \sim 10$ s 26 s @ reduced power $T_e \sim 5$ keV, $T_i \sim 4$ keV $n_e \sim 1.6 \times 10^{20}$ m ⁻³
				
OP2 2022-	Water cooled CFC divertor (HHF), steady-state plasmas	~ 18 GJ (cooling water reservoir) (10 MW for 30 min.)	$P_{\text{ECRH}} \sim 10$ MW (cw) $P_{\text{NBI}}^D \sim 10$ MW (10s) $P_{\text{ICRH}} \sim 4$ MW (2s)	$T_e \sim 5$ keV, $T_i \sim 5$ keV $n_e \sim 2.4 \times 10^{20}$ m ⁻³
				

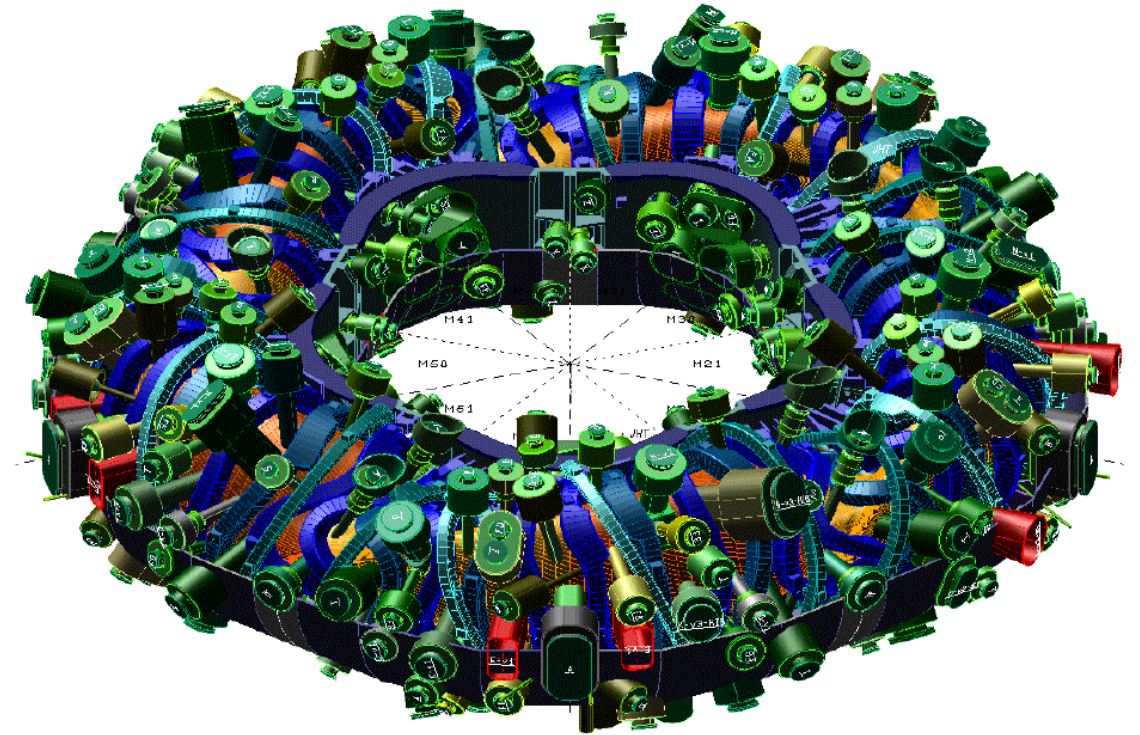
W7-X diagnostics

Impurity control is a very important task in the magnetic confinement fusion.

Because of non axis-symmetric 3D magnetic fields in stellarator, impurity transport in the plasma core is expected to be different in comparison with tokamaks.

Understanding the impurity transport is a one of the key issue for steady-state operation.

At W7-X several diagnostics are dedicated to study this purpose and also impurity injection systems (like gas-puff, laser blow-off, TESPEL or pellet injection) are installed.



Plasma impurities

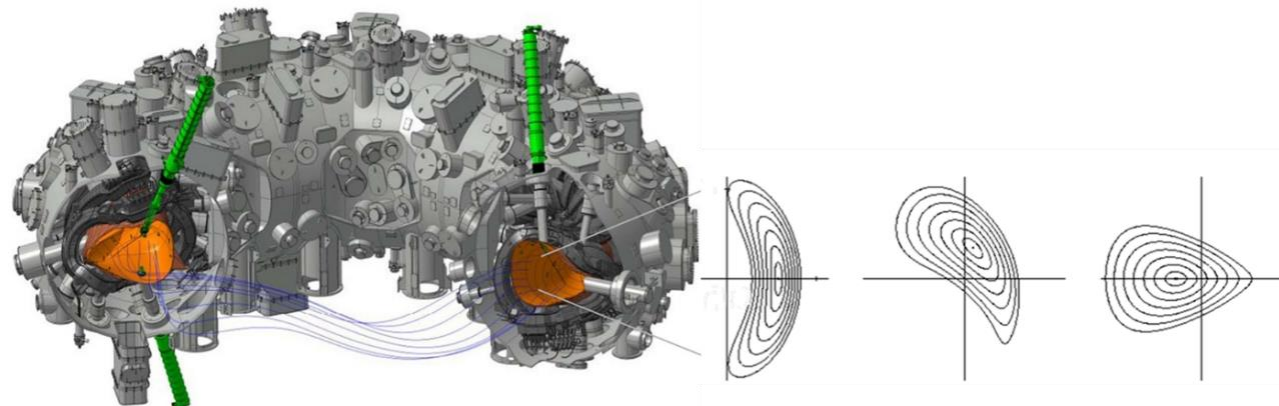
Impurity transport study is important:

- To avoid high Z accumulation scenarios
- For long pulse, steady state experimental programs

From experiment:

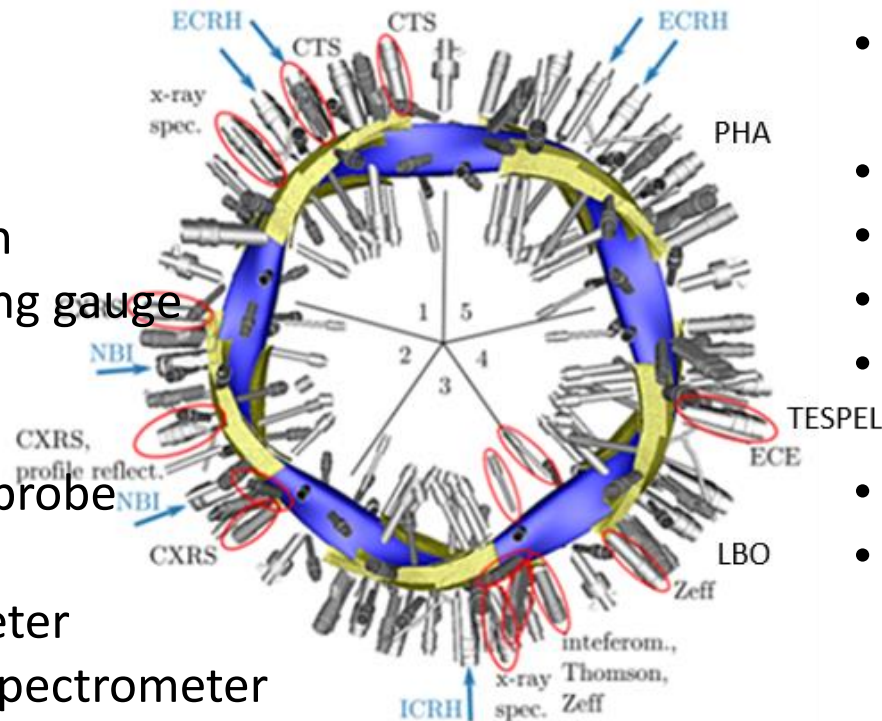
- Monitor temporal **intrinsic** impurity emissivities (identify accumulation or non accumulation scenarios)
- Monitor temporal **injected** impurity emissivities (by gas puff system, laser blow-off, TESPEL)

→ Transport relevant parameters: impurity transport times τ_i ,
radial electric field $E_r(r)$, diffusive $D(r)$ and convective $v(r)$ transport coefficients



W7-X Diagnostics

- Flux surface measurement
- Video diagnostic
- Thomson scattering
- Interferometer
- ECE
- H_{α} and NIR cameras observation
- Neutral gas manometers/Penning gauge
- Helium beam (gas injection)
- Filterscope (several single los)
- Multipurpose fast manipulator probe
- Langmuir probes
- X-ray Imaging Crystal spectrometer
- High Resolution X-ray Imaging Spectrometer
- High Efficiency XUV Overview Spectrometer
- Pulse Height Analysis
- Bolometer

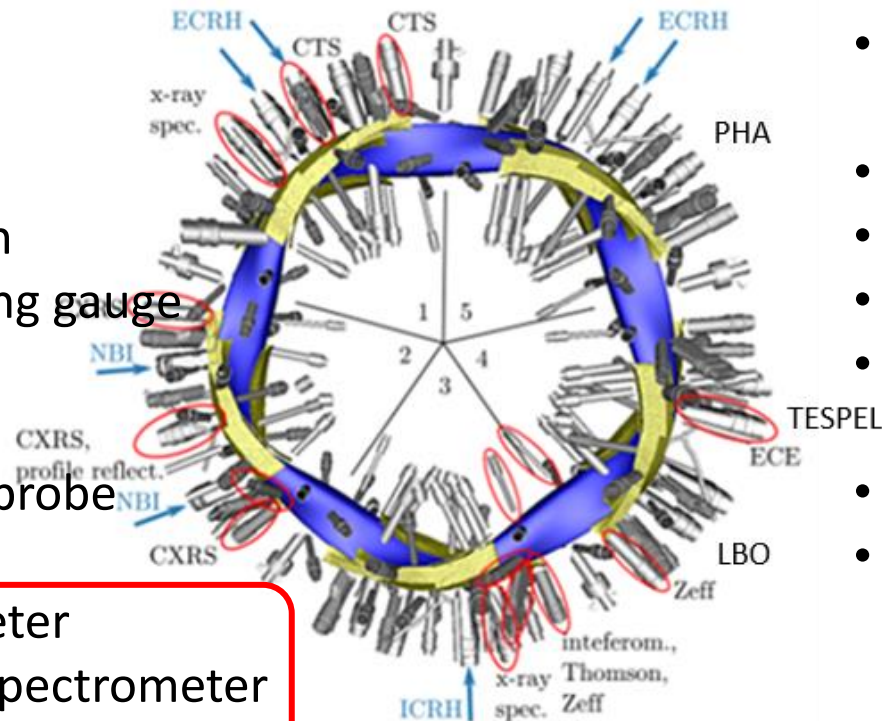


- ECRH sniffer probes
- Neutron counter
- Magnetics (diam. loops, Rogowski/Mirnov coils)
- Reflectometer
- Z_{eff} (single los)
- UV-VIS overview spectrometer
- X-Ray Multi-Camera System (MHD tomography)
- Laser blow-off
-

M. Krychowiak, et al. Rev. Sci. Instr. 87 (2016) 11D304
H. Thomsen, et al. Journal of Instrumentation 10 (2015) P10015

W7-X Diagnostics

- Flux surface measurement
- Video diagnostic
- Thomson scattering
- Interferometer
- ECE
- H_{α} and NIR cameras observation
- Neutral gas manometers/Penning gauge
- Helium beam (gas injection)
- Filterscope (several single los)
- Multipurpose fast manipulator probe
- Langmuir probes
- X-ray Imaging Crystal spectrometer
- High Resolution X-ray Imaging Spectrometer
- High Efficiency XUV Overview Spectrometer
- Pulse Height Analysis
- Bolometer



- ECRH sniffer probes
- Neutron counter
- Magnetics (diam. loops, Rogowski/Mirnov coils)
- Reflectometer
- Z_{eff} (single los)
- UV-VIS overview spectrometer
- X-Ray Multi-Camera System (MHD tomography)
- Laser blow-off
-

PHA detectors

PNDetector

1st and 2nd energy channels

SDD-10-130 BeW ic

10.0 mm² x 450 μm
round design
polysilicon technology

round TO8 housing
outer diameter 15 mm
Ø 3.2 mm Zr collimator
1-stage peltier cooler
8 μm Beryllium window

typ. 132 eV FWHM
@ MnK, -20°C, 10 kcps
typ. 133 eV FWHM
@ MnK, -20°C, 100 kcps
P/B typ. 2,500 @ MnK

bestseller



- for medium- and high-Z impurity observation

3rd energy channel

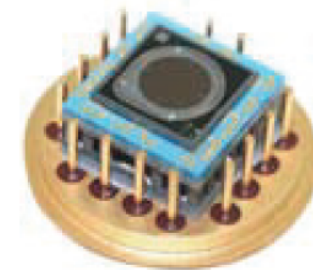
SD3-10-128pnW UTW ic

10.0 mm² x 450 μm
droplet design
polysilicon technology
pnWindow

round TO8 housing
outer diameter 15 mm
Ø 3.1 mm Zr collimator
1-stage peltier cooler
thin polymere window
non-magnetic cap

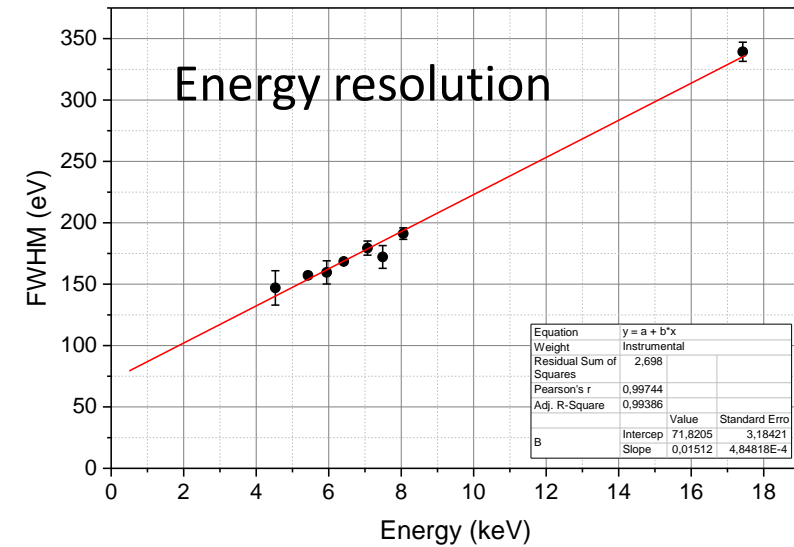
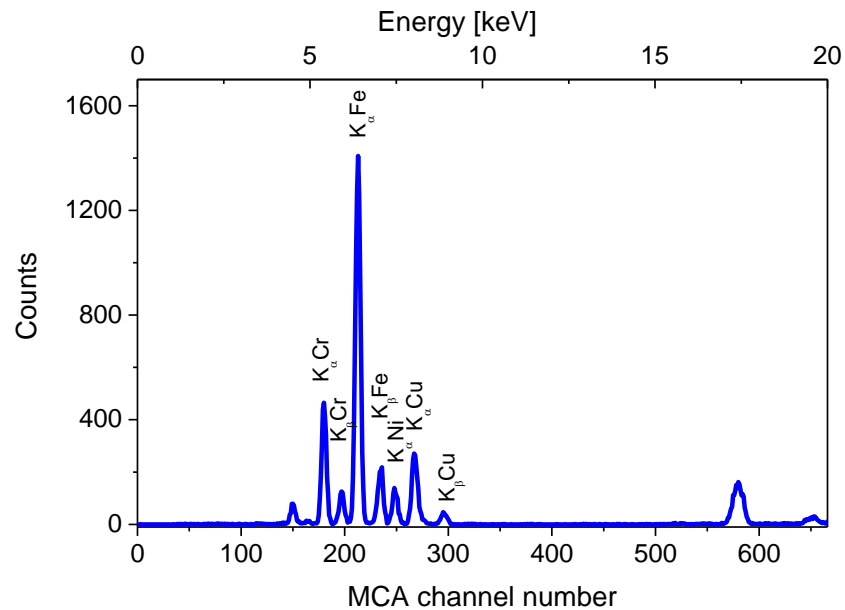
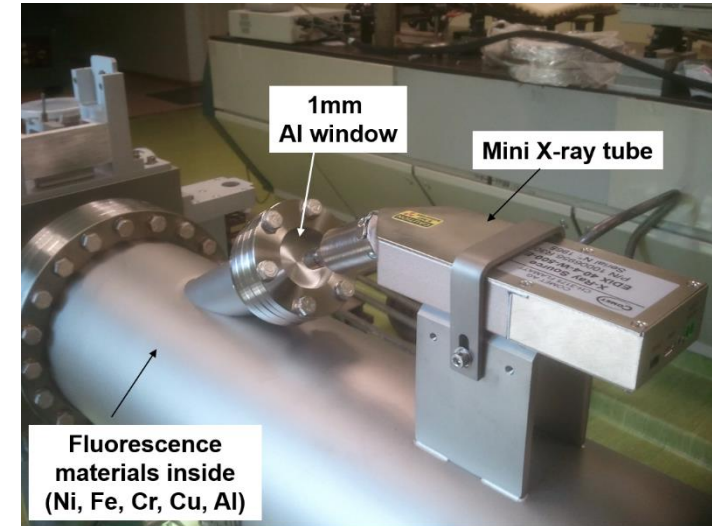
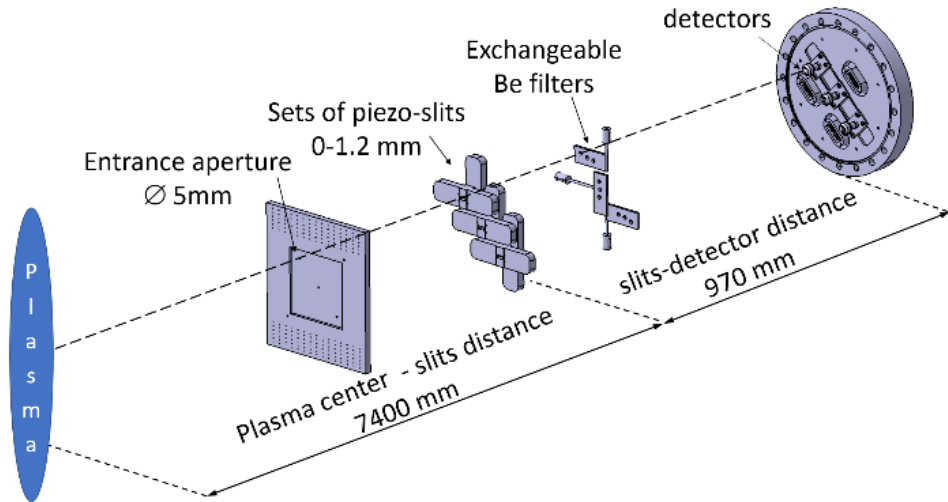
typ. 127 eV FWHM
@ MnK, -20°C, 10 kcps
typ. 129 eV FWHM
@ MnK, -20°C, 100 kcps
typ. 48 eV FWHM
@ C_K and B_K, -20°C, 10 kcps
P/B typ. 15,000 @ MnK

bestseller



- for light impurity observation

PHA system



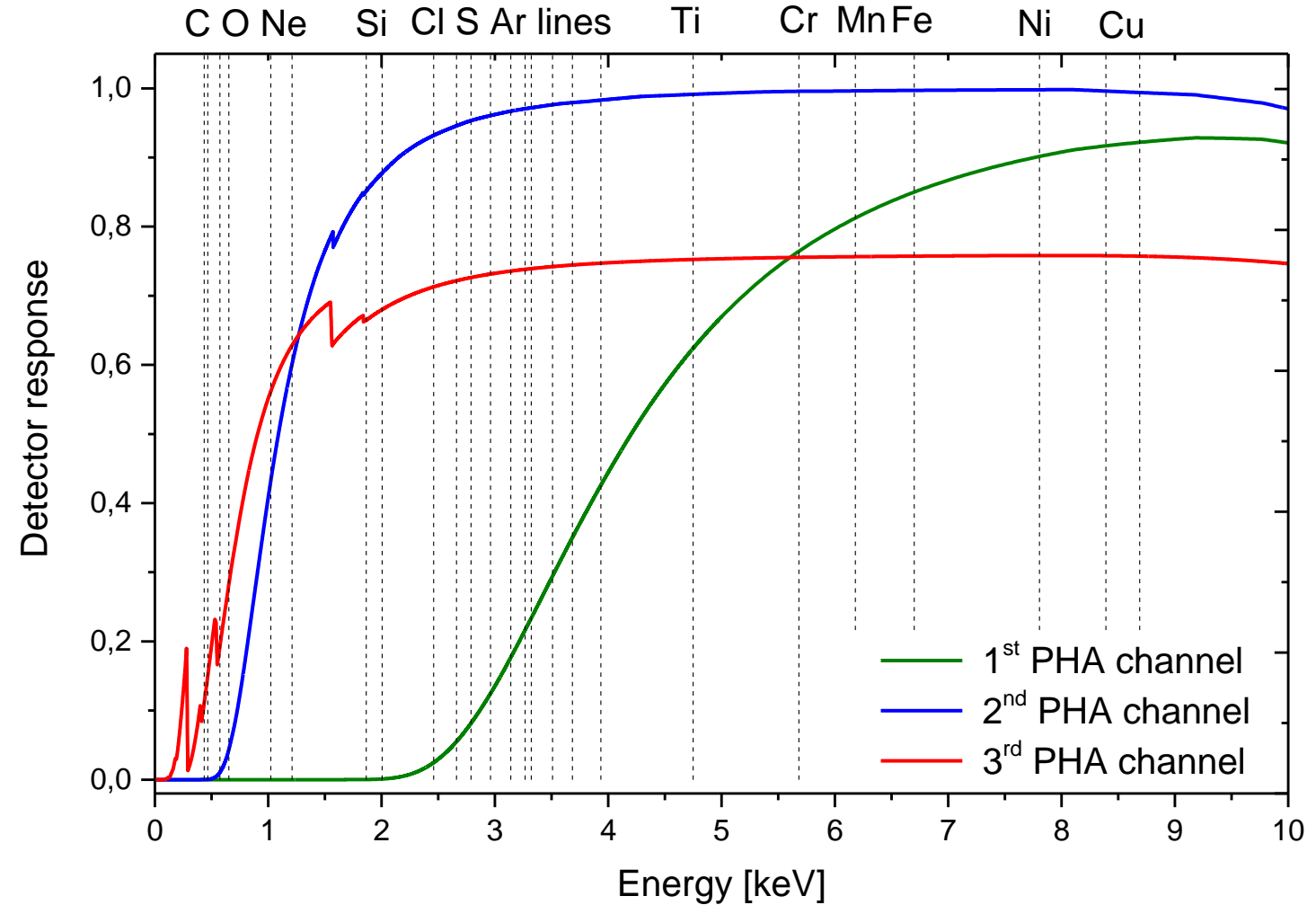
PHA system

- Consists of 3 channels:

1st (SDD (8+500) μm Be): 1.55–19.60 keV,

2nd (SDD 8 μm Be) 0.96–19.60 keV,

3rd (SD3 Polymer window) 0.6–19.60 keV,
assuming 1/e transmission



First Hydrogen Plasma in W7-X, OP1.1

3.2.2016, 15:21:25.822 (local time)

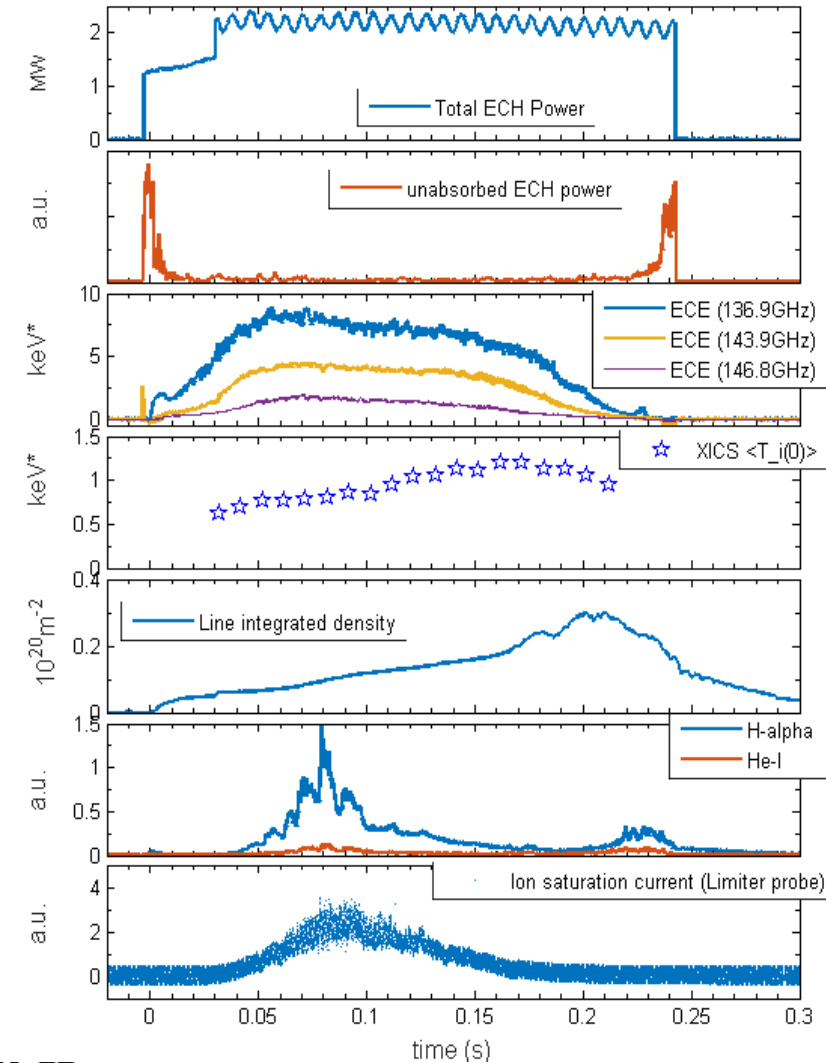


First hydrogen plasma in Wendelstein 7-X

- total heating power ECRH: ~ **2 MW**
- pulse lengths: ~ **250 ms**
- $T_e \sim 7 \text{ keV}$, $T_i \sim 1.2 \text{ keV}$
- $\langle n \rangle \sim 2 \times 10^{19} \text{ m}^{-3}$
- $a < 49 \text{ cm}$ ($V \sim 26 \text{ m}^3$)

... 60 s later

W7X Program 20160203.006 (UTC: Wed 03.02.2016 14:22:25.822)



Observation of plasma impurities during OP1.2

Commissioning and operation of the LBO (laser blow-off) and TESPEL (tracer-encapsulated solid pellet) systems.

Diagnostics are dedicated for impurity transport studies.

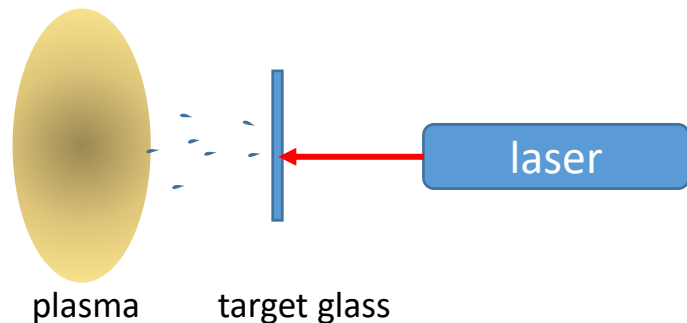
LBO

Deposition in the edge

Th. Wegner et al., RSI 89 (7) 2018

Deposited materials:

Al, C, B, Fe, Mo, Si, Ni, Ti, W



TESPEL

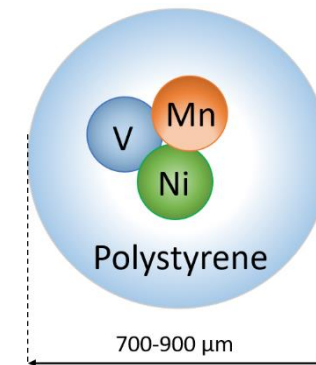
Deposition in the core

R. Bussiahn et al., RSI 89 (10K112) 2018

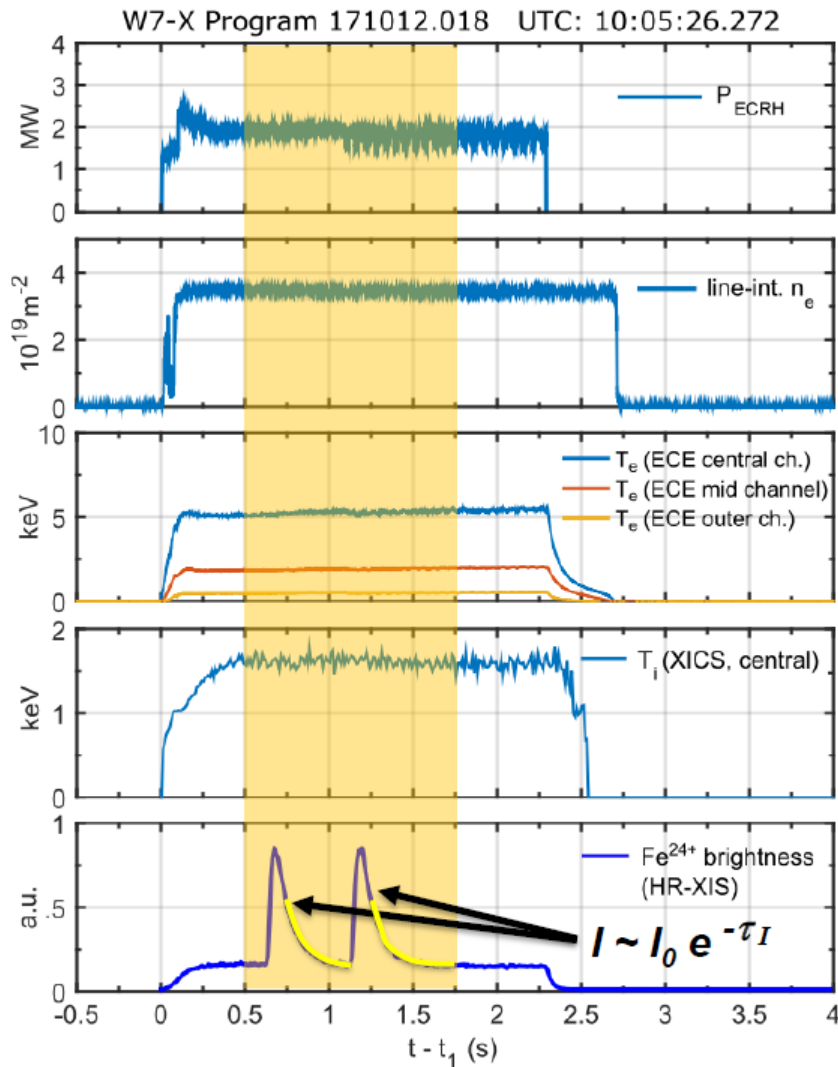
S. Sudo et al., Nuc. Fus. 52 (2012) 063012

Deposited materials:

Al, Si, Ti, V, Mn, Fe, Ni, Cu, Mo, W



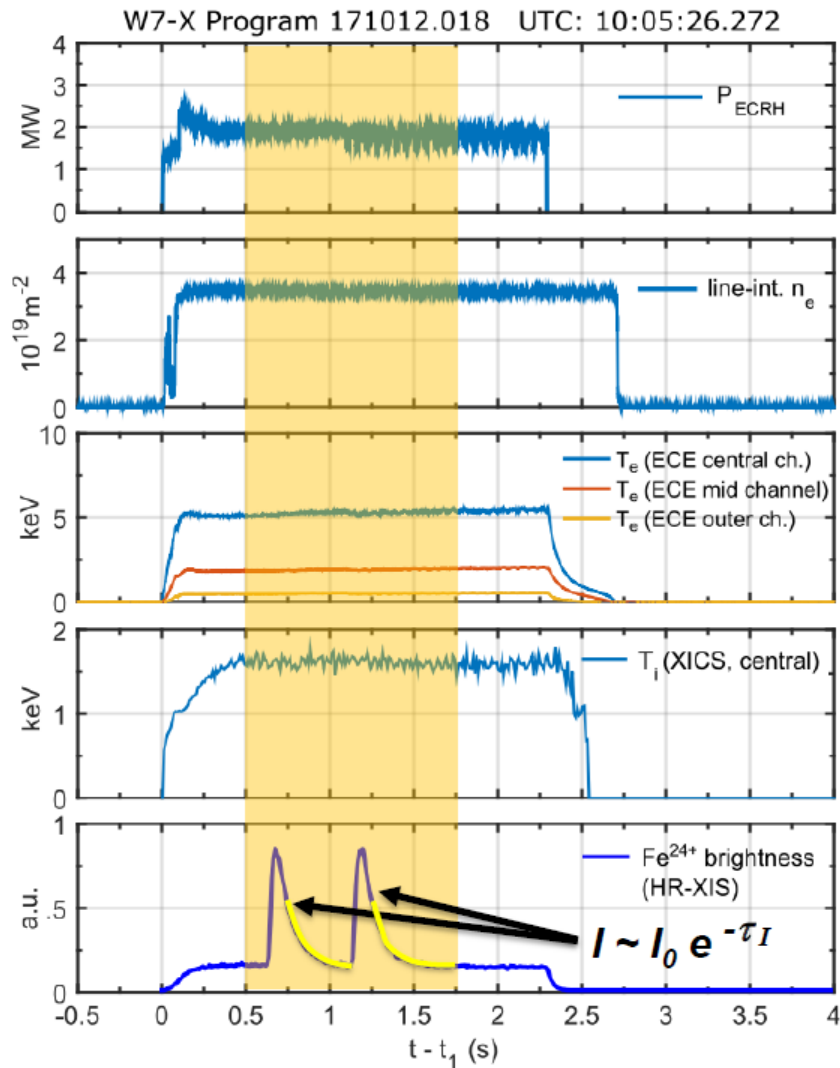
Measurement of Impurity Transport Times - XICS



Prerequisites:

- Stationary plasma conditions
 - (signal $\sim n_e$ and T_e)
- Pulsed injection of non recycling impurities, e.g. Fe
- Fit of exponential signal:
 - Ionization equilibrium

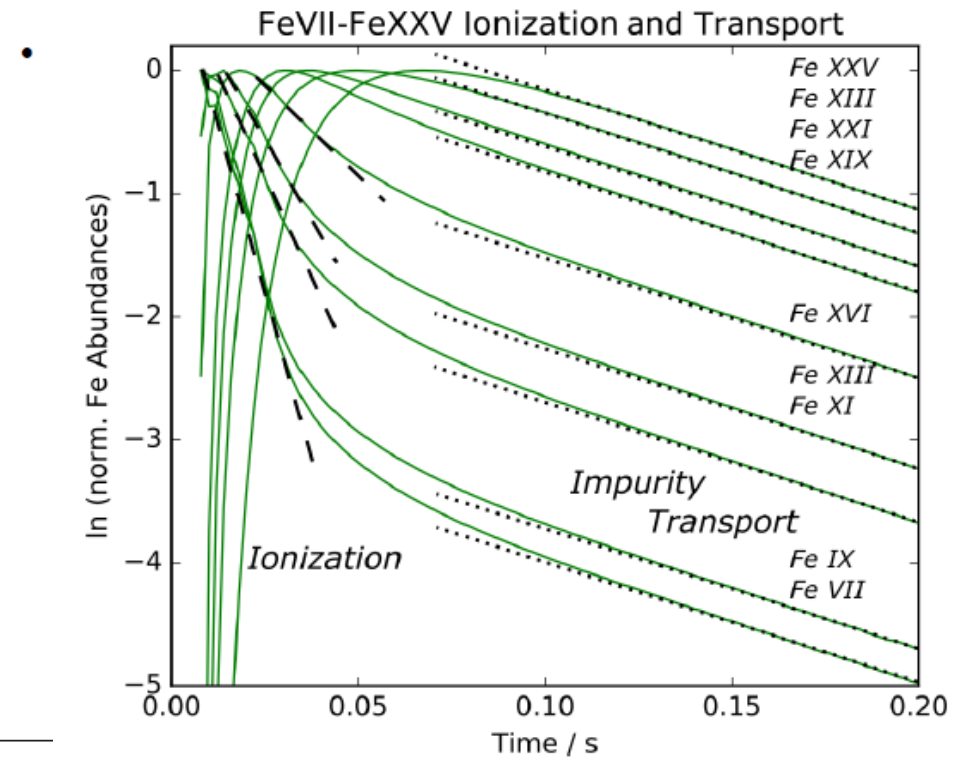
Measurement of Impurity Transport Times - XICS



A. Langenberg

Prerequisites:

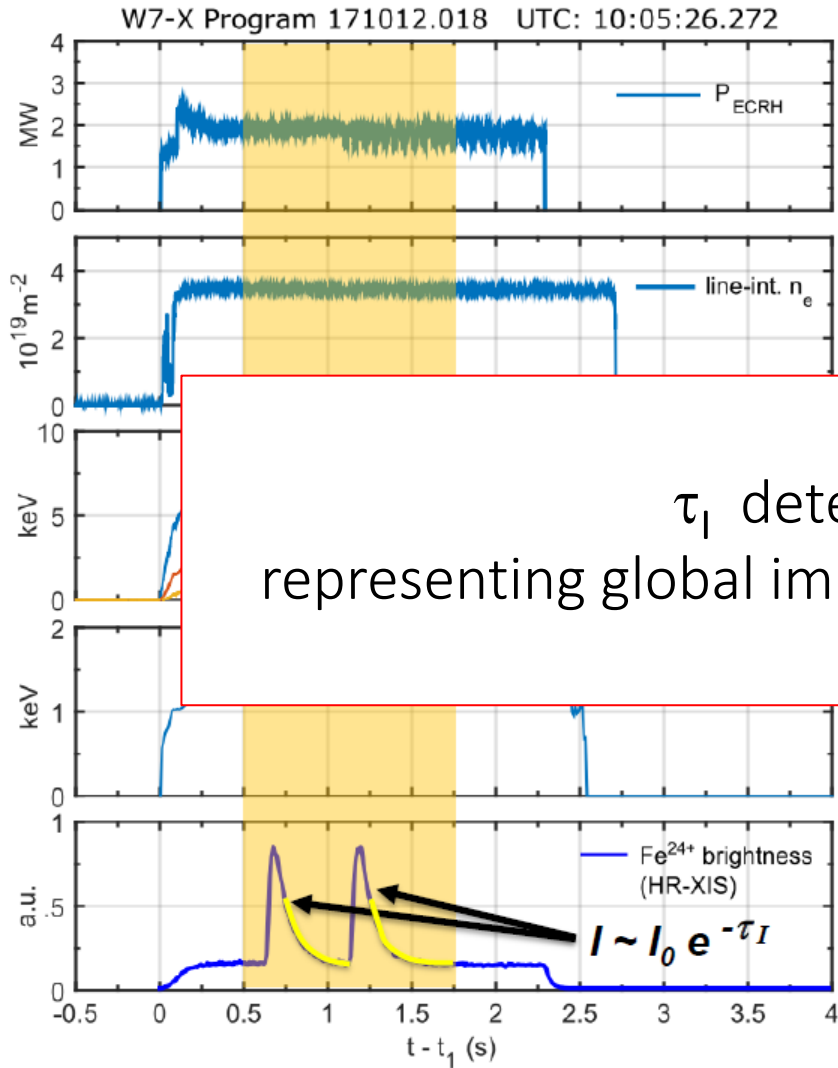
- Stationary plasma conditions
 - (signal $\sim n_e$ and T_e)
- Pulsed injection of non recycling impurities, e.g. Fe



EPS 2018, Prague



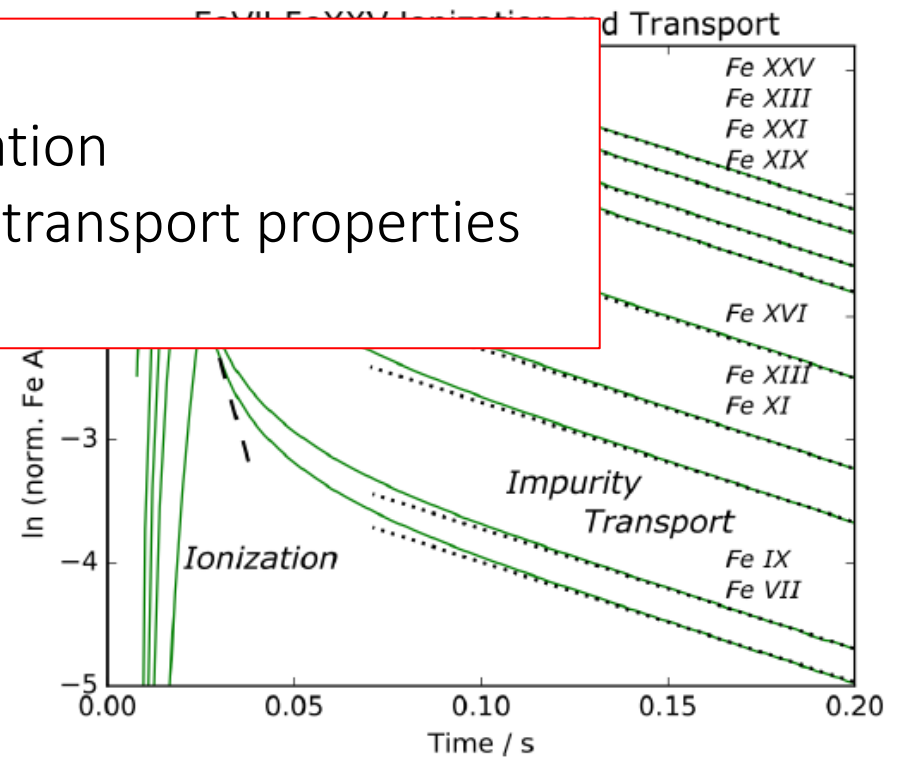
Measurement of Impurity Transport Times - XICS



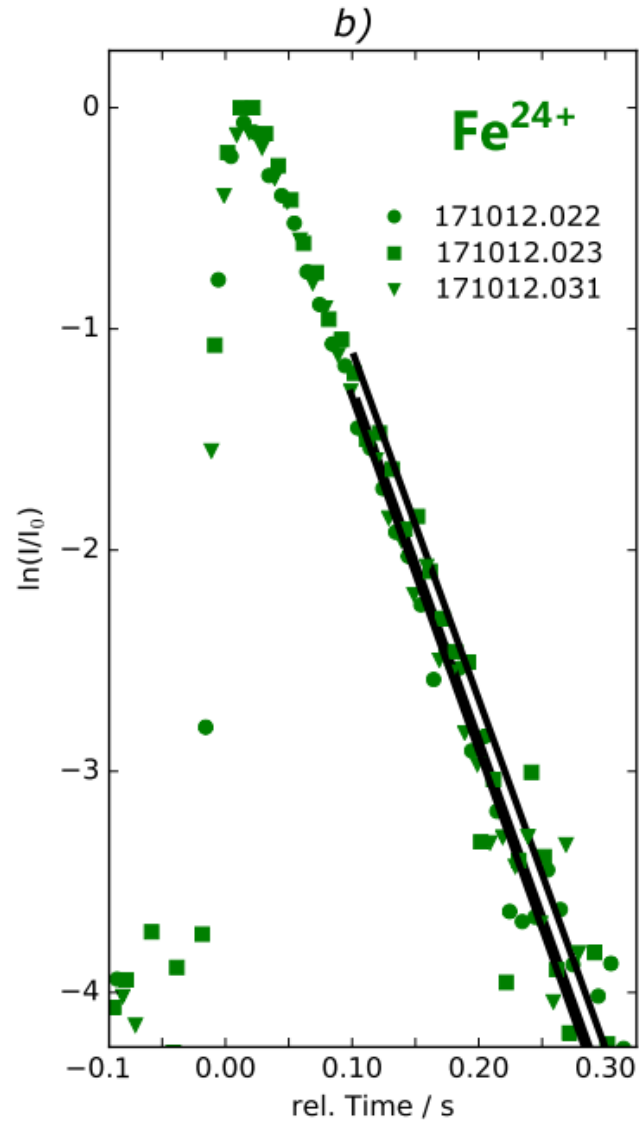
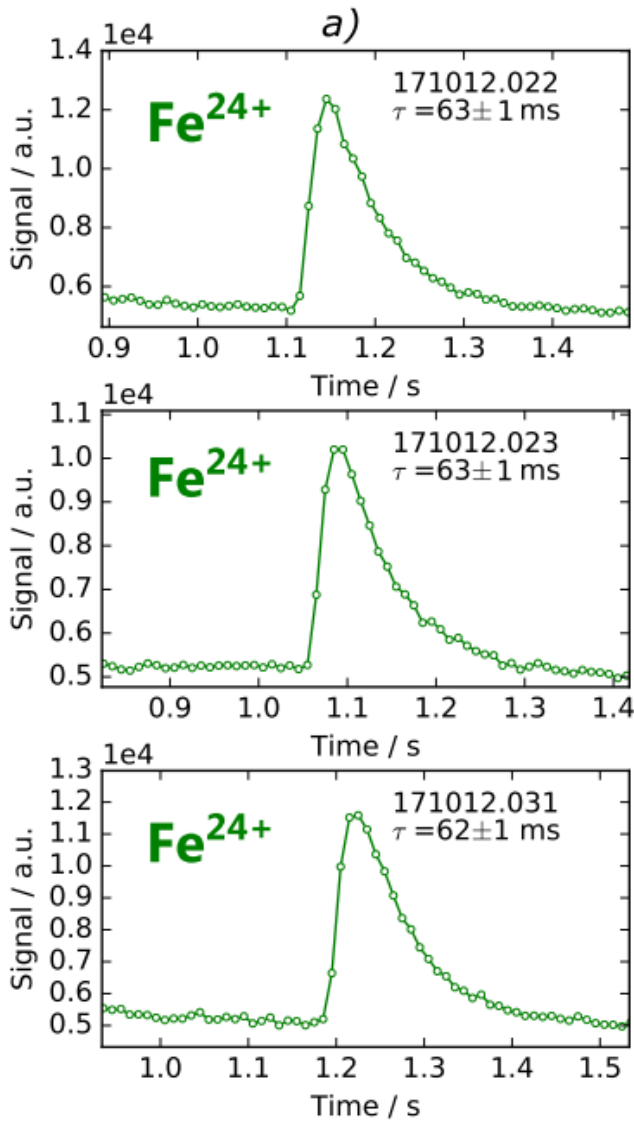
Prerequisites:

- Stationary plasma conditions
 - (signal $\sim n_e$ and T_e)
- Pulsed injection of non recycling impurities, e.g. Fe

τ_I determination
representing global impurity transport properties

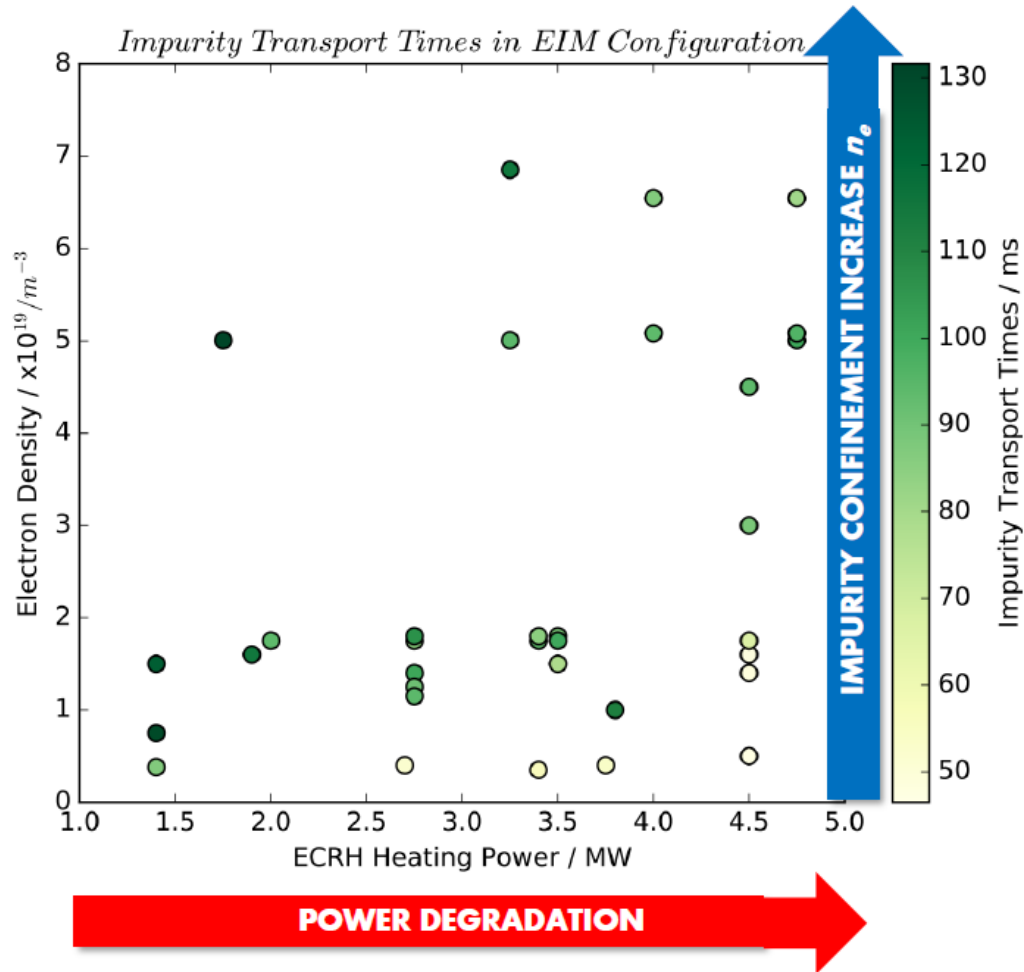


Measurement of Impurity Transport Times - XICS



- double Fe injections from LBO into stationary phase of He plasmas
- $T_e(0) = 4.3$ keV, $n_e(0) = 1.5 \times 10^{-19}$ cm⁻³
- accurate and reproducible determination of impurity confinement times t : $\Delta t = \pm 1$ ms

Measurement of Impurity Transport Times - XICS



- Impurity confinement times show a clear n_e and P_{ECRH} dependence
- similarly observed in other experiments

$$\tau_I \propto \gamma \cdot P_{ECRH}^{\alpha} \cdot n_e^{\beta}$$

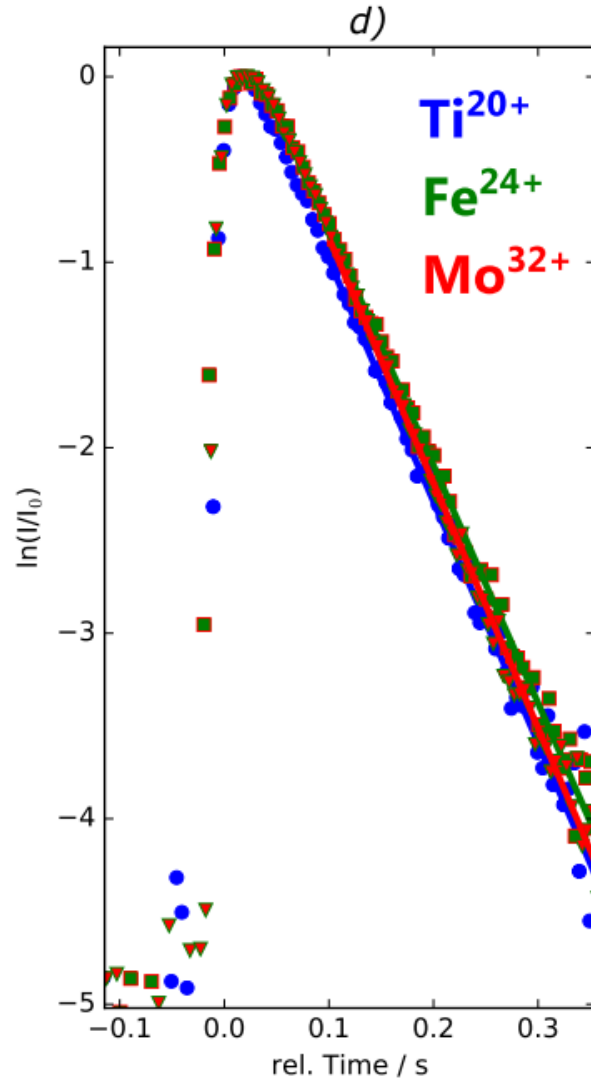
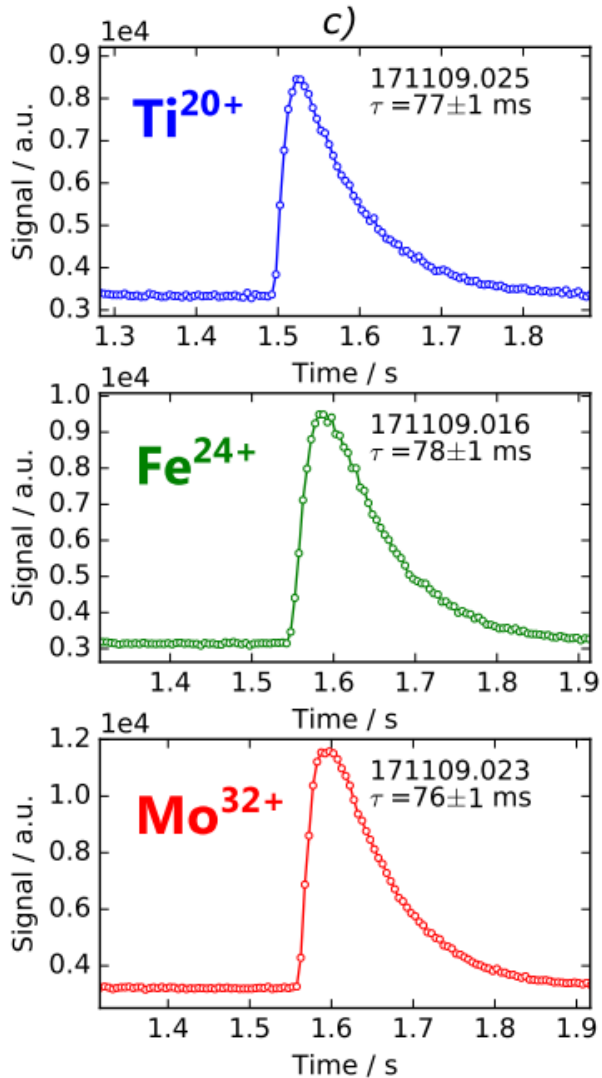
τ_I scaling parameters	EIM
α	-0.49 ± 0.07
β	0.19 ± 0.03
γ	140 ± 10
CoD	0.66

R. Burhenn, Y. Feng, K. Ida et al. *Nuclear Fusion* **49** 065005 (2009)

A. Langenberg et al. EPS 2018

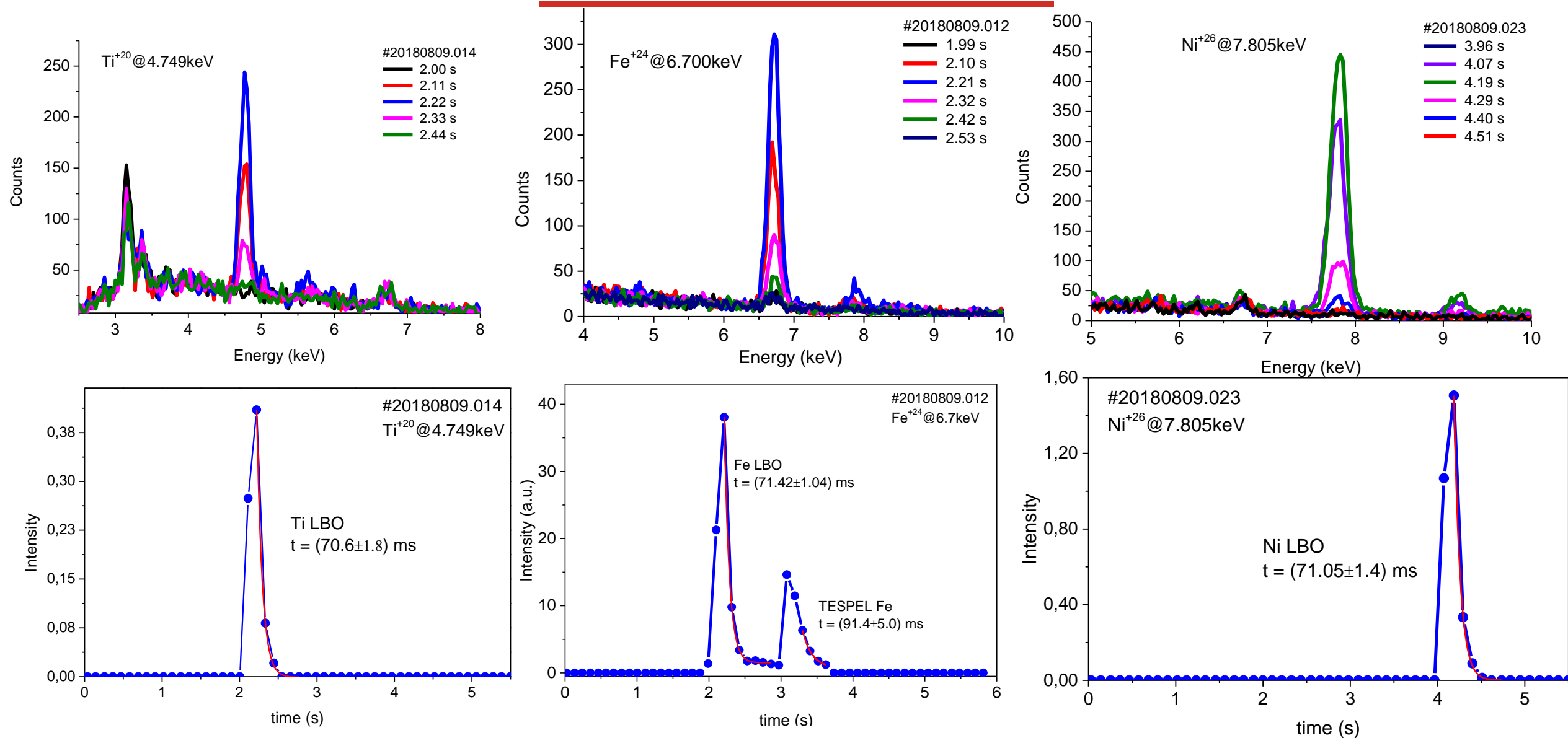
Measurement of Impurity Transport Times - XICS

Z dependance

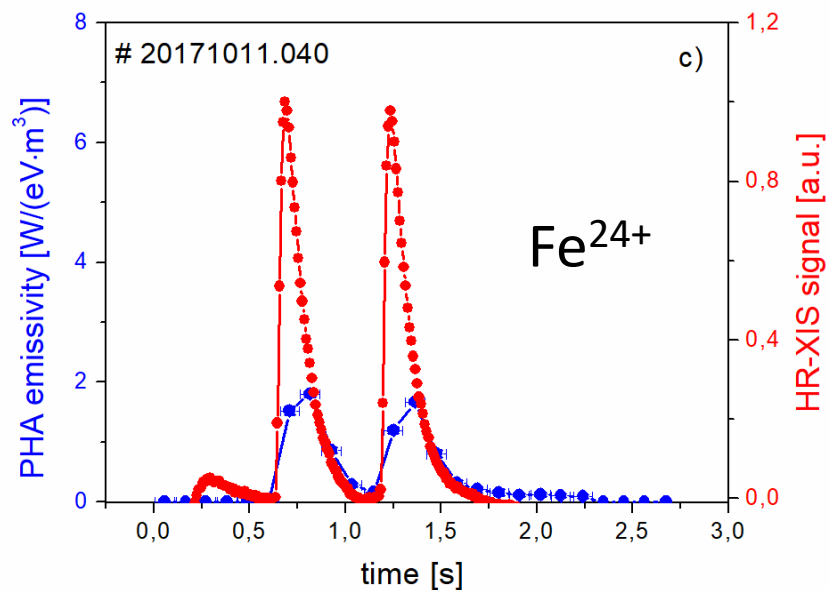
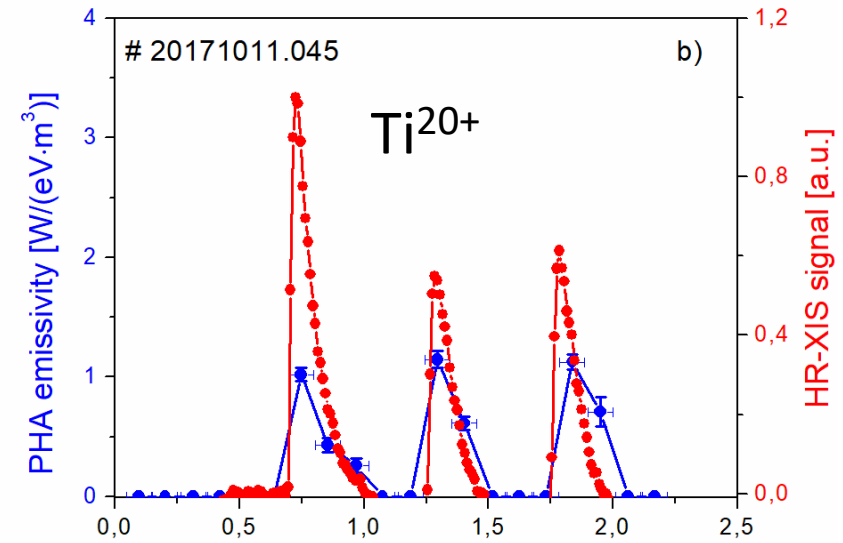
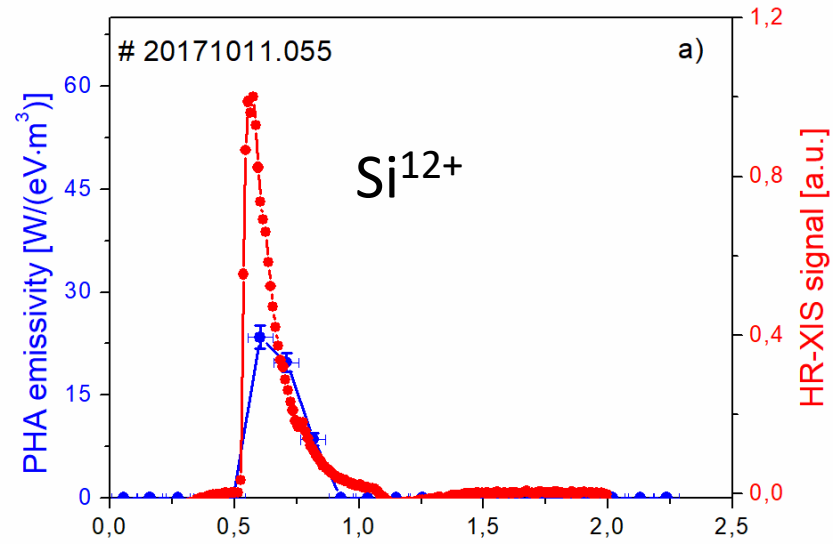


- transport study varying Z within identical plasma scenarios in He
- $T_e(0) = 5.0$ keV, $n_e(0) = 8.5 \times 10^{-19}$ cm $^{-3}$
- similar confinement times for Ti^{20+} , Fe^{24+} , and Mo^{32+} impurities $t = 77 \pm 1$ ms
- no clear Z dependance observed

Measurement of Impurity Transport Times - PHA



Measurement of Impurity Transport Times – XICS & PHA



Comparison of time traces of Si XIII (a), Ti XXI (b) and Fe XXV (c) lines during the laser blow-off injection.

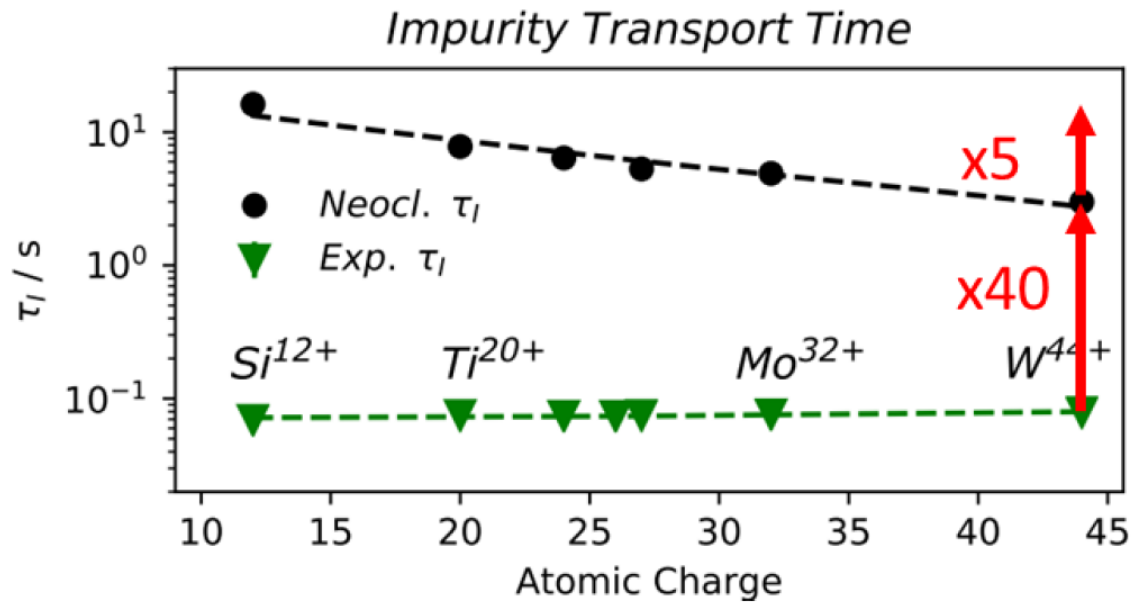
—●— corresponds to PHA signal and

—●— corresponds to HR-XIS signal

Measurement of Impurity Transport Times

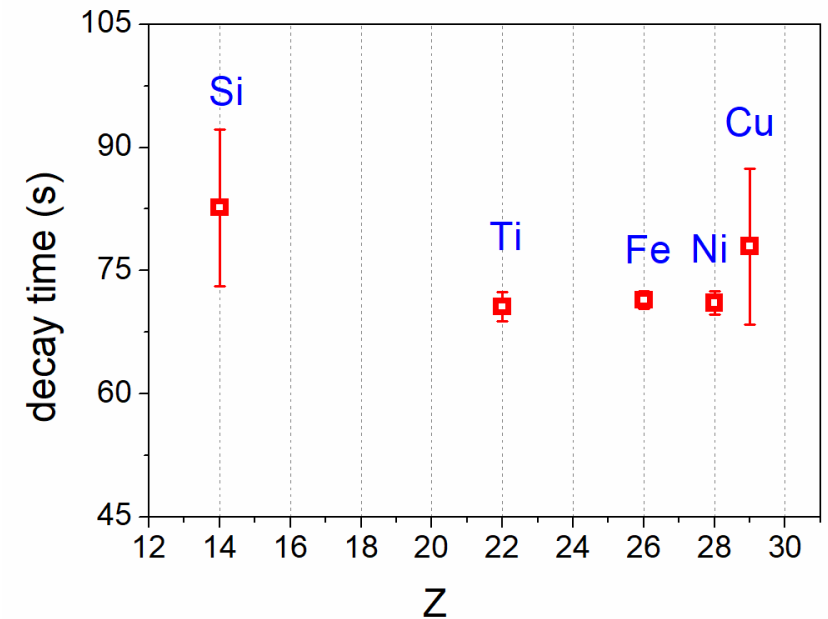
Turbulent impurity transport compared to neoclassics (collisional transport)

From XICS



A. Langenberg et al., PoP27 (2020)

From PHA

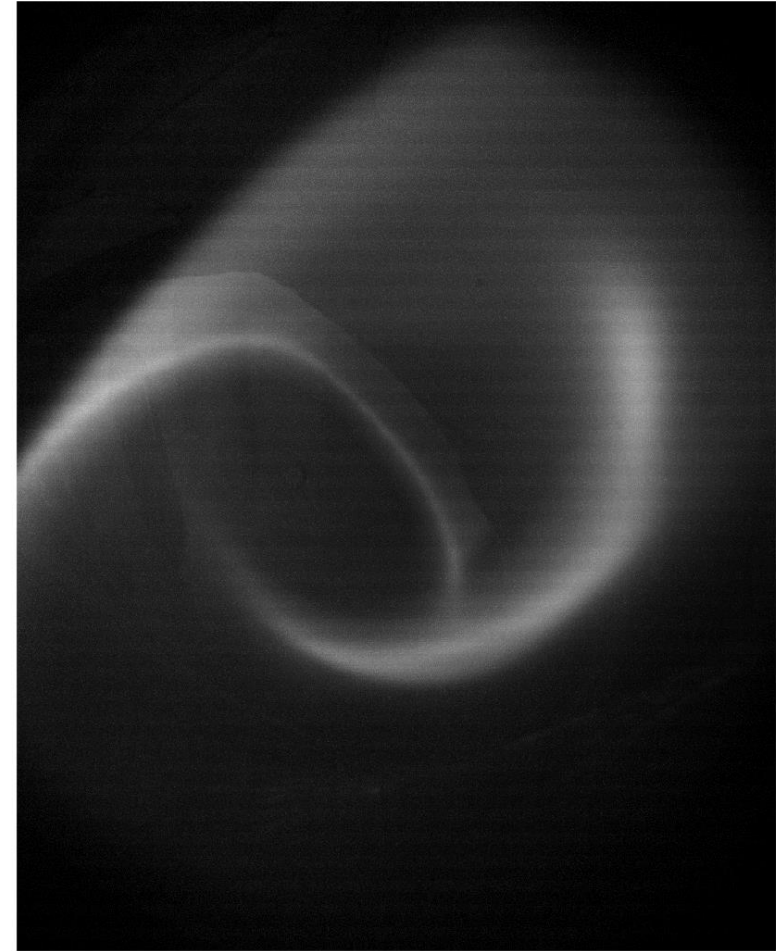
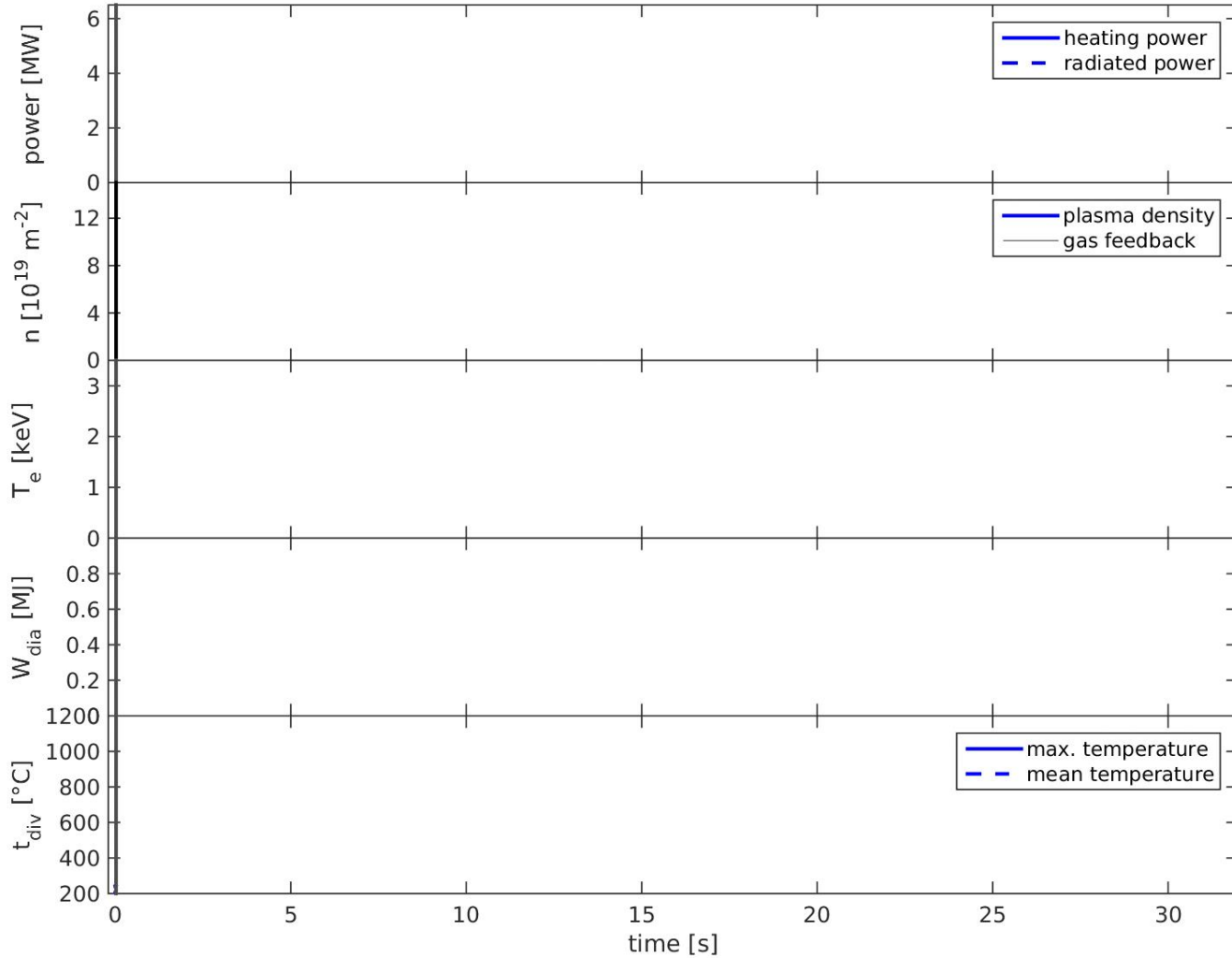


M. Kubkowska et al 2020 JINST 15 C01019

weak Z and M dependence of the transport time as expected from theory for turbulent diffusion.
Simulations done by STHRAL code.

[P. Helander et al., PPCF 60 (2018)]

ECRH plasma with detached divertor from OP1.2



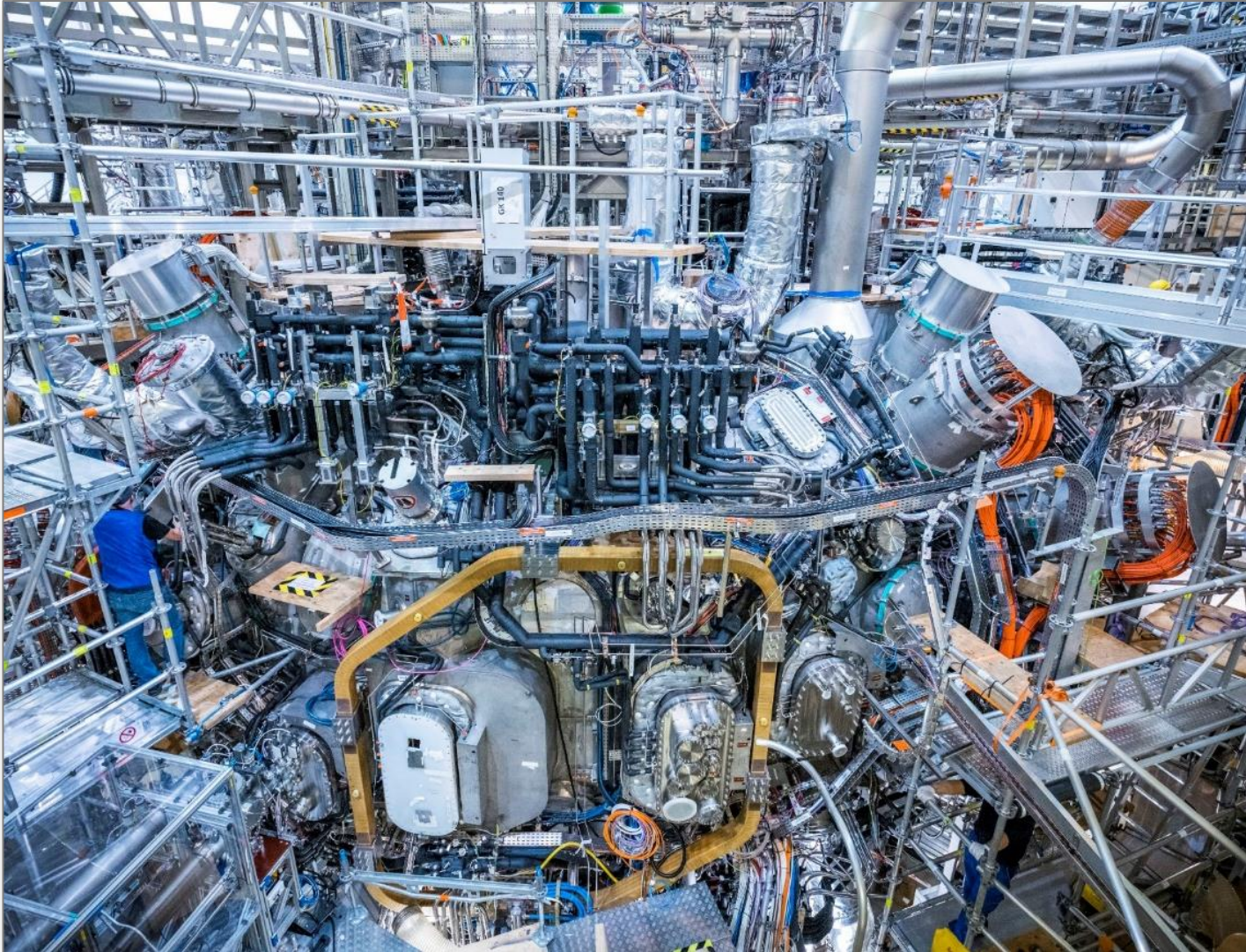
Current W7-X experimental campaign OP2.1

OP1.2b finished in October 2018

3 years break for preparation to OP2.1

– campaign with actively cooled CFC divertor

Preparation to OP2.1



- pressure water cooling circuits
- cryo supply system for cryo pumps
- second cryo valve box

- second NBI box 3.5 MW
- new ICRH heating system 1.5 MW
- development 1.5 MW gyrotron
- aim > 20 MW heating power

- total 70 diagnostic systems
- 50 diagnostics revamped/extended

Wendelstein 7.X completed with
in total 1.3 million assembly hours

Preparation to OP2.1



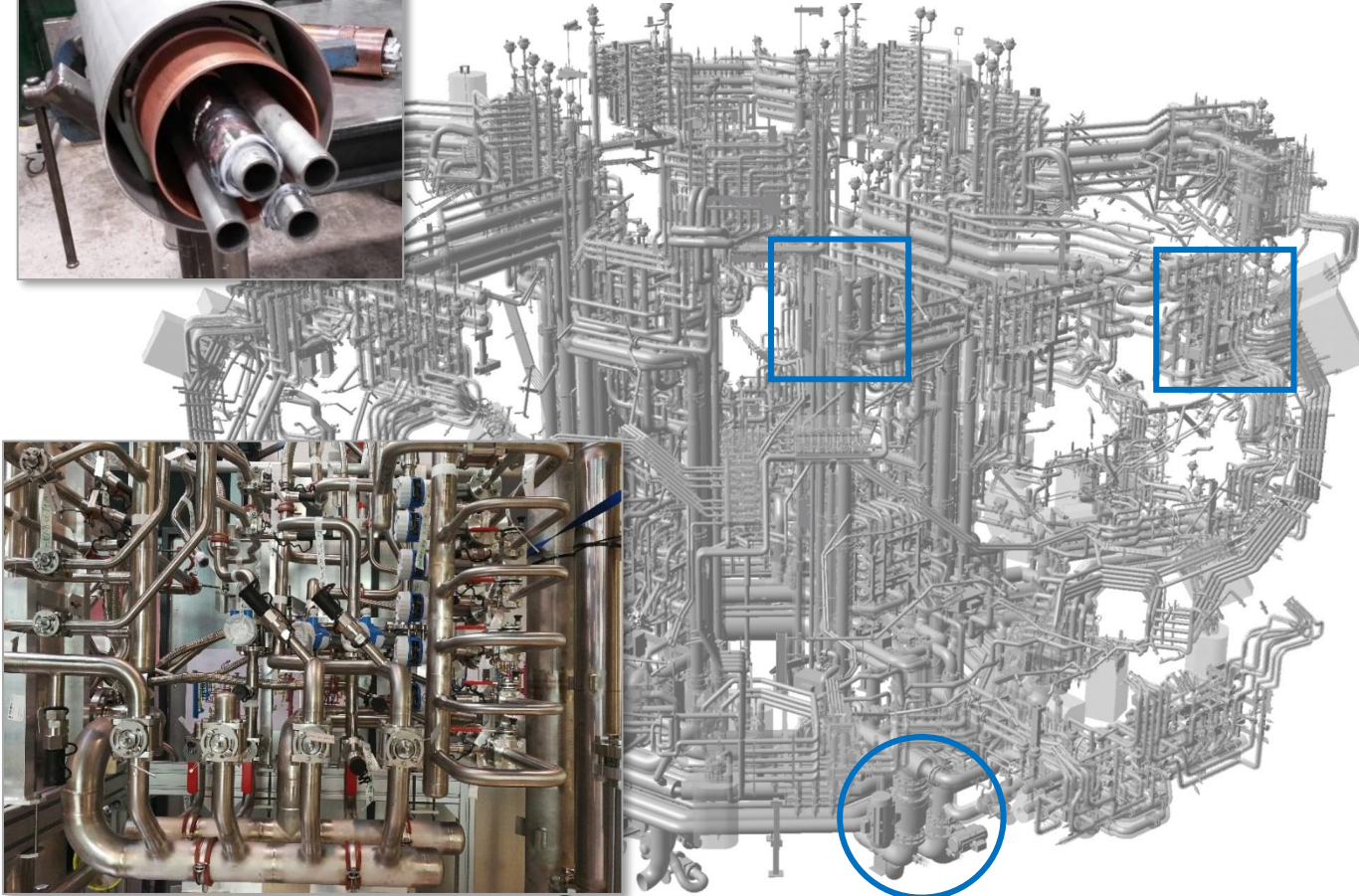
- 10 CFC island divertor modules
- 60 pumping gap panels
- 10 divertor cryo pumps
- 580 cooling circuits in-vessel
 - 6.800 m pipework
 - 1.500 screw joints
 - 450 welds
- 80 actively cooled port liners
- 4.500 redesigned graphite tiles
- 430 thermocouples + wiring
- actively cooled in-vessel diagnostics
- infrared wall monitoring system

Preparation to OP2.1

Water cooling and cryo pipe work



10 cryo supply lines

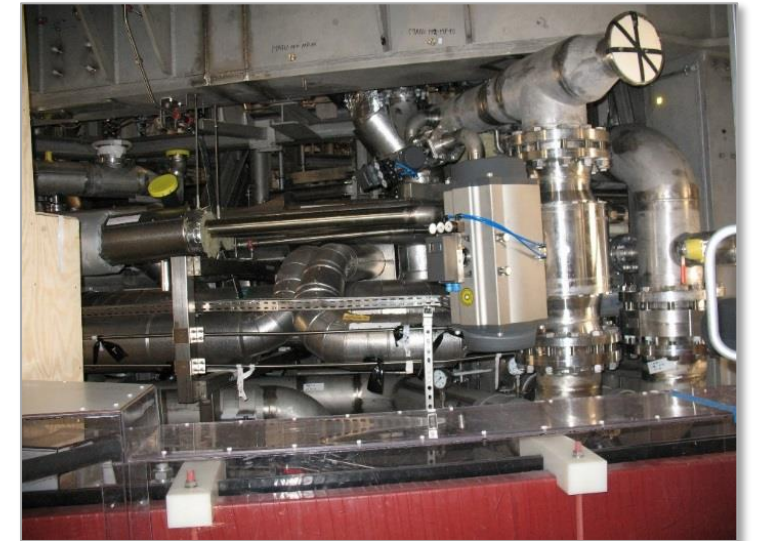


40 manifold-units

5 main divertor feedings

Complicated structure due to ...

- about 500 openings and ports
- avoid collisions with diagnostics
- general lack of space



pipework accuracy +/-5 mm

Commissioning from Jan 2022 onwards

Routine commissioning steps

- safety system validation according to DIN/ISO 16511
- cryostat and plasma vessel pump-down (few minor leaks in the cryostat)
- cool-down (3 weeks)
- magnet system testing
- plasma vessel bakeout (2 weeks in two steps 80°C and 150°C) and glow discharge cleaning

New commissioning steps

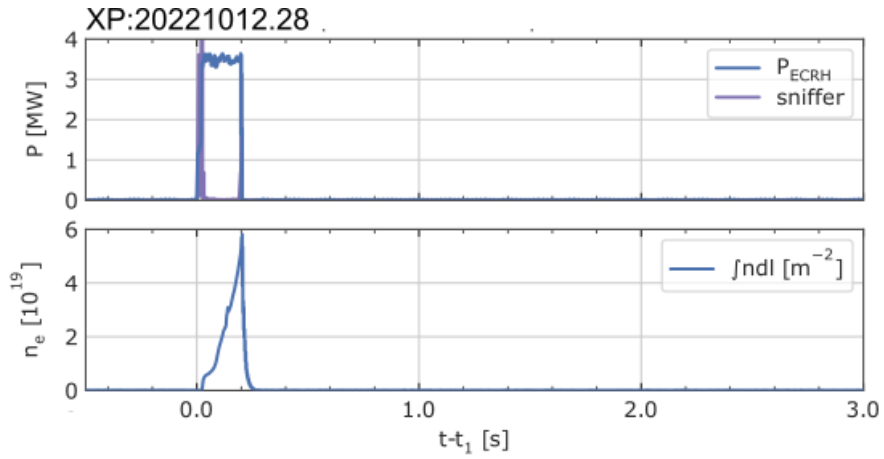
- water cooling circuit overpressure leak tests
- cooling water circuits filling and hydraulic balancing (3 months)
- cryo pump commissioning and integrated cryo operation

Plasma operation

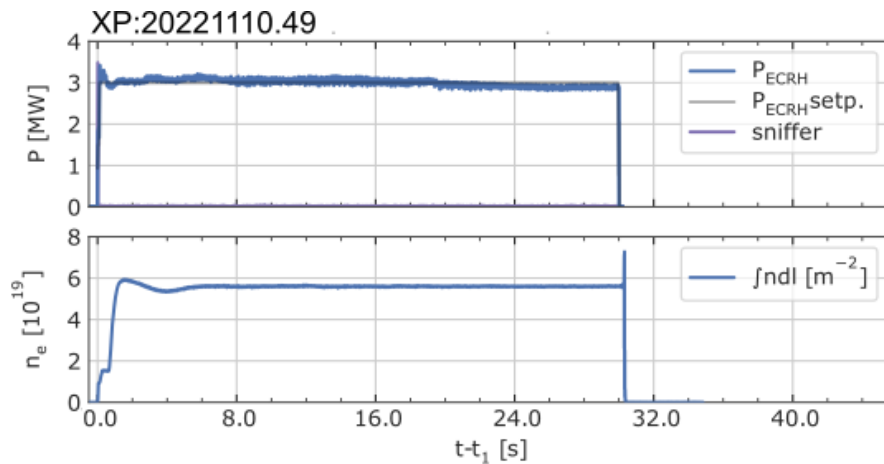
- first plasma operation Sept 28, 2022
- science program since Nov 22, 2022

OP2.1 starts

He plasma dominated by impurities/radiation



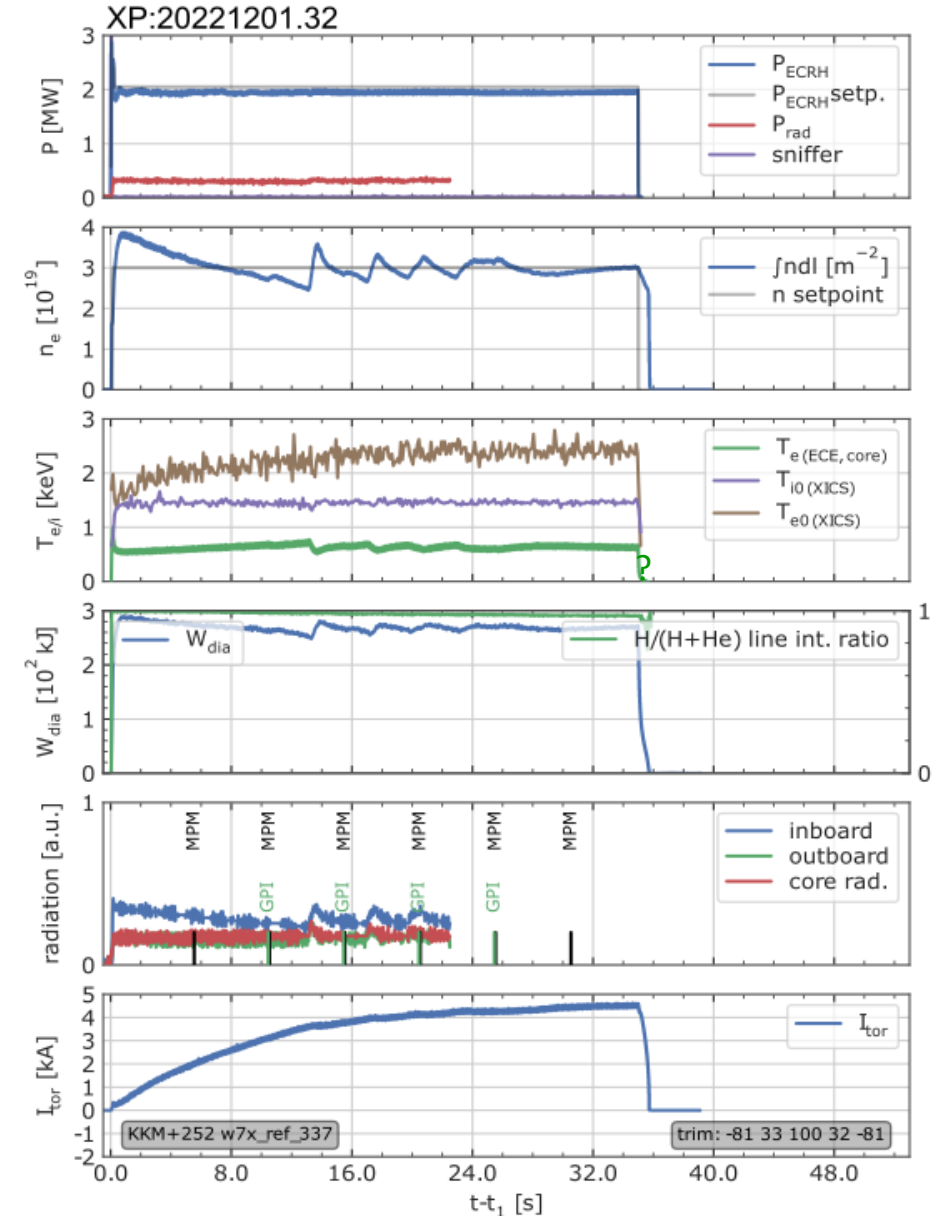
He plasma after intense wall cleaning



boronization

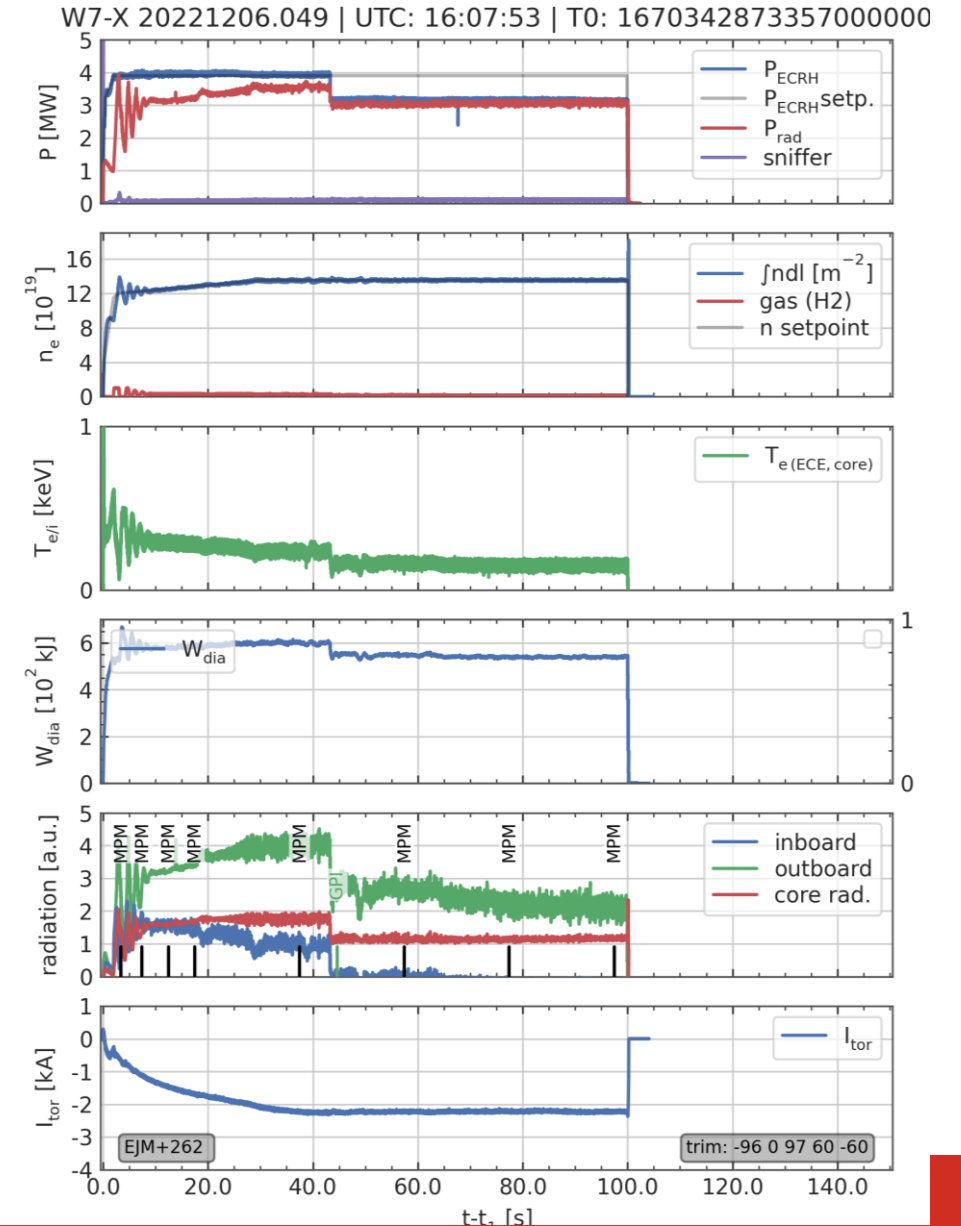


H plasmas



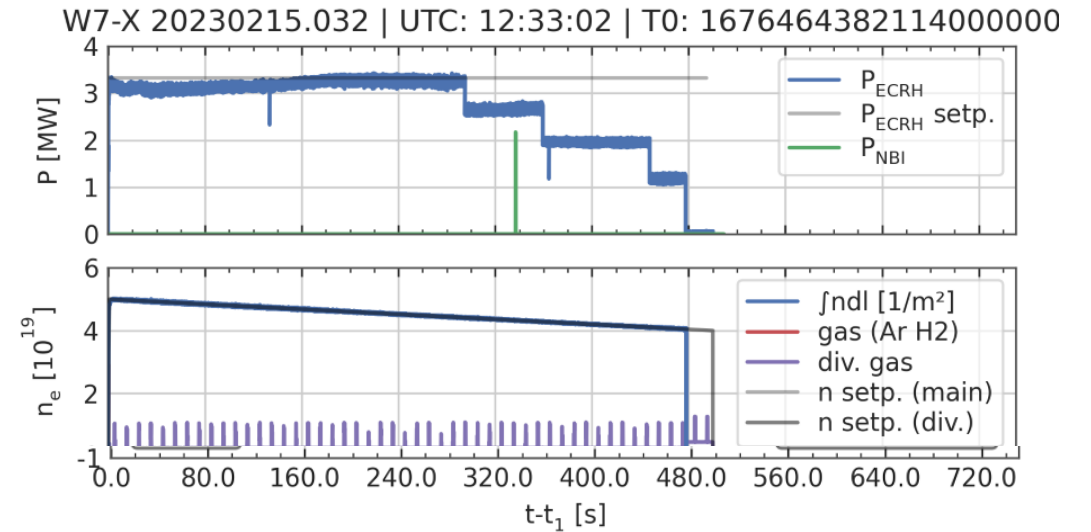
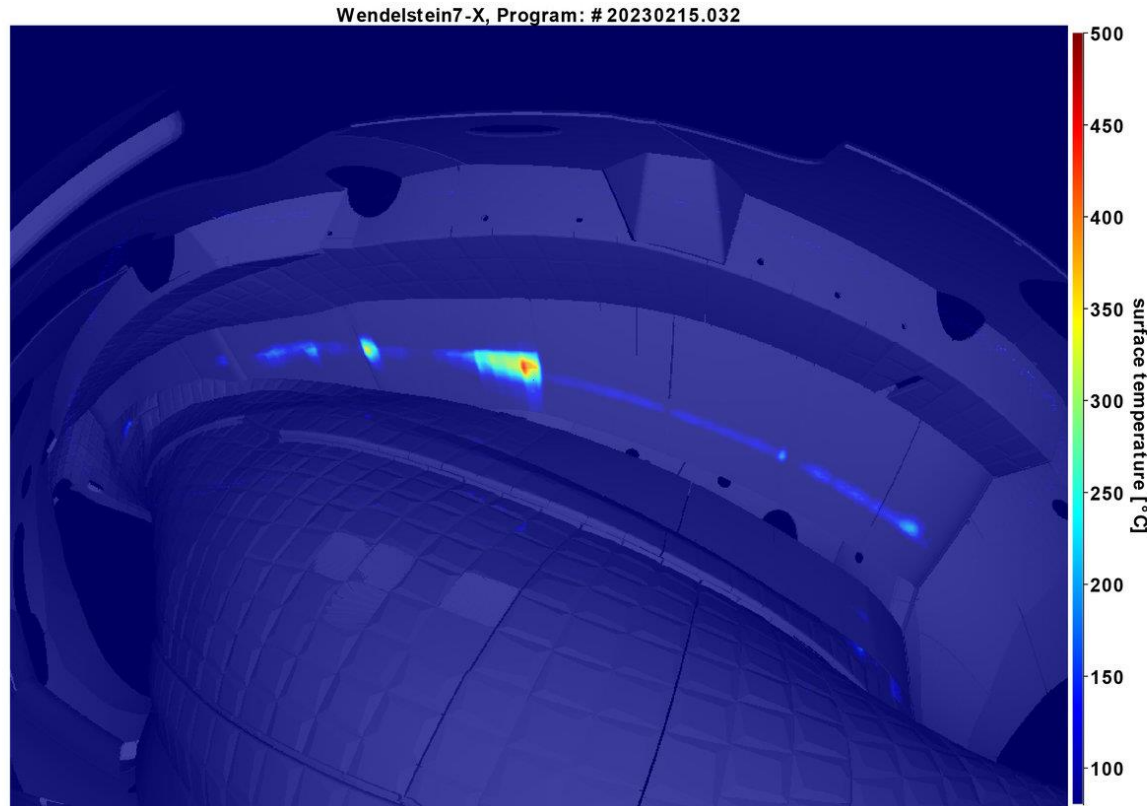
Divertor detachment

- 350 MJ energy turnaround – step towards 1 GJ
- long + stationary divertor detachment
- large fraction of radiated power
- detachment stable even at gyrotron drop-out
- long time scale evolution of bootstrap current
- no visible influence of strike line modification



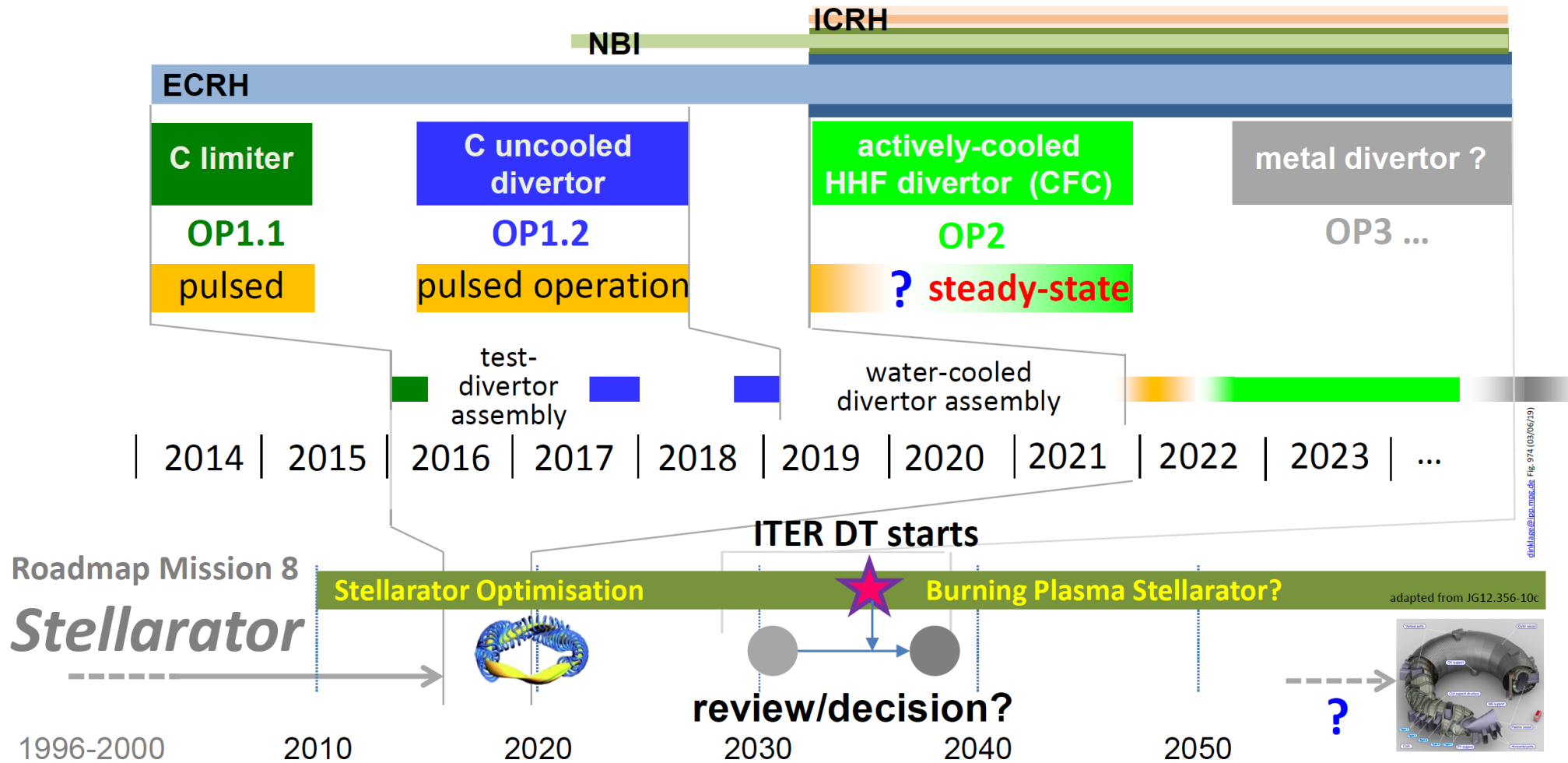
1 GJ achieved!

On 15 February 2023, the researchers reached a new milestone: for the first time, they were able to achieve an energy turnover of 1.3 gigajoules in W7-X.



Infrared image from the vacuum vessel of Wendelstein 7-X. In individual areas, temperatures of up to 600°C are reached.

Plans for W7-X

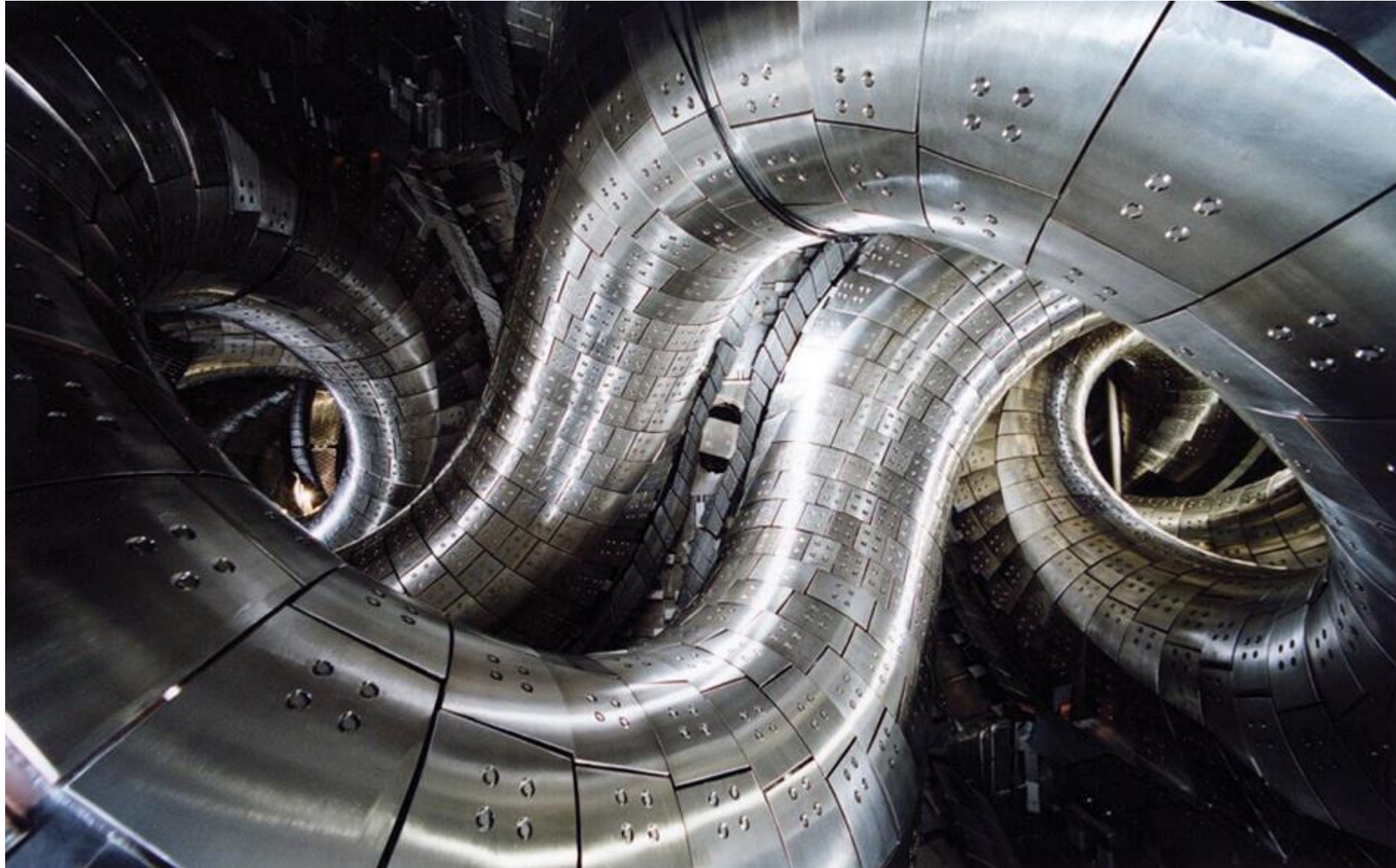


Long term mission: Physics and technological basis for a HELIAS FPP

Summary

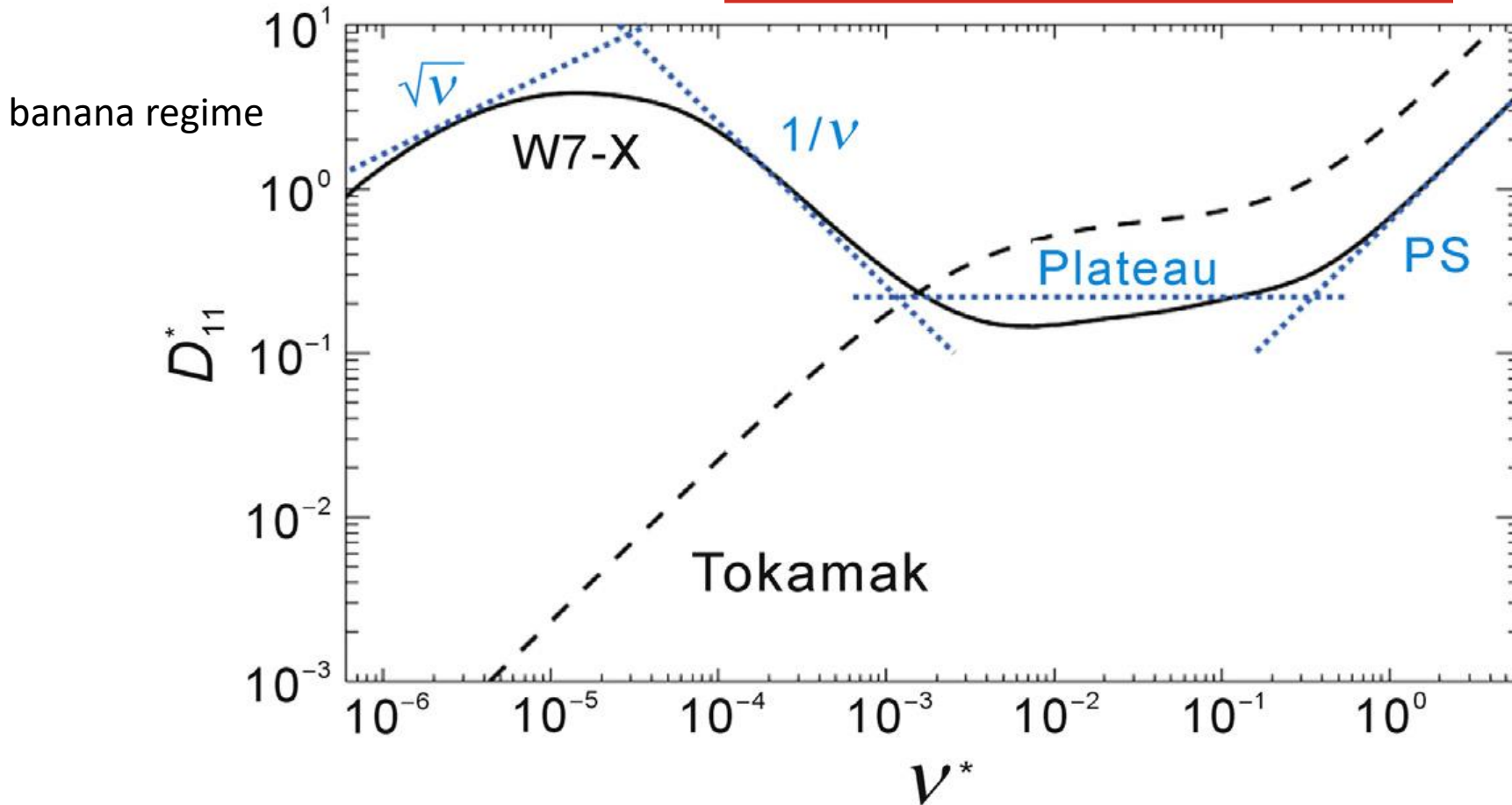
- W7-X programme is still at the beginning of its way to FPP.
- It is big international project where researchers from all over the world work under one W7-X team to achieve the main goal – steady state operation, reaching up to 30 min.
- Polish contribution is significant – two diagnostics systems, involvement in experiments
- W7-X is ready to explore unprecedented plasma conditions in stellarators

Large Helical Device, NIFS, Japan



Heliotron





Pfirsche-Schluter regime

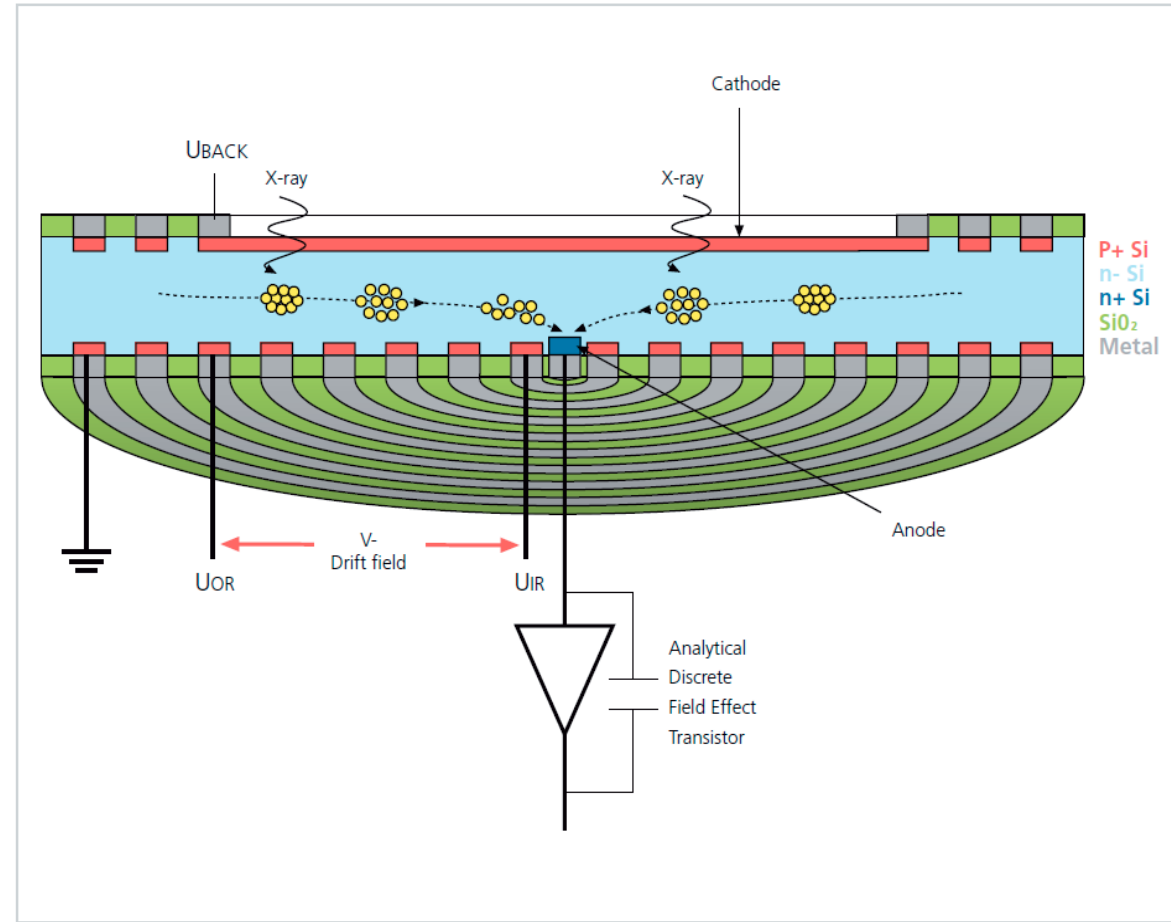
Comparison of diffusion coefficient versus collisionality between tokamaks (dotted curve) and the W7-X stellarator (solid curve) in different regimes

the electrons and ions are often in different regimes, and the larger diffusivity of ions than electrons often violates the ambipolarity. For electrons they usually lie in the $1/\nu$ regime. At low collisionality, the diffusion coefficient in stellarators is much larger than in tokamak

PHA detectors

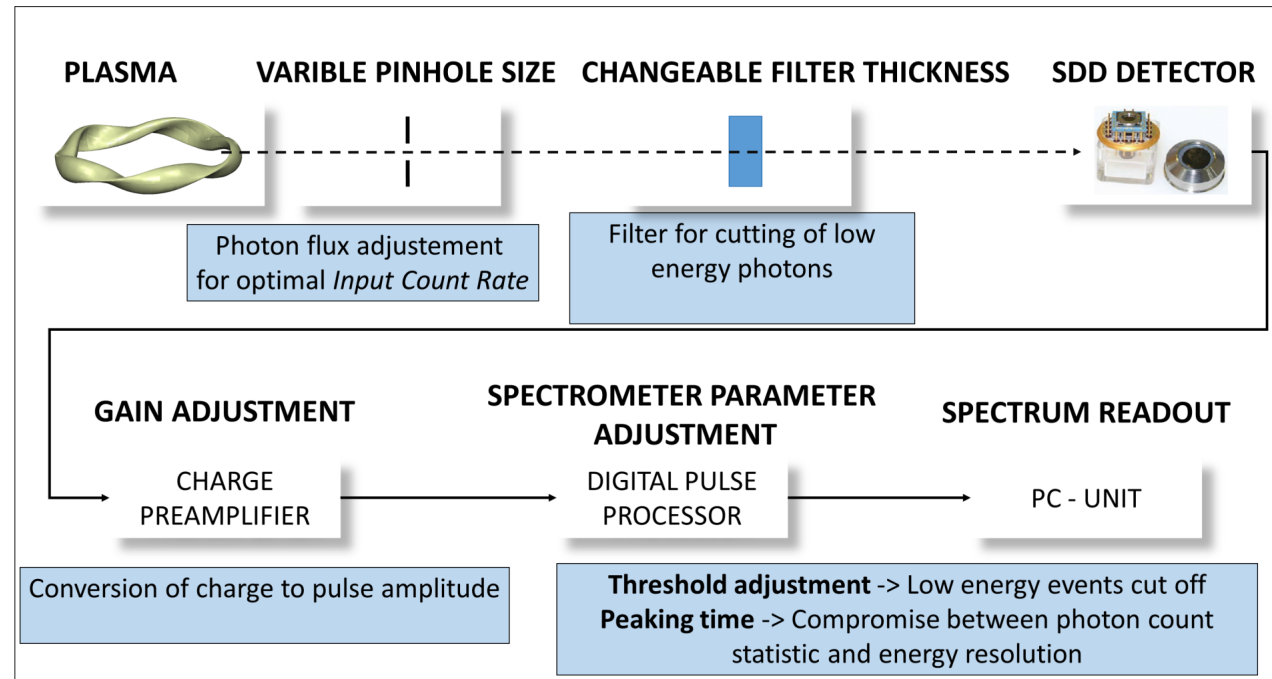
Silicon Drift Detetor (SDD)

When a bias is applied to the SDD detector chip and the detector is exposed to X-rays, it converts each X-ray detected into an electron cloud with a charge that is proportional to the characteristic energy of that X-ray. These electrons are raised into the conduction band of the silicon semiconductor and leave behind holes that behave like free positive charges within the sensor. The electrons are then 'drifted' down a field gradient applied between the drift rings to be collected at the anode. The charge that accumulates at the anode is converted to a voltage signal by the FET preamplifier.



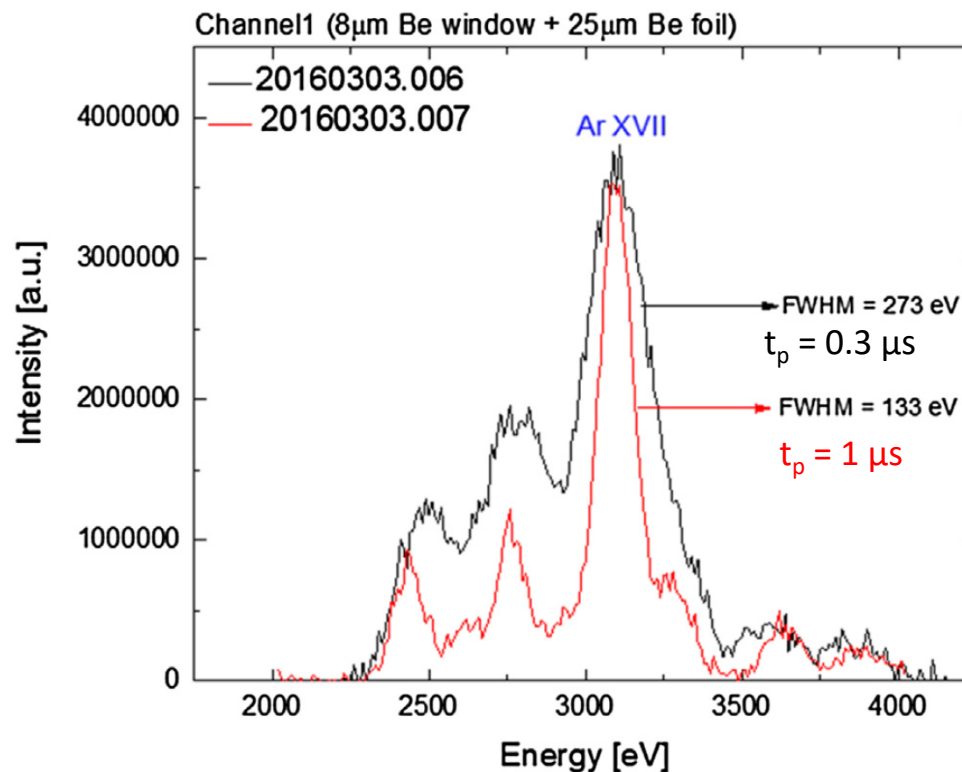
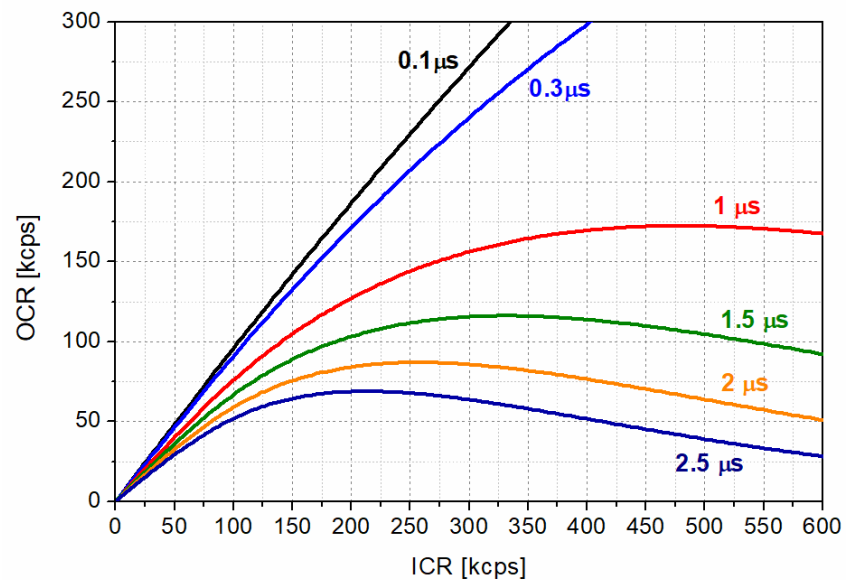
PHA system at W7-X

The charge liberated by an individual X-ray photon appears at the output of the preamplifier as a voltage step on a linearly increasing voltage ramp. The fundamental job of the pulse processor is to accurately measure the energy of the incoming X-ray and give it a digital count in the corresponding channel in the computer. With digital pulse shaping the signal from the preamplifier is digitised at the input of the pulse processor and shaping and noise reduction are achieved by digital computation. The preamplifier output is sampled continuously by an analogue to digital converter and X-ray pulse heights are typically measured by subtracting the average of one set of values, measured before an X-ray event, from that for another set, measured after the event. The resultant value of the step measurement is then sent directly to the computer multi-channel analyser.



PHA settings

- Energy range - additional filter
- Pinhole size - photon flux
- Peaking time - energy resolution



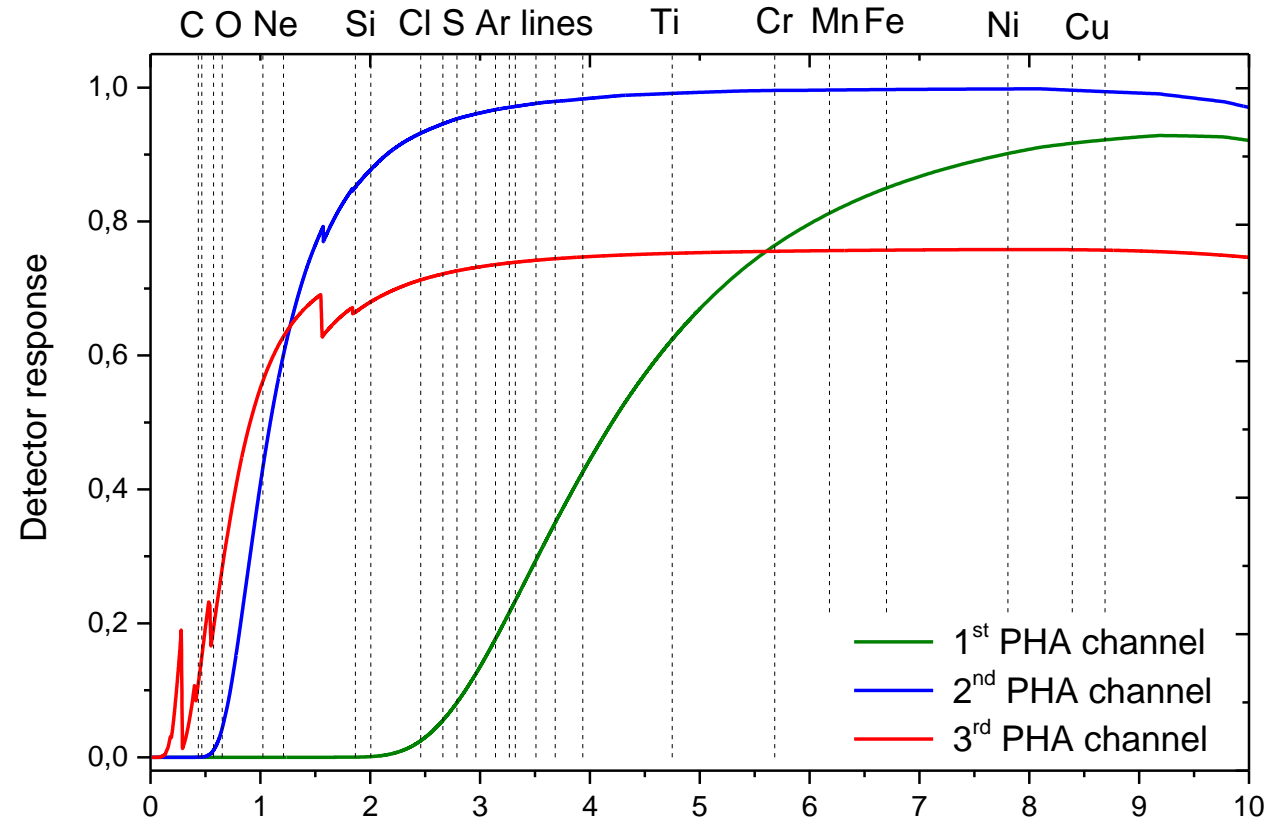
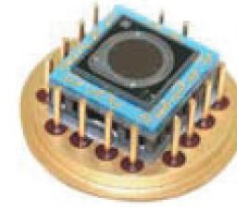
PHA system for W7-X

- Consists of 3 channels:

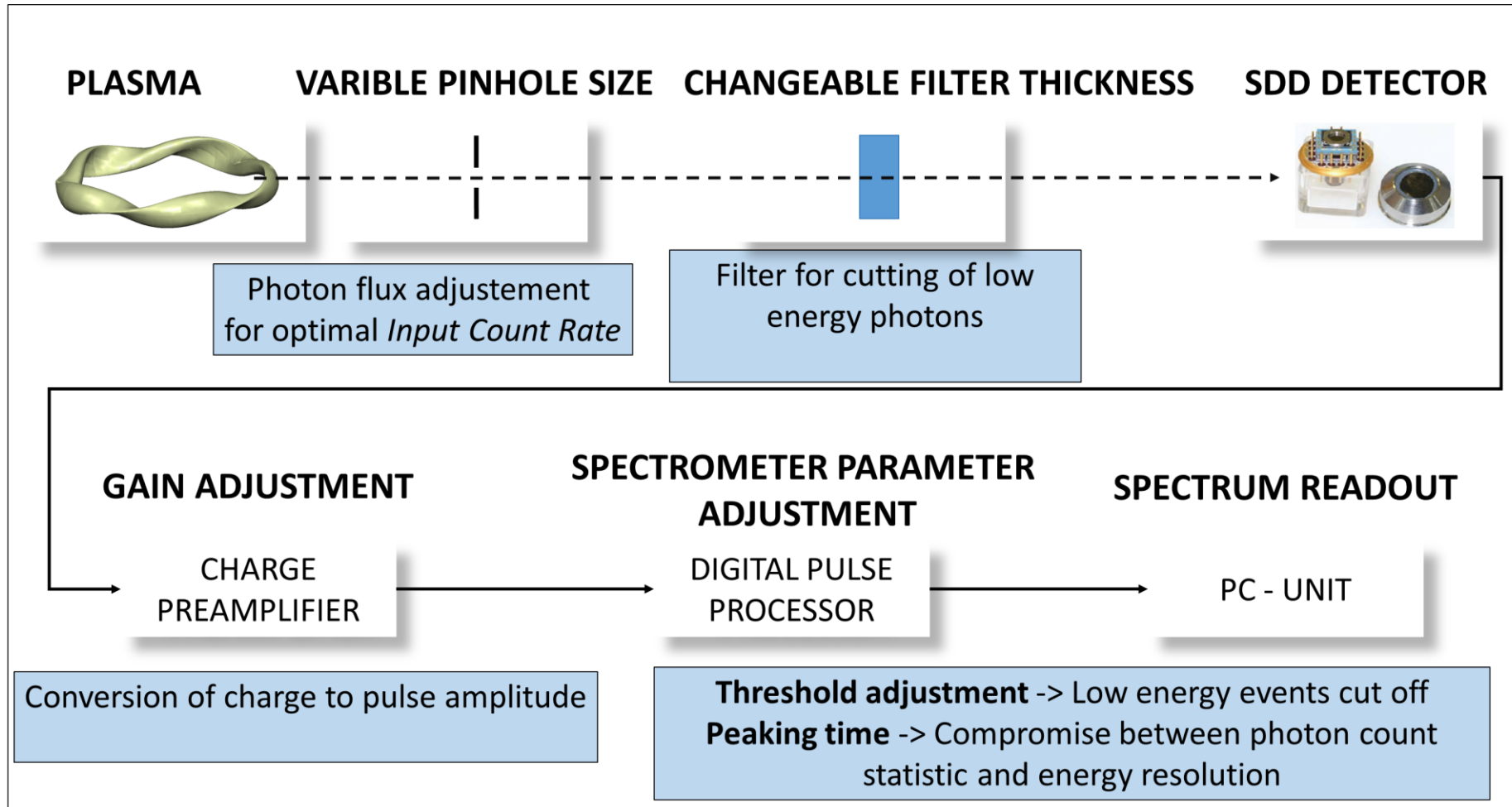
1st (SDD (8+500) μm Be): 1.55–19.60 keV,

2nd (SDD 8 μm Be) 0.96–19.60 keV,

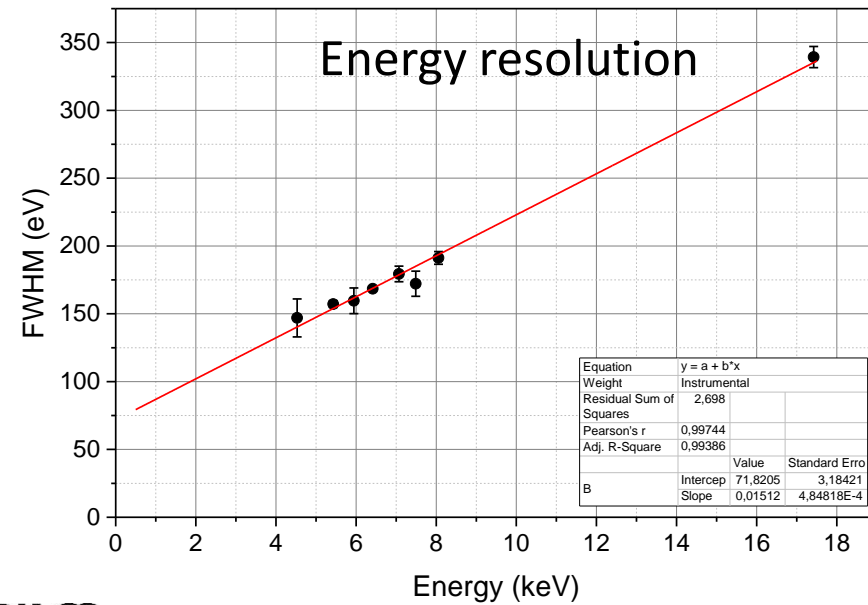
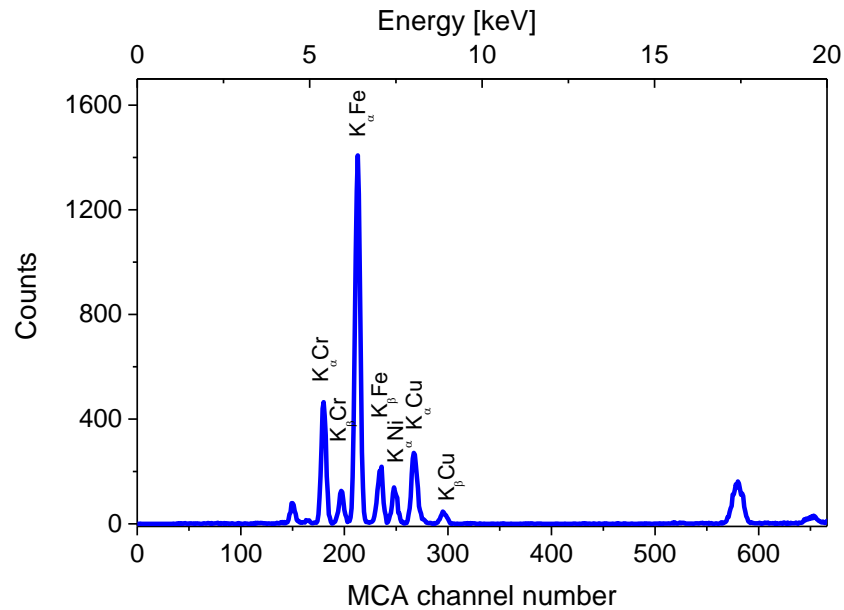
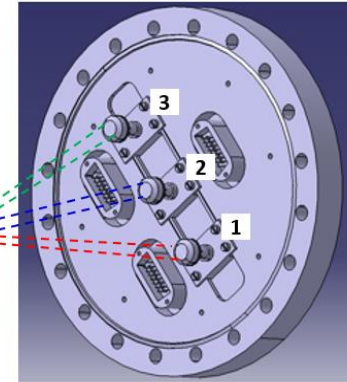
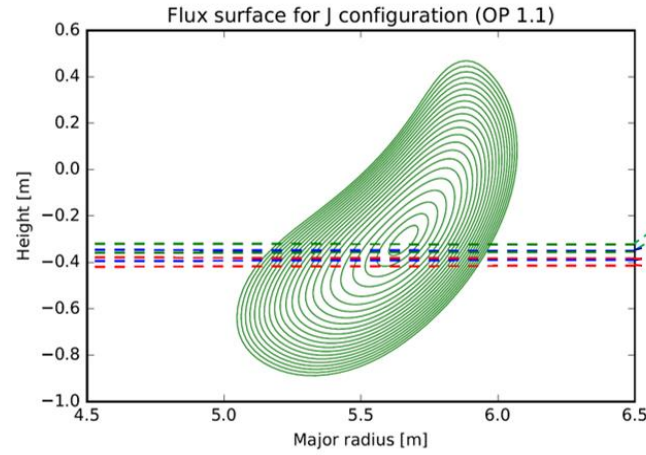
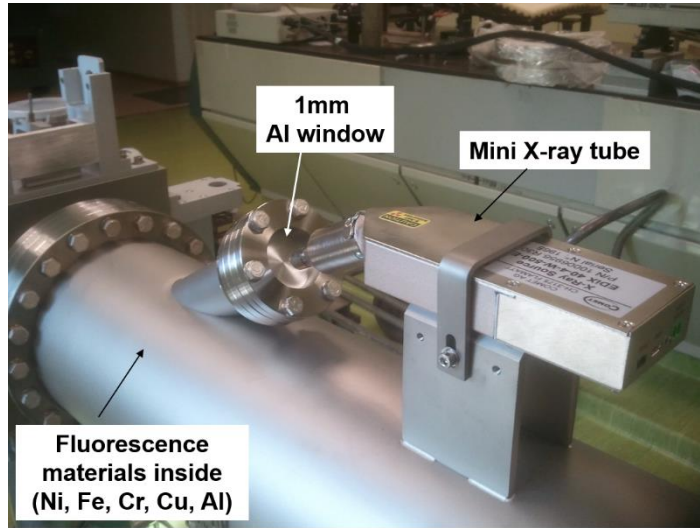
3rd (SD3 Polymer window) 0.6–19.60 keV, assuming 1/e transmission

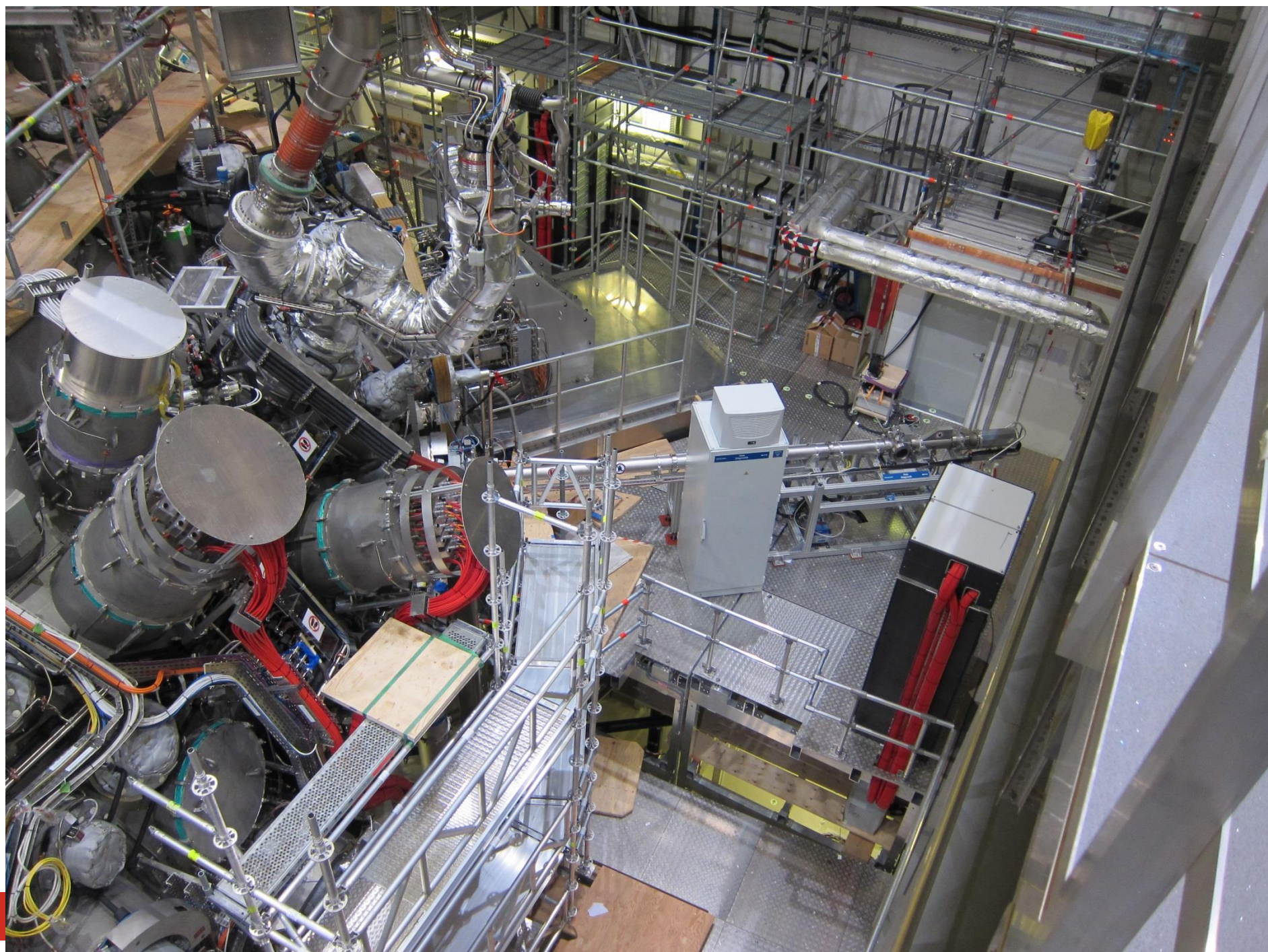


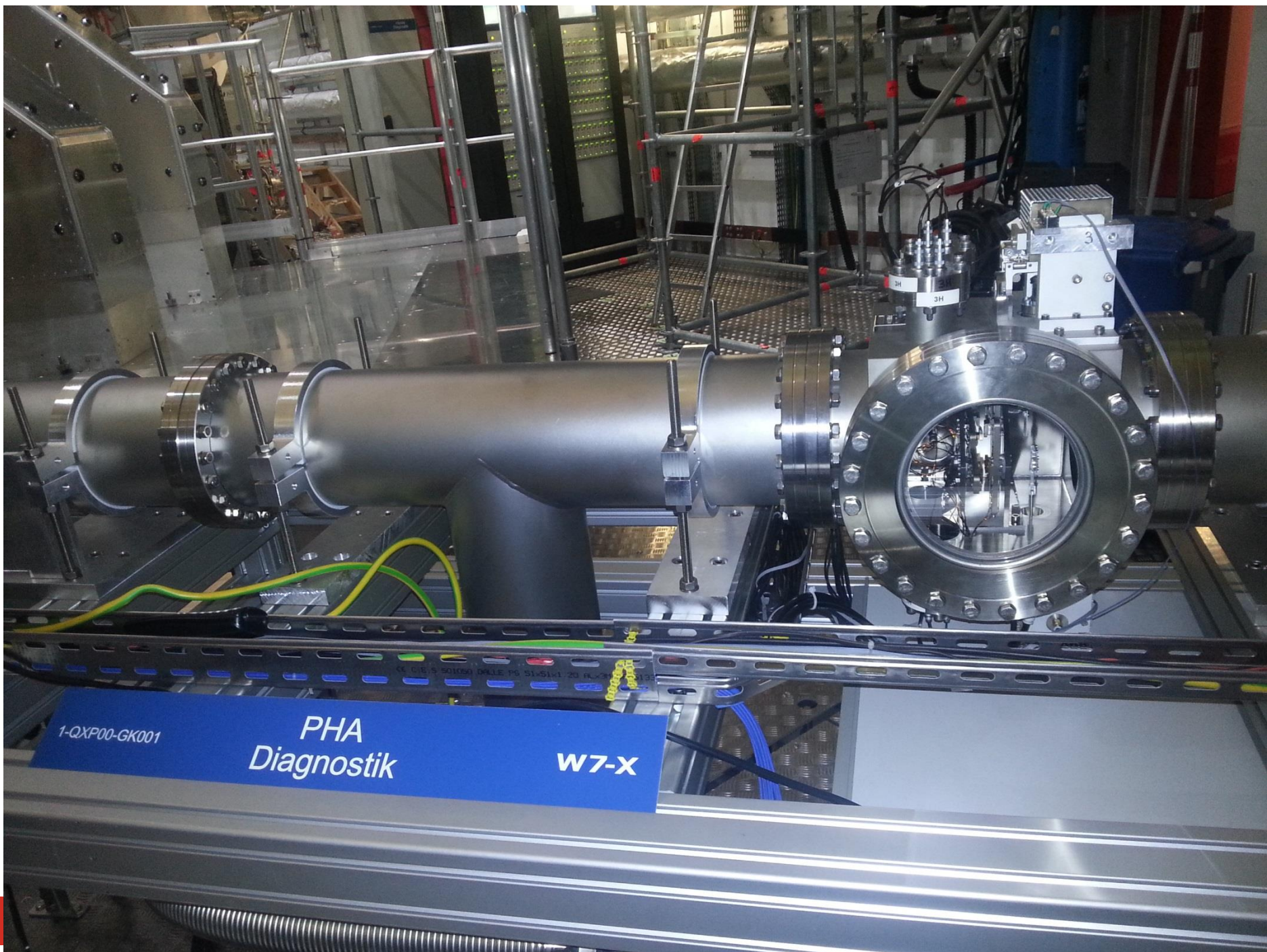
PHA system at W7-X



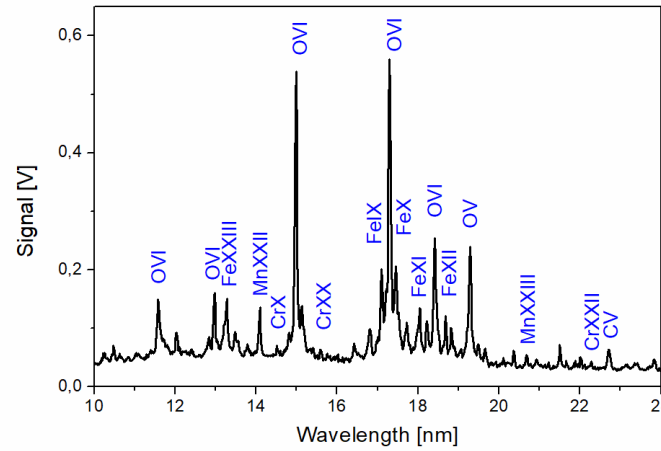
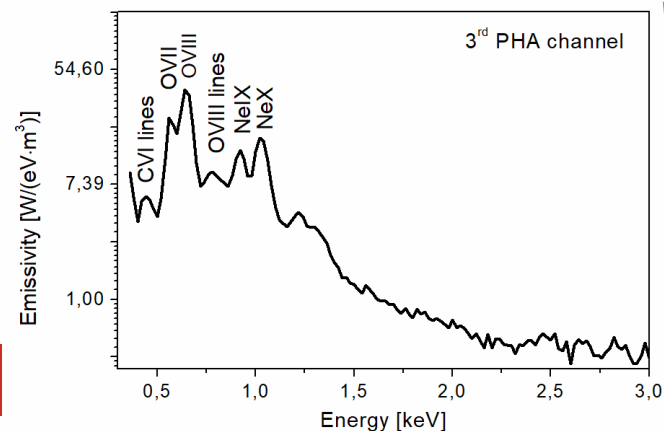
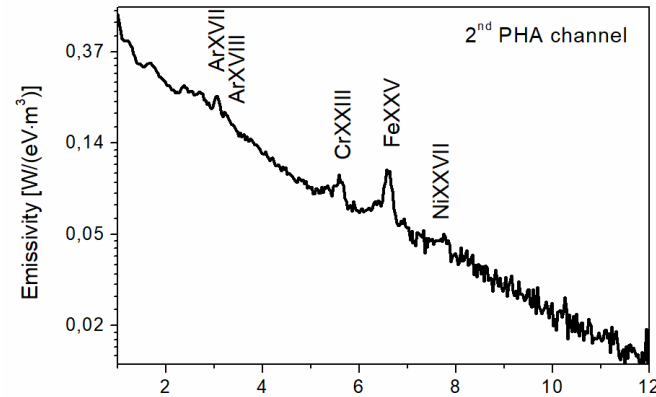
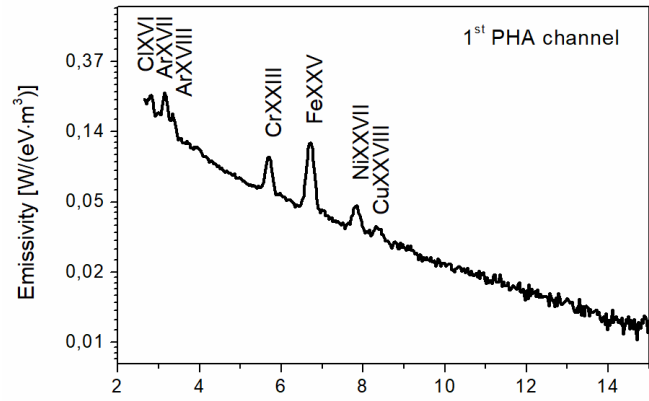
Energy calibration of the PHA system







Example results from OP1.2a



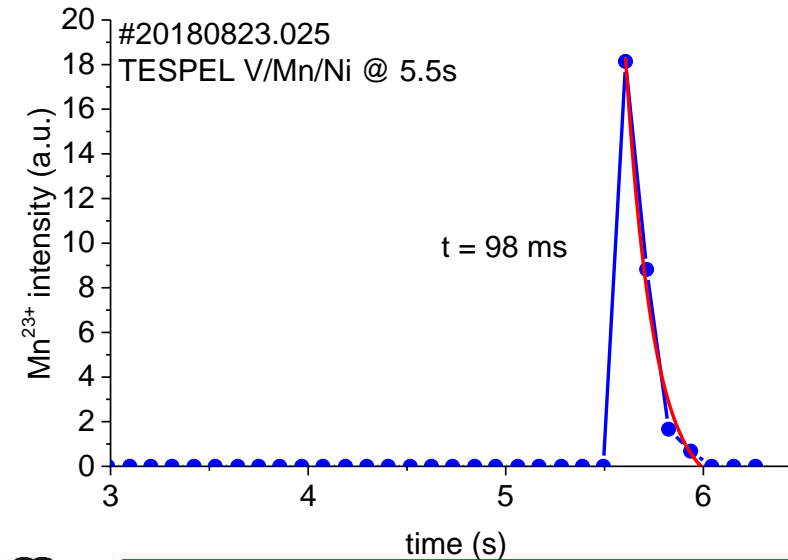
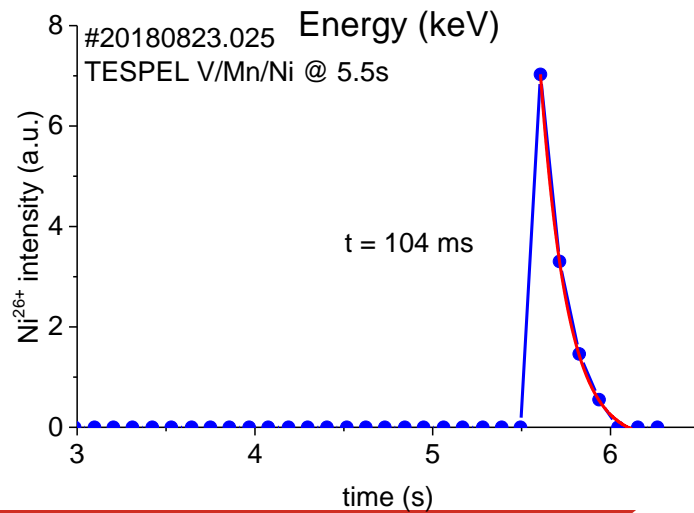
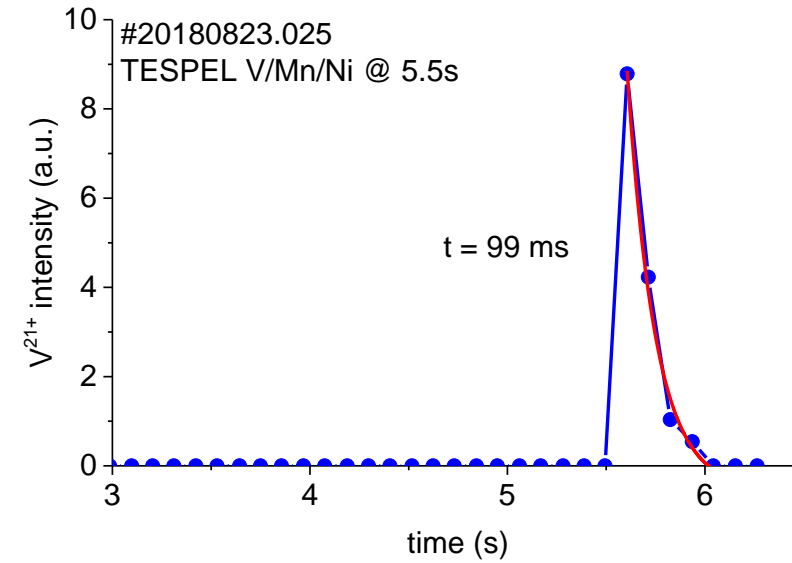
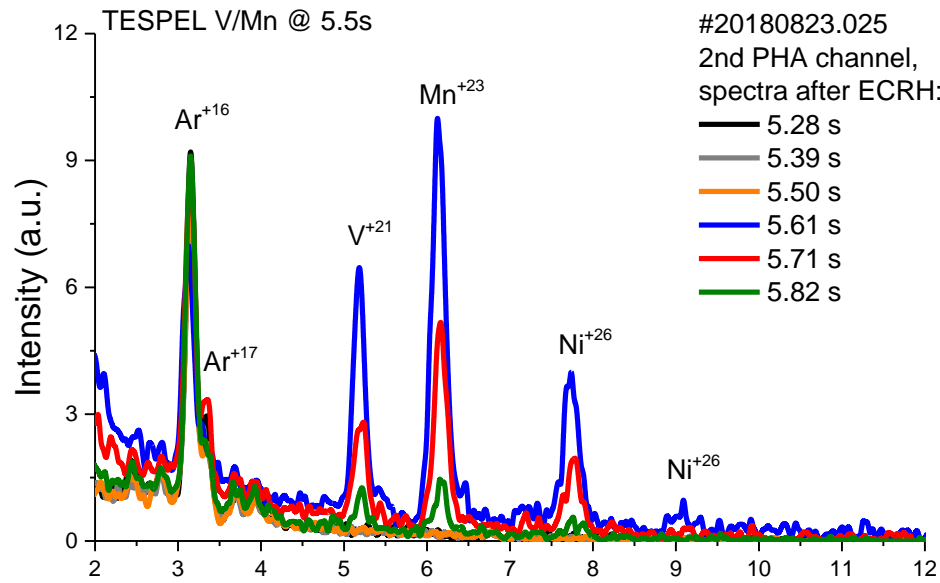
An example of a spectrum for discharge 20171129.025 with identified lines observed by the HEXOS spectrometer

An example of collected by 3 PHA channels spectra for discharge #20171129.021 during OP1.2a experimental campaign at W7-X.

M. Kubkowska et al. RSI, 2018

Type of line	Energy [keV]
H-like C (C ⁺⁵)	0.436
H-like C (C ⁺⁵)	0.459
He-like O (O ⁺⁶)	0.574
H-like O (O ⁺⁷)	0.653
He-like Ne (Ne ⁺⁸)	0.922
H-like Ne (Ne ⁺⁹)	1.022
He-like Si (Si ⁺¹²)	1.865
H-like Si (Si ⁺¹³)	2.005
He-like S (S ⁺¹⁴)	2.460
H-like S (S ⁺¹⁵)	2.662
He-like Cl (Cl ⁺¹⁵)	2.789
H-like Cl (Cl ⁺¹⁶)	2.961
He-like Ar (Ar ⁺¹⁶)	3.140
He-like Cl (Cl ⁺¹⁵)	3.267
H-like Ar (Ar ⁺¹⁷)	3.321
H-like Cl (Cl ⁺¹⁶)	3.508
He-like Ar (Ar ⁺¹⁶)	3.684
H-like Ar (Ar ⁺¹⁷)	3.935
He-like Ti (Ti ⁺²⁰)	4.749
He-like Cr (Cr ⁺²²)	5.682
He-like Mn (Mn ⁺²³)	6.180
He-like Fe (Fe ^{+24*})	6.700
He-like Ni (Ni ⁺²⁶)	7.805
He-like Cu (Cu ⁺²⁷)	8.391

Example results from OP1.2b



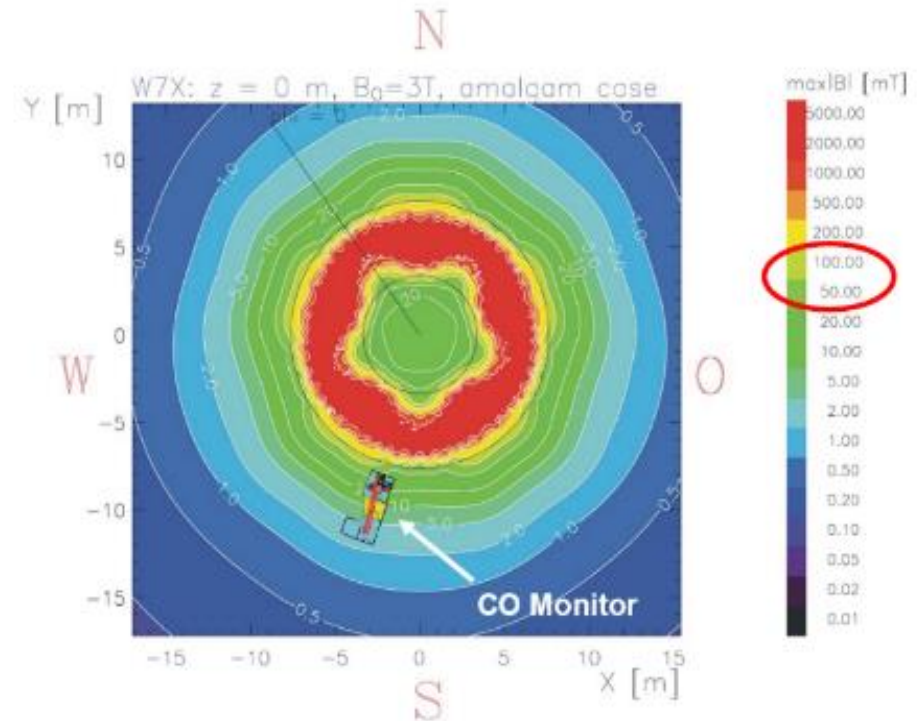
C/O monitor system for W7-X

The “CO Monitor” system for the Wendelstein 7-X (W7-X)

- a dedicated spectrometer with high throughput and high time resolution;
- for monitoring of low-Z impurities in the plasma; based on intensities of Lyman- α lines of H-like ions of
 - carbon (3.4 nm; plasma-wall interaction),
 - oxygen (1.9 nm; the wall condition),
 - nitrogen (2.5 nm; vacuum leakage),
 - boron (4.9 nm; plasma-boronized wall interaction, quality of boron layer).
- will be fixed in a nearly horizontal position;
- will be divided into two subspectrometers, each containing two spectral channels assigned to two impurity species;
- each channel will consist of a separate dispersive element and detector.

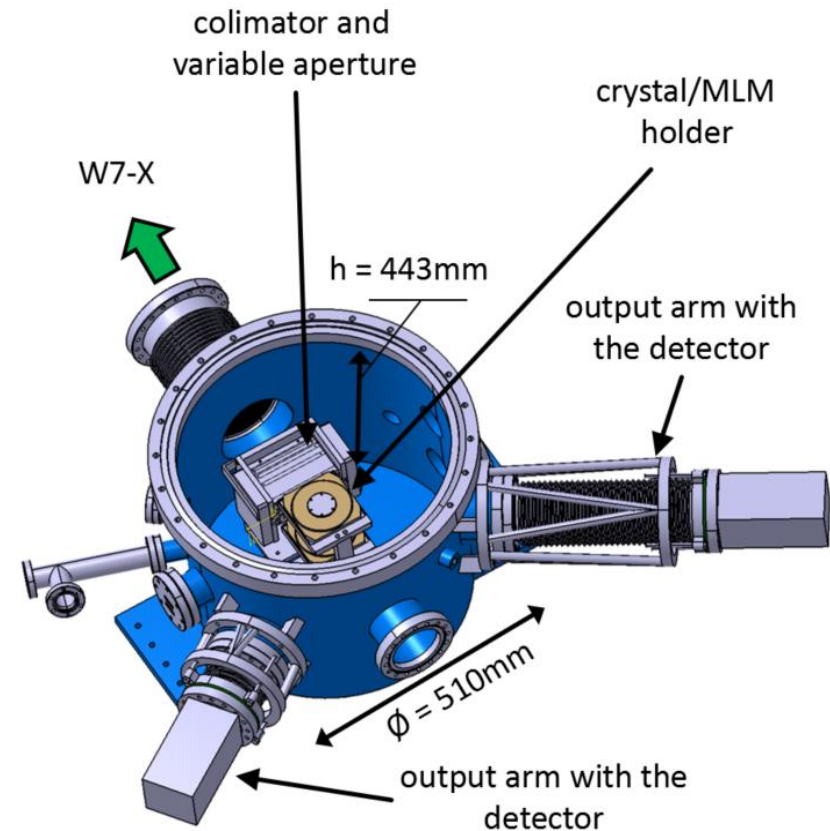
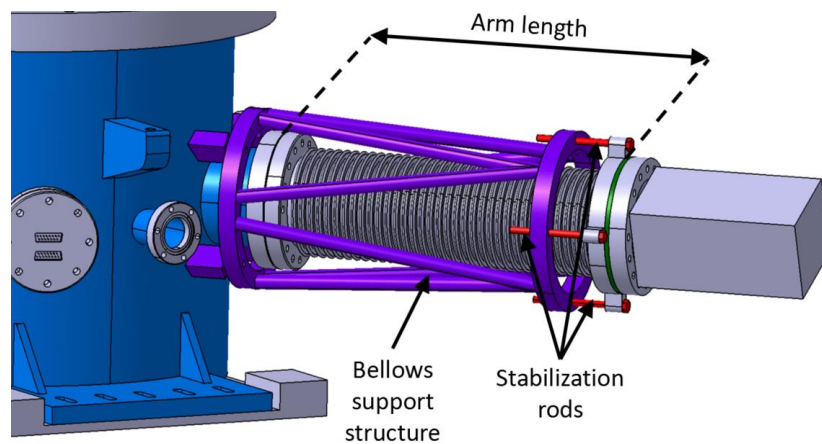
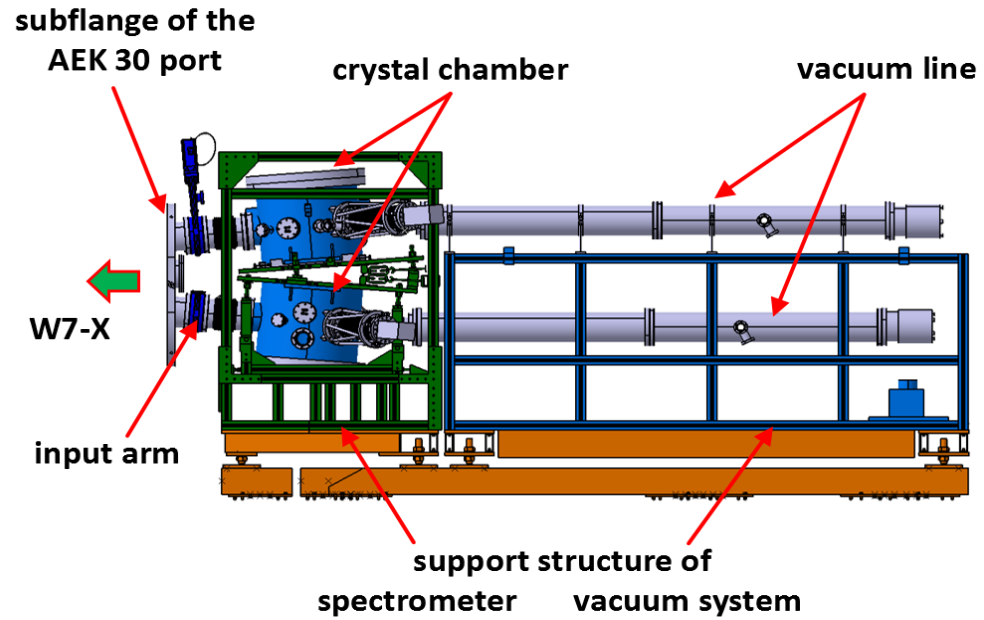
W7-X requirements for CO monitor

- High magnetic field in the area of 'CO Monitor' (approx. 100 mT);
- Low magnetic permeability of the materials (e.g. steel 316LN);
- Proper vacuum level and relevant vacuum system;
- Protection from the ECRH stray radiation;
- High reflectivity of the dispersive elements;



- Adjustment of input aperture and crystal angle;
- Detection system with relevant parameters (sensitivity, time resolution, etc.)

Concept of the CO monitor for the W7-X



CO monitor – first results

